Research Final Report

for
Research Project T2696, Task 02
Development Of High Performance Concrete And
Evaluation Of Construction Joints In
Concrete Floating Bridges

DEVELOPMENT OF HIGH PERFORMANCE CONCRETE AND EVALUATION OF CONSTRUCTION JOINTS IN CONCRETE FLOATING BRIDGES

by

Rafik Itani, Eyad Masad, Bart Balko and Brian Bayne
Washington State Transportation Center (TRAC)
Department of Civil and Environmental Engineering
Washington State University
Pullman, WA 99164

Washington State Department of Transportation
Technical Monitor
Geoff Swett, Bridge Engineer

Prepared for

Washington State Transportation Commission
Department of Transportation
and in cooperation with
US Department of Transportation
Federal Highway Administration

July, 2003

TECHNICAL REPORT DOCUMENTATION PAGE

1. Report No. WA-RD 649.1	2. Government Accession No.	3. Recipient's Catalog No.
4. Title and Subtitle DEVELOPMENT OF HIGH PERFORMANCE CONCRETE AND EVALUATION OF CONSTRUCTION JOINTS IN CONCRETE FLOATING BRIDGES		5. Report Date July 2003 6. Performing Organization Code
7. Author(s) Rafik Itani, Eyad Masad, Bart Balko, Brian Bayne		8. Performing Organization Report No.
9. Performing Organization Name and Address Washington State Transportation Center (TRAC) Civil and Environmental Engineering; Sloan Hall, Room 101 Washington State University Pullman, Washington 99164-2910		10. Work Unit No. 11. Contract or Grant No. T2696 Task 02
12. Sponsoring Agency Name and Address Research Office Washington State Department of Transportation Transportation Building, MS 7370 Olympia, Washington 98504-7370		13. Type of Report and Period Covered Final Report 14. Sponsoring Agency Code

15. Supplementary Notes

This study was conducted in cooperation with the U.S. Department of Transportation, Federal Highway Administration.

16. Abstract

Floating bridge concrete must be watertight, durable, workable, and must have sufficient cohesiveness to prevent segregation in heavily congested deep walls. The mix design must experience minimal creep and shrinkage to reduce prestress losses, and shrinkage cracking. As a result of recent concrete research, new mixes were created incorporating various quantities of fly ash, silica fume, metakaolin, poly-carboxylate ether superplasticizers, and Caltite waterproofing admixture. This research focuses on concrete with a water binder ratio of 0.33 and a slump in the range of 8 to 9 inches. Workability characteristics of the fresh concrete are analyzed and hardened concrete properties tested in this research are compressive strength, chloride ion permeability, and creep and drying shrinkage properties.

It was found that metakaolin was successful in producing mix designs with similar properties as Silica fume modified concrete. Satisfactory strength was achieved through increasing the fly ash and lowering the silica fume contents, though, chloride ion permeability was negatively affected. The removal of silica fume and the inclusion of Caltite decreased the concrete's resistance to chloride ion permeability and produced concrete that failed to attain the required 28-day ultimate compressive strength of 6500 psi. The second part of this study focuses on developing an experimental setup to evaluate products and construction methods to help prevent water leakage through construction joints in pontoon floating bridges. A pressure system was used to apply significant pressures to concrete test specimens containing a construction joint. Different products and construction methods were used in constructing the joints to determine the most effective methods for preventing water penetration in the field.

The testing results have shown compaction effort is the most important factor in water leakage through a joint. Increased compaction in laboratory specimens leads to less water leakage through construction joints. Product selection was ineffective in preventing water leakage if concrete compaction was inadequate.

17. Key Words	18. Distribution Statement
Concrete, Performance, Fly Ash, Silica Fume, Metakaolin, Polycarboxylate, Caltite, Creep, Shrinkage, Compressive Strength, Permeability, Construction Joint, Leakage, Waterstop, Compaction, Watertight	No restrictions. This document is available through the National Technical Information Service, Springfield, VA 22161.

19. Security Classif. (of this report)	20. Security Classif. (of this page)	21. No. of Pages	22. Price
None	None	239	

DISCLAIMER

The contents of this report reflect the views of the authors, who are responsible for the facts and accuracy of the data presented herein. The contents do not necessarily reflect the official views or policies of the Washington State Transportation Commission, Department of Transportation, or the Federal Highway Administration. The report does not constitute a standard, specification, or regulation.

TABLE OF CONTENTS

LIST OF TABLES

LIST OF FIGURES

SUMMARY

Floating bridge concrete must be watertight, durable, workable, and must have sufficient cohesiveness to prevent segregation in heavily congested deep walls. The mix design must experience minimal creep and shrinkage to reduce prestress losses, and shrinkage cracking. As a result of recent concrete research, new mixes were created incorporating various quantities of fly ash, silica fume, metakaolin, poly-carboxylate ether superplasticizers, and Caltite waterproofing admixture. This research focuses on concrete with a water binder ratio of 0.33 and a slump in the range of 8 to 9 inches. Workability characteristics of the fresh concrete are analyzed and hardened concrete properties tested in this research are compressive strength, chloride ion permeability, and creep and drying shrinkage properties.

It was found that metakaolin was successful in producing mix designs with similar properties as Silica fume modified concrete. Satisfactory strength was achieved through increasing the fly ash and lowering the silica fume contents, though, chloride ion permeability was negatively affected. The removal of silica fume and the inclusion of Caltite decreased the concrete's resistance to chloride ion permeability and produced concrete that failed to attain the required 28-day ultimate compressive strength of 6500 psi.

The second part of this study focuses on developing an experimental setup to evaluate products and construction methods to help prevent water leakage through construction joints in pontoon floating bridges. A pressure system was used to apply significant pressures to concrete test specimens containing a construction joint. Different products and construction methods were used in constructing the joints to determine the most effective methods for preventing water penetration in the field.

The testing results have shown compaction effort is the most important factor in water leakage through a joint. Increased compaction in laboratory specimens leads to less water leakage through construction joints. Product selection was ineffective in preventing water leakage if concrete compaction was inadequate.

CHAPTER 1: INTRODUCTION

1.1 BACKGROUND

The State of Washington has been designing and building concrete floating bridges since 1938. The original Lacey V. Murrow floating bridge opened to traffic in 1940, and was considered at that time to be one of the most innovative and controversial bridges in the world (Lwin el al. 1994). Since that time, Washington State has become a worldwide authority in the design and implementation of this practical and economically viable structure. Four floating bridges are currently in service in the state including the new Lacey V. Murrow Bridge, the Evergreen Point Floating Bridge (or the Second Lake Washington Bridge), the Third Lake Washington Bridge, and the Hood Canal Floating Bridge.

The most recent of the floating bridges constructed in Washington is the new Lacey V. Murrow Floating Bridge. During the design phase of this bridge, extensive research was performed to determine a mix design that would deliver superior performance for the demands that the structure would experience. The concrete was developed and named the LVM mix design, representing the bridge in which it was first used, the Lacey V. Murrow.

The Hood Canal Floating Bridge was originally constructed in 1961 as a vital link between the Olympic Peninsula and the central Puget Sound region. On February 13, 1979, the bridge was subject to its 100-year design storm and the West half was unable to withstand the forces induced by the storm; the West half of the bridge was destroyed and sank. Following this structural failure, the West half was rebuilt and the East half was rehabilitated to maintain this important structure for the years to come. Currently, the

East half of the Hood Canal Floating Bridge is nearing the end of its design life and scheduled for replacement

1.2 PROBLEM STATEMENT

It is the desire of the Washington State Department of Transportation to use a state of the art concrete mix design for the floating pontoon sections of the new Hood Canal Floating Bridge. The LVM mix design has worked well in the past, but there is room for improvements, which are discussed in detail in the forthcoming pages.

Concrete, similar to most construction materials, deforms under constant load sustained for a long period. This deformation is known as creep deflection and must be understood and accounted for in structural design. One main area of impact that creep has within concrete structures, and in particular prestressed concrete structures, is loss of prestressing force due to the shortening of the concrete member.

Concrete is very strong in compression resistance, but weak in tension and must be reinforced with steel. Prestressing is done for the basic purpose of dramatically reducing or eliminating the tensile force that the concrete member will have to resist during its design life. The compressive force that is induced into the concrete member through prestressing is a moderately high, sustained load and, therefore, has the potential to cause the concrete to creep. When the concrete member length is shortened, the length of the elastically strained, tensioned cable is shortened as well, reducing the strain in the cable, and thus reducing the tensile stress. This reduction in tensile stress in the cable translates to a reduction in compressive stress in the concrete member, which in turn, causes a stress reversal in the "tensile zone" of that member. If the stress reversal is large, the

concrete must resist the tensile force. Tensile forces in the concrete cause cracks to form and if the cracks become too dramatic, failure would become eminent.

Floating bridges designers throughout Washington State utilize this prestressing technique to create floating concrete pontoons. These pontoons are essentially hollow, concrete beams resting on an elastic foundation. The pontoons used as the floating structure in the Hood Canal floating bridge are 360 feet long, 18 feet high and 60 feet wide. The length of a pontoon is subdivided into three rows of 14 cells each, with outside wall and floor thickness between 8 and 12 inches. These pontoons float due to the buoyant force of the water, and it must be noted that the air filled cells are key to the equation of equilibrium. With the pontoons being constructed of concrete that has been prestressed, creep of the concrete will occur. If the concrete creep is not controlled and prestress loss occurs, cracks can form in the "tensile zones" of these beams. The tensile zone is generally on the bottom face of the pontoons, as is usually the case with supporting beams. Tensile zones are also on either of the sides of the pontoon, depending on the direction of the dynamic forces induced by wind and wave action. If the tensile stresses are large enough so that the concrete has to resist a portion of it, the concrete may crack due to its inadequacy in this application. The cracked concrete would allow water passage into the air filled cells, which will result in undermining the buoyancy of the structure. Creep must be minimized so that prestress loss is controlled.

Shrinkage must also be analyzed in concrete used for floating bridges. Shrinkage in concrete can cause large internal stresses in the concrete matrix and which can lead to cracking. These cracks are passageways for water to penetrate the outer walls of the pontoons and enter into the cells. Also, the concrete bridge pontoons have differing wall

and floor thickness. This difference in thickness can lead to localized stresses due to shrinkage and lead to differential shrinkage cracking, and thus, allowing water to enter the pontoon cells. A concrete of low shrinkage potential is necessary for its use in floating bridges.

The Hood Canal is a body of salt water that is highly corrosive. Care must be taken such that structural steel is protected. Included in this list of critical steel members are steel reinforcing bars and steel prestressing tendons within the concrete pontoons. The chloride ion penetrability of concrete mixes to be used in floating bridges must be tested.

Water leakage through joints in the pontoons of floating bridges has been a problem in previous pontoon construction projects. Water trapped within pontoons can cause excessive damage that if left unchecked can lead to pontoon failure. This water leakage occurs mainly during or immediately after construction of the pontoon causing a need for expensive post-construction repairs. Currently pontoon joint leakage is halted through repairs to the inner surface of the pontoons such as through the use of sealing or epoxy injection after completion.

Research has been performed in the past to improve mix designs for floating bridges. The new mix designs have improved workability, durability and limit concrete permeability. Little research has been performed on construction joint improvements. Construction joint improvements are needed in pontoon floating bridges to reduce water leakage and thereby reduce maintenance costs while lengthening pontoon service life.

1.3 OBJECTIVES

The overall goals of this research are to improve the concrete mix design currently used in concrete floating bridges and to develop a watertight construction joint for these bridges. The LVM mix design is used as a baseline for the development of new mix designs suitable for use in concrete floating bridges. The intent is to explore new concrete technology and new materials that have emerged since the LVM creation in 1990, and to implement these into LVM alterations. Tests will be performed to determine properties in each mix and the results will be compared to the performance of the LVM. Conclusions will be formulated based on these results.

Some concrete properties are of primary importance in selecting a mix design for use in concrete floating bridges. These properties include fresh concrete workability, creep, shrinkage, compressive strength, and chloride permeability. Creep of concrete will be discussed in detail due to the relatively rare implementation of this test into mix design performance studies.

Research objectives for the study of watertight construction joints include:

1. To investigate different alternatives for developing a watertight construction joint suitable for floating bridge pontoons.
2. To design a laboratory experiment to simulate water infiltration in concrete pontoon joints under conditions similar to those experienced in the field.
3. To recommend guidelines for reducing water penetration through a construction joint to be included in specifications for future floating bridges and other similar projects.

1.4 TASK SUMMARY

This research consisted of six tasks grouped in two phases described below.

Phase 1 – Review and Development

Task 1: Literature Review, Broad Scope

Collect and review relevant literature, mix design specifications, materials, new or existing products, research findings and current practices used to produce durable concrete for submerged concrete structures. Also, collect information relevant to construction joints in submerged concrete structures. The review will focus on current construction practices for a floating bridge; mix designs used and new or existing products for sealing construction joints.

Task 2: Literature Review, Concentrated

Utilize the information obtained after the construction of the last floating bridge in the early 90's and other recent knowledge to develop new and improved mix designs. The improvements would be based on high performance concrete (HPC) properties especially chloride permeability, compressive strength, creep and shrinkage, and self-consolidation.

Task 3: Review Synthesis

Based on the information gathered in tasks 1 and 2, identify and discuss material properties, mix proportions and other factors that affect the durability of concrete in a salt water environment. Also, based on information from manufacturers and product vendors, a product's ability to meet the design needs determined during task 1 is quantified.

Products are chosen for laboratory testing to determine their ability to reduce water leakage through a construction joint.

Task 4: Research Development

Develop a detailed experimental work plan to investigate the influence of the modifications in the mix design on the strength, durability, and long-term properties of the concrete. In this task, a work plan to determine the effectiveness of different products at reducing water penetration through the joint is also developed. The work plan will include specimen dimensions, the design and construction of a water pressure system and a testing procedure for determining the necessary requirements for passing the tests.

Phase 2 – Realization and Analysis

Task 5: Implementation

Conduct concrete tests including compressive strength, chloride ion permeability, creep and shrinkage to determine the influence of any modifications to the mix design performance. This task also includes performing the experiments developed in task three to determine product effectiveness at preventing water penetration through the joint. The data gathered from the experiments will be analyzed to determine the most effective product or construction method for use in the field.

Task 6: Production

The final report documenting research procedure and findings is provided. This report will include the following: a synthesis of all pertinent literature from Tasks 1 and 2; a detailed documentation of the experimental work plan: materials used, number of specimens and testing procedures; a statistical analysis of the testing results; proposed

methods for improving the performance of the mix design. The final task also involves developing a set of construction joint procedures or guidelines to be included in the specifications for the Hood Canal Floating Bridge East Half Replacement Project. The guidelines will list a set of construction procedures or product guidelines for reducing water penetration at the joint.

This report is split into two parts. The first part focuses on the concrete mix design research to improve the LVM and includes Chapters 2 through 5. The second part focuses on the construction joint research and includes Chapters 6 through 9.

CHAPTER 2: LITERATURE REVIEW

This literature review focuses on the key aspects of concrete mix design development and performance for use in concrete floating bridges. Topics of interest for this research were a previous floating bridge mix design study and mechanisms of concrete creep. Other noted literature included admixture and supplementary cementitious material effects on freshly mixed and hardened concrete properties.

2.1 CONCRETE FOR THE LACEY V. MURROW FLOATING BRIDGE

Concrete for the Lacey V. Murrow floating bridge was first developed with water tightness and durability of the concrete as the prime importance. The research committee conducted a concrete mix development program consisting of three phases. The first phase included the investigation of many trial mixes. These mixes were used to verify the resulting concrete properties produced by the inclusion of different supplementary cementitious materials and concrete admixtures. Silica fume was found to reduce permeability, increase early compressive strengths, reduce bleeding, and increase the heat of hydration. Fly ash was found to increased workability, reduce heat of hydration, and increase ultimate compressive strengths of the concrete. Retarders added to the mixes increased workability, extended slump life, and improved concrete set control. Superplasticizers increased workability and decreased the water demand for concrete mixes.

The second phase of the research was to develop the mix design to be used in the

Lacey V. Murrow floating bridge. This was done based on the results from the first phase. Watertightness, durability, constructability, and compressive strengths were the key properties that were tested in selecting an appropriate mix design. The third stage involved constructing full size test sections to test the constructability of the concrete mix. Wall and slab sections were built and the mix design was evaluated for effectiveness for the particular application of floating bridges.

The general mix design was created using the three phases for research. WSDOT and fellow researchers set minimum and maximum quantity extents on different concrete constituent proportions to be used in the contractor specified mix design. Proportions selected by the project contractor and approved for use were as follows:

Portland cement type II:	624 lb
Silica Fume* (AASHTO M307):	50 lb
Fly Ash Class F (AASHTO M295):	100 lb
Paving Sand (WSDOT Class 1):	1,295 lb
Coarse Aggregate** (3/8 inch max agg.):	1,770 lb
Water: 225 lb	
Water Reducer (ASTM C494, type A or D):	965 mL (25 oz)
Superplasticizer (ASTM C494, type F or G):	5065 mL (131 oz)
Air Entrainment:	none
Water/Cementitious Material ratio:	0.33
Slump:	7 in.

*- Silica Fume slurry – 45% Silica fume solids, water and a small amount of superplasticizer

**- Gradation similar to that of ½ inch coarse aggregate

2.2 CREEP OF CONCRETE

Creep is defined by a deformation occurring under, and induced by, a constant sustained stress. Creep strains are considered proportional to the applied stress for stress values below 0.40*f'c (Carriera et.al. 2000). According to the Portland Cement Association, the amount of creep is dependant upon the magnitude of the applied stress, the age and strength of the concrete when the stress is applied, and the length of time the concrete is stressed. Other factors that affect the creep potential of concrete have to do with the quality of the concrete and the conditions of exposure. These factors include: type, amount and maximum size of aggregate; type of cementitious materials; amount of cement paste; volume to surface ratio of the concrete element; amount of steel reinforcement; curing conditions prior to the load application; and the ambient temperature and humidity (Design and Control of Concrete Mixtures, PCA, p269).

A paper by Dilger and Wang (2000) provided definitions of creep terminology. Basic creep is the creep without moisture exchange between the concrete and the ambient environment. Drying creep is the additional creep caused by drying, i.e. by the loss of moisture to the environment. Total creep of the concrete exposed to the environment is the sum of basic and drying creep. The quantities defined here can be seen graphically in Figure 2.1. The statement was made that high performance concrete (HPC) behaves differently than normal strength concrete and therefore, property characteristics are different with time. The current prediction models in codes and practice at the time this paper was written did not apply to HPC. New creep prediction model equations are provided in this paper for the use with high performance concrete.

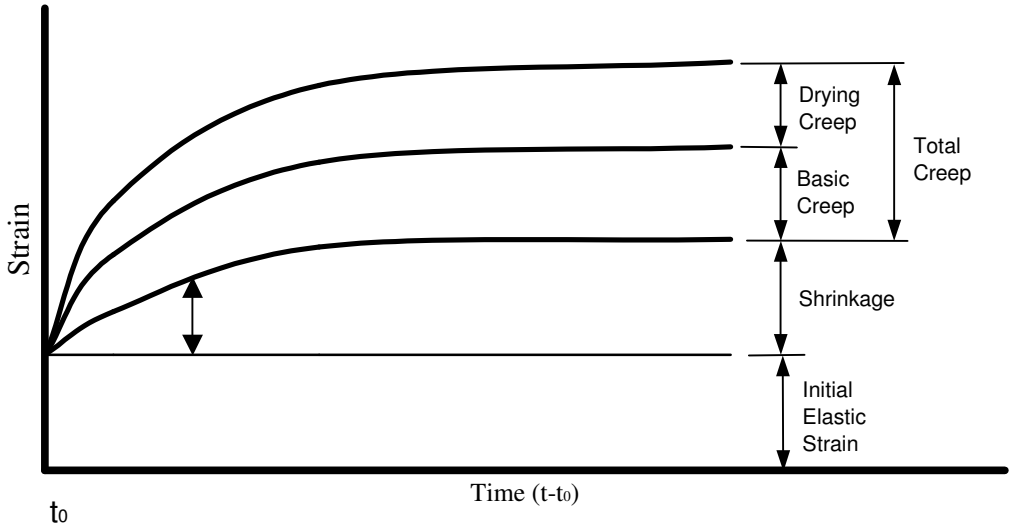

Figure 2.1 - Concrete Time Dependant Strains

In the book Creep of Plain and Structural Concrete, Neville, Dilger and Brooks (1983) asserted that the deformation characteristics of a material are a critical element in the knowledge of their behavior and an essential feature of their properties. The authors insisted that creep deformation could be substantial and must be taken into account in addition to initial elastic strain. This is demonstrated by sited test results showing creep strains after one year of load as high as 2 to 3 times that of the initial elastic strains. A fundamental generalization was made claiming hydrated cement paste is the seat of concrete creep. This statement has been verified by tests cited in this book researching creep of concrete with varying degrees of hydration.

Brooks and Neville (1975) studied concrete creep with the intent developing extrapolation equations to estimate long-term creep from short-term tests. They determined that creep and shrinkage at one year could be predicted from measured values at between seven and 28 days by means of linear and power equations. From their research, conclusions were made that creep tests of approximately 100 days can be used to very accurately predict the values at 1 year with an acceptable error coefficient. They surmised that 1-year deformation, measured in microstrain, could be predicted from experimentally determined 28-day values by the use of the following equations:

- basic creep: $c_{365}=6.0+1.59c_{28}$
- total creep: $c_{365}=18.4+1.70c_{28}$

and further extrapolated to:

$$c_t = \left(\frac{t}{57.4+t}\right)1.15c_{365} -> (Ross)$$

or

$$c_t = \left(\frac{t^{0.6}}{15.45+t^{0.6}}\right)1.45c_{365} -> (Meyers)$$

with an error coefficient of :

$$M = \frac{1}{c}\sqrt{\frac{(c_t - c)^2}{n}}$$

c=actual creep after 1 year

c_t=predicted creep after t days
n=number of tests

Brooks and Neville (1978) wrote a second paper with the intent of verifying or altering their previous prediction equations using a larger database of creep test results. The equations in this paper are based on 5-year creep data. The equations are provided to predict creep and shrinkage at any age up to 5 years from values determined experimentally at 28 days, within quoted accuracies. It should be noted that these equations are different from those previously published. The results are statistically based on a 95% confidence interval. The relationships are sensibly independent of mix properties, type of aggregate, size of specimen and age at testing. The expressions provided in this paper are as follows:

basic creep- $c_t=c_{28}*0.50t^{0.21}$; $M_{bc}=16\%$

total creep- $c_t=c_{28}[-6.19+2.15\ln(t-t_{28})]^{1/2.64}$; $M_{tc}=19\%$

shrinkage- $\varepsilon_{sh}(t,t_{sh,0}) = A'(\varepsilon_{sh28})^{a'}$; $M_{sh}=14\%$

where $A' = [1.53\log_e(t-t_{sh,0})-4.17]^2$

and $$a' = \frac{100}{2.90 + 29.2\log_e(t - t_{sh,0})}$$

Brooks and Neville noted that improved prediction accuracies can be obtained by increasing the duration of the short-term test, but testing costs increase with test continuance. The required accuracy for the particular application must be assessed so that appropriate creep test duration can be determined.

2.2.1 CREEP AFFECTED BY CONCRETE COMPOSITION

Zia (1993) made generalizations about concrete creep in *High Performance Concrete, A State of the Art Report*. These are similar to the generalizations that can be

made about shrinkage of concrete. Main points included were: when the water to cement ratio is increased, the creep potential of the concrete is increased; when the cement content is increased, the creep potential of the concrete is increased; with an increase in aggregate content and stiffness, creep is decreased due to the restraining action of the aggregate.

Collins (1989) studied high strength concrete mixes with compressive strengths between 8,700 and 9,300 psi were tested. Test results of the different mix designs showed that creep was less for concrete mixes with lower cement paste content and larger aggregate. The tests also showed that creep was not significantly affected by the inclusion of a high range water reducer into the mix design.

Carrette, Bilodeau, Chevrier, and Malhotra (1993) tested high performance concretes with high volumes of fly ash. Concrete mixes had excellent mechanical properties with relatively low levels of creep deformation.

Zia (1993) researched high strength concretes with different aggregate types including crushed granite, marine marl, and rounded gravel were evaluated for creep deformation. These high strength concretes, with compressive strengths exceeding 10,000 psi, showed creep strains ranging from 20% - 50% of that of ordinary concrete. The concrete consisting of marine marl aggregate had a much higher specific creep than that of either the crushed granite of the rounded gravel concretes.

The forth chapter of a book by Neville, Dilger, and Brooks (1983) discussed the influence of aggregate on creep. The authors' findings based on prior research was that it is acceptable to assume that the maximum size and grading of aggregate do not affect creep given that full compaction within the concrete has been achieved.

Brooks (1999) assessed the affects of admixtures and supplementary cementitious materials by a relative deformation approach. This was done by comparing the deformation of the admixture concrete with that of the control concrete having the same mix proportions by mass, with ultimate values for creep obtained by extrapolation.

Various chemical admixtures were tested and it was determined that no significant differences in creep strain occurred between types of plasticizers and superplasticizers. However, a general increase in creep of 20% was shown, as compared with the control concrete having the same mix proportions (σ=23%). The likely reason for this increase is thought to be the chemical admixture ability to entrain air, which in turn makes the hardened cement paste weaker. However, a point of note is that this increase of 20% is conflicting within the article and may be a decrease of 20%. This should be investigated further to determine the correct finding.

Blast furnace slag, fly ash, and silica fume, were used as supplementary cementitious materials in the test mixes in this paper as well. The inclusion of blast furnace slag (BFS) showed a decrease of average ultimate creep with an increase of replacement of cement with slag. Shrinkage of the concrete was unaffected by the increase in slag content. It was also shown that with BFS, lower creep values were associated with slower development of strength. Fly ash concrete was shown to have

reduced average ultimate creep values with an increase of the cement replacement percentage with fly ash. This trend was explained by looking at the concrete strength development: fly ash concrete continues to develop strength through a very long hydration process. As was the case with BFS, shrinkage was unaffected by the use of fly ash in the concrete mix. A small reduction in creep was shown for small quantities of cement replacement with silica fume. Creep increases with silica fume replacement of over 16% of ordinary Portland cement.

Brooks and Neville (1992) published findings for creep deformations determined first hand as well as findings published by other researchers. The results were summarized into effects of different admixtures and different supplementary cementitious materials separately. Water reducers showed a very wide range of effects on concrete creep. Results of various tests ranged from 34% to 166% of creep strain, as compared to a reference mix. However, water reducers created from different chemical bases showed differing results. Lignosulphonate admixtures lead to a higher basic creep than carboxylic acid admixtures. Carboxylic acid admixtures often result in a reduction in basic creep compared with plain concrete. No consistent trend for concrete creep can be observed when there is a change in cement paste content, in the type of aggregate, or in cement composition.

There have been no publications regarding retarding admixtures (ASTM C494-82 type B) and their effect on concrete creep. Calcium chloride used as an accelerator has been shown to increase creep in the range of 122% to 136%. Lignosulphonate / triethanolamine based accelerators increased basic creep in the range of 110% to 125%

and affected total creep (under drying conditions) in the range of 92% to 135%. A wide variation of relative deformations have been shown for superplasticizer inclusion in concrete mixes, however, an increase in concrete creep is the general trend.

Fly ash, blast furnace slag, and silica fume were the supplementary cementitious materials reviewed in this paper. Fly ash concrete has shown reduced creep values for up to 35% ordinary Portland cement replacement. Reduced creep values have been shown for blast furnace slag with replacement quantities of up to 75% of ordinary Portland cement. With 30% of ordinary Portland cement replaced by silica fume and various water cement ratios, approximately 50% more creep was observed under drying conditions after moist curing. Less basic creep was observed for the silica fume concrete if the concrete was autoclaved, but more basic creep occurred after moist curing.

Brooks (2000) reviewed different admixtures and supplementary cementitious materials for their effect on concrete creep. Lignosulphonate and carboxylic acid water reducers both result in greater mean deformations, however the results were not very different between the two admixtures or their respective control concretes. Sulfonated melamine formaldehyde condensates (SMFC), sulfonated naphthalene formaldehyde condensates (SNFC), and copolymers used as superplasticizers all showed a general increase in the mean creep deformation compared with plain concrete. However, the basic creep of concrete with the copolymer admixture was not significantly different from that of plain concrete. Ground granulated blast furnace slag (GGBFS) tended to decrease total creep as the slag levels increase in the concrete mix, but only for low water cement ratios. For higher water cement ratios, creep appears to increase. It has been determined

that fly ash inclusion into concrete mixes reduces basic creep. Silica fume used as a supplementary cementitious material increases basic creep as the silica fume content increases. However, total creep decreases for low levels of silica fume. Autoclaved concrete showed a large reduction in creep at high levels of silica fume addition, up to about 30%. Relationship equations were included in this article to estimate creep based on the replacement percentages of ordinary Portland cement with the supplementary cementitious materials.

Based on the results of this research, Table 2.1 was created and included in the article showing the general influence trends that the admixtures and supplementary materials have on concrete creep. The variable R in the table stands for replacement percentage

Table 2.1 - Trends in Concrete Creep

Ingredient	Creep at constant stress-strength ratio	
	Basic	Total
Plasticizers/ Superplasticizers	increase by 20%	increase by 20%
Blast Furnace Slag	decrease with increase of R	No Change
Fly Ash	decrease with increase of R	decrease for R>=10%
Silica Fume	increase with R>7.5% no change for R<7.5%	increase with R>15% decrease for R<15%

.

Khatri (1995) studied a concrete mix with water to cementitious material ratio of .35, and a constant binder content of 430 kg/m^3. Results of this study showed that silica fume at about 10% replacement marginally decreased the workability of the concrete but significantly improved the mechanical properties. These improvements included a

decrease in creep at all ages and refined pore size, which increases the concrete compressive strength. The strain due to creep was said to be caused by the removal of adsorbed water. When silica fume was added to high slag concrete, the creep was not affected. When a ternary mixture, or one with three cementitious materials, was created containing fly ash, general-purpose cement, and silica fume, strain due to creep was increased.

A study performed by Jianyong and Yan (2001) was a comparison of the creep of different materials used as concrete binders. The materials of interest included ordinary Portland cement (OPC), ultra fine ground granulated blast furnace slag (GGBS), and silica fume (SF). The creep tests were performed at a temperature of 20±3°C, with a testing duration of 180 days, and the test cylinders were loaded at 40% of their respective 28 day compressive strength. For comparison, drying shrinkage specimens were studied simultaneously in the same environmental conditions as the loaded creep specimens. The strains due to creep and shrinkage were measured using a mechanical comparator. In this study, replacing OPC with 30% (by weight) GGBS and 10% (by weight) SF delivered the best results for creep strain. The proportions of material for this mix was 360 kg/m^3 OPC, 180 kg/m^3 GGBS, 60 kg/m^3 SF, and 156 kg/m^3 of water, producing a water to cementitious material ratio of 0.26.

The mineral and chemical admixtures examined in the study by Memon, Radin, Zain and Trothier (2002) included fly ash, ground granulated blast furnace slag, silica fume, and superplasticizers. Blended mixtures, or a combination of the mineral and

chemical admixtures, performed better in strength and showed a general result of lower permeability. This result was achieved by greater pore refinement due to the better distribution of particle sizes in the blended mixes.

Ramachandran (1995) discussed concrete creep in the Concrete Admixtures Handbook for various reasons having to do with the causes and effects that mix design and proportioning have on the creep potential of the concrete. Summaries of the author's conclusions based on previous studies are divided into admixture categories below.

- Accelerators

Based on previous tests, calcium chloride and triethanolamine admixtures increase the creep of concrete. With 1.5% $CaCl_2$ addition, the percentage increase in creep of the concrete cylinders loaded at 7 and 28 days was 36% and 22 % respectively. Creep was increased by triethanolamine only at early age loading (7 days) when lignosulfonate was added to the concrete as well. Calcium formate addition tends to increase shrinkage.

- Water reducers / Retarders

Listed in this section of the book were several of the basic causes of concrete creep. Factors listed were type of cement, mix composition, type of cement, age at loading, degree of hydration at loading, incremental hydration under loading, moisture loss from concrete under sustained load, and movement of moisture in the cement gel under conditions of hygral equilibrium between the ambient medium and the concrete. Studies have shown that lignosulfonate admixtures increase the rate and total creep for concrete with type I cement but there is no significant effect with type V cement. The

rates and formation changes of the hydration process caused by water reducers and retarders altars the creep potential of a concrete when loaded at different times or ages with a sustained load. Hydroxycarboxylic acid based water reducers/retarders tend to increase long term creep except for lightweight concrete, however the initial creep rate is low. The claims were made that in general, water reducers have either no effect or they increase the creep of concrete and retarders increase the creep of concrete.

- Superplasticizers

The author of this section observed that superplasticizers generally decrease shrinkage of concrete, though exceptions do occur. The general consensus is that the addition of superplasticizers into a mix results in approximately the same creep as the reference mix. In on instance, an identical mix design was altered three times by adding one different chemical superplasticizer at a time. The superplasticizer based on melamine added into the mix decreased creep, one based on napthalene showed approximately the same creep as the reference and one based on Lignosulphonate increased the creep of the concrete mix.

- Air Entrainment

The use of air entrainment is not permitted in the LVM concrete mix and is not an important factor for the creep of concrete.

- Polymer modified Concrete

In general the use of polymers to modify a concrete mix design leads to large creep deformations. Catastrophic failures of the concrete occur at 50°C

- Mineral Admixtures

The mineral admixtures of interest in this book are fly ash and silica fume, and are used as supplementary cementitious materials. A study showed that fly ash type F with replacement values of up to 15% of the ordinary Portland cement, the creep remains the same. When more than 15% of the OPC by weight is replaced by fly ash type F, the creep is slightly higher. High strength concretes containing silica fume were shown to have significantly less creep than normal strength concretes due to the fact that SF accelerates the strength development of the concrete. The general trend of concrete is that as compressive strength of the concrete increases, the creep potential of the concrete decreases.

2.2.2 CREEP RELATED TO COMPRESSIVE STRENGTH AND SHRINKAGE

Zia (1993) reported a trend in concrete creep that for higher strength concrete, creep potential is lower. Another important trend is that creep deformations are similar for silica fume concrete, fly ash concrete, and ordinary Portland cement concrete with similar compressive strengths.

A study by Paulson, Nilson and Hover (1991) dealt with the long-term deflection of high strength concrete beams. The study showed that the creep coefficient for high strength concrete under steady and continuous axial compression was considerably less than the creep coefficient of ordinary strength concrete.

The research done by Yamamoto (1990) demonstrated that creep deformation of high strength concrete columns was much less than that of normal strength concrete.

Burg and Ost (1994) studied the engineering properties of five high strength concrete mixes. The concrete had components of no mineral admixtures, silica fume only, or both fly ash and silica fume in addition to the ordinary Portland cement. The creep strain was measured under about 39% of f'_c (at 28 days) for a test duration of 430 days, and then unloaded so that creep recovery was measured. Specific creep was determined to be the lowest for the concretes with the highest compressive strengths. This was attributed to the paste composition and internal structure of the concrete. Specifically, proportions of the mix (per cubic yard) with the lowest creep values were 800 lbs of cement type I, 125 lbs of silica fume, 175 lbs of fly ash, 425 fl oz. of high range water reducer, 39 fl oz of retarder type D, a water to cement ratio of 0.318 and a water to cementitious material ratio of 0.231. The value of the specific creep for this mix was .24 millions of an inch/psi.

Neville, Dilger and Brooks (1983) reviewed research of the influence of stress strength ratios and concrete age effects on creep. The authors placed the linear relationship between concrete creep and applied stress from a ratio of about 0 to between 0.30 and 0.75. Above that limit of linearity, creep increases with stress at an increasing rate. Also determined was that for a given stress strength ratio, creep is the same regardless of how strength or stress have been altered, as long as their ratio is the same.

When humidity is a variable in research, it can be said that the relation between creep and stress to strength ratio seems to be approximately the same for different relative humidity values, provided considerable shrinkage does not occur. For this to occur, the

concrete must reach hygral equilibrium with the medium prior to the application of the load.

Regarding age at application of load, loading older concrete would definitely tend to decrease creep due to the more mature hydration. After about 28 days, however, differences are minor since strength gain is very slow at this point and the concrete hydration is more mature. The creep at this point is only really dependant on the stress to strength ratio. A section on maturity of concrete was included and the term reflects the degree of hydration and therefore the amount of cement gel in the concrete matrix. It has been shown that strength and maturity are not linearly related, and it is the maturity of the hydration, not the strength of the concrete, that is the fundamental factor of creep.

Persson (2001) performed an experimental and numerical study on the similarities and differences in mechanical properties of self-compacting concrete (SCC) and normal compacting concrete (NCC). Properties of interest included strength, elastic modulus, creep and shrinkage. Eight mix designs were tested with water-cementitious material ratios ranging from .24 to .80. Four mixes were self-compacting and each of these mixes had a corresponding normal compacting concrete of similar water-cementitious material ratio. To increase the viscosity of normal compacting concrete, fillers such as fly ash and silica were used, in addition to superplasticizer introduction into the mixes. Spring loading frames were used to perform the creep tests, and parallel specimens were used to study shrinkage. For creep analysis, four different stress levels were studied including 0.20, 0.40, 0.55, and 0.70. Several conclusions reached as a result of this on going study. First, the creep, shrinkage and elastic modulus of the two types of concrete corresponded

well when the strength was held constant. When the strength loading for the creep tests was held constant, the creep coefficient of mature concrete was similar between the two types of concrete. The creep coefficient of concrete increased greatly, when the concrete was loaded at a young age, though this increase was similar for both types of concrete. When the compressive strength of the concrete was high, the creep coefficient was greatly reduced, which is similar to many results from previous literature. A graphical display of these findings is shown here in Figure 2.2.

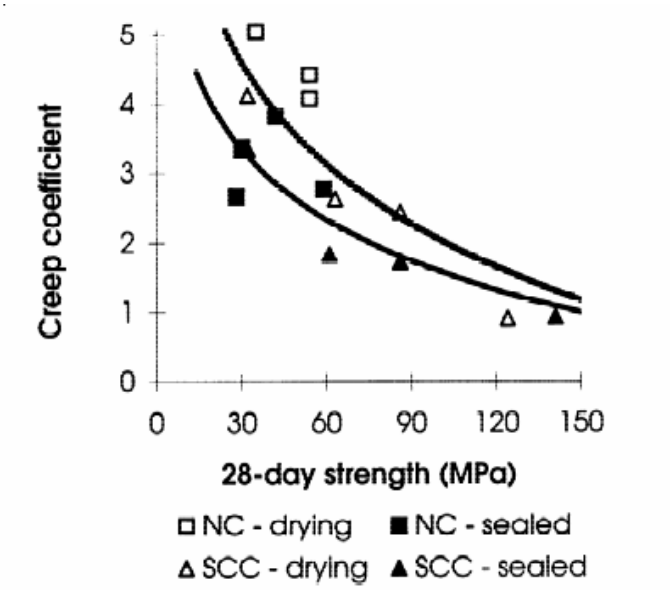

Figure 2.2 - Compressive Strength vs Creep Coefficient (Persson)

Zia (1993) surmised that concrete resistant to shrinkage also has low creep potential.

2.3 OTHER CONCRETE MATERIALS AND ADMIXTURES

Metakaolin is a highly effective pozzolanic material that can be used as a supplementary cementitious material. Brooks and Johari (2001) found that total creep, basic creep, as well as drying creep were significantly reduced particularly at higher metakaolin replacement levels. This effect can be attributed to a denser pore structure, stronger paste matrix, and improved paste aggregate interface of the metakaolin concrete mixtures. This is a result of the formation of additional hydrate phases from secondary pozzolanic reaction of metakaolin and its filler effect. The research showed the 200-day drying creep was reduced for metakaolin concrete at high levels of replacement (15% ordinary Portland cement replacement). Shrinkage tests showed an increase in total autogenous shrinkage at the 5% replacement level, but at the higher 10 to 15% levels of replacement, total autogenous shrinkage was decreased.

Calderone, Gruber and Burg (1994) discussed some general properties of high reactivity metakaolin (HRM) and its effect on freshly mixed and hardened concrete. HRM is not an industrial byproduct, as are many other supplementary cementitious materials. HRM is specifically manufactured for its particular uses, is nearly 100% reactive, and conforms to ASTM C618, class N pozzolan specifications. This study compares the relative performance of five mixtures produced with HRM and silica fume at various contents including two mixes with HRM, 5% and 10% replacement, two mixes with silica fume, 5% and 10% replacement, and one control mix with neither HRM nor silica fume. The required additions for high range water reducer (HRWR) are 25% to

35% less for mixes containing HRM than for the mixes containing SF to obtain similar slumps. The HRM mixes were also less sticky and provided similar set times to that of SF concrete. The HRM concretes had higher compressive strengths, lower chloride ion penetration, and similar drying shrinkage to the SF concrete with values for 28-day shrinkage of 280 microstrain for the metakaolin concrete and 260 microstrain for the silica fume concrete. The values for shrinkage for the two mixes were equal after 156 days of drying. HRM used in powder form was in some cases better than the SF in slurry form.

The conclusions of a study by Ding and Li (2002) were that metakaolin is comparable to silica fume as a supplementary cementitious material, but is lower in price. Metakaolin is produced by a well-controlled manufacturing process, and is typically incorporated into concrete to replace 5-20% by weight of cement. Ding and Li systematically studied and compared the effects of metakaolin as a cementitious replacement to those effects of silica fume. Seven mix designs were created using 0, 5, 10, and 15% ordinary cement replacement by metakaolin or silica fume. All of the mixes had a water to binder ratio of 0.35, a sand to aggregate ratio of 0.40, 1.0% (by weight of cement) addition of napthalene sulfonate-based superplasticizer, and 0.25% addition of a set retarder.

All of the metakaolin concrete mixes had much higher slump values than that of the silica fume concrete mixes, and they showed higher slump values than the control mix at the 5 and 10% levels. The compressive strength test results indicated that the introduction of metakaolin into concrete produces much higher strength than the control

at all levels, and very similar results to that of the silica fume concrete at the same replacement levels.

Metakaolin concrete shows a faster initial rate of shrinkage than the control and the silica fume concrete, but the rate levels off within days and leads to lower values over time. The results showed lower values for shrinkage for greater levels of replacement of cement with metakaolin, and the same was true for silica fume. The lowest shrinkage values observed were from the mix with 15% metakaolin replacement.

The tests for chloride diffusivity showed that metakaolin is less effective than silica fume at all similar replacement levels, but is still better than the control mix. After 90 days of observation, the 15% replacement levels of metakaolin and silica fume had equivalent values for chloride diffusivity.

The purpose of a study by Sicker and Huhn (1997) was to characterize the influence of silica fume and high reactivity metakaolin and of superplasticizers on the rheological properties of mortars by means of fluidity measurements. New generation superplasticizers such as polycarboxilic ether based superplasticizers were compared with the commonly used, older types. The effect of superplasticizers in fresh concrete is a mix with significantly lower flow resistance, while the viscosity remains almost unchanged. Thus, the risk of segregation is no greater, as it would be with the addition of water. The rheological properties of mortars are extremely dependant on the type of superplasticizer and pozzolans in the mix design. The results of this study indicated that concrete made with metakaolin and the polycarboxilic ether based superplasticizers had the longest effective period for good rheological performance.

A study by Feng, Chan, He, and Tsang (1997) showed that when 10% of ordinary Portland cement was replaced by an equal weight of shale ash, the compressive strength of the concrete increased 5 to 10%. Oil shale ash is an industrial waste product that can be utilized as a pozzolana and can also be used as a carrier for superplasticizer to form a carrier-fluidifying agent (CFA). When the shale ash was used as a carrier for the superplasticizer, the resulting CFA could control slump loss. One such test showed that when a 1.5% dosage of CFA was used, the slump was maintained for 90 minutes.

Xu and Chung (2000) performed research to show the effects of silica fume as a supplementary cementitious material in concrete. The research was also to show the increased benefits of using silane in conjunction with the silica fume. Silica fume was shown in this paper, and has been shown in applications previously, to have significant effects on the properties of the resulting concrete mixes. It has also been shown to degrade the workability of the concrete.

Silane is a concrete additive that can be introduced in two ways: first in the form of a coating on the silica fume particles, and second in the form of an admixture. Both of the methods of silane uses were shown to enhance the workability and increase the strength of the concrete. The method of coating the silica fume with silane was shown to be the better method in terms of mechanical properties; however, this method is more difficult to perform in the mixing process. There was no data recorded for creep effects but the results for shrinkage in the concrete containing silane and silica fume showed an improvement over the concrete mixes with no silane.

CHAPTER 3: EXPERIMENTAL METHODS

3.1 MATERIALS AND MIX DESIGNS

Concrete used in floating bridges must be designed with compressive strength, durability, and long-term properties as the critical factors for successful performance. The LVM mix design, of which the origin was previously described in detail, has these characteristics and was used as the reference mix for use in the development of new mix designs. The LVM concrete is Mix Design number 1 and Mix Design number 5 in this research. The concrete constituent quantities are shown in Table 3.1 and Table 3.5.

During the construction of the Lacey V. Murrow floating bridge, Wiss, Janney, Elstner Associates (WJE), Inc analyzed the suitability of the mix design. Within their published report (1993), they discussed mix design development, suitability testing criteria, and the conclusions based on their findings. This report included several recommendations for future construction of watertight structures. It was stated that mix alterations could be made such that the silica fume content be reduced to the 4 to 5 percent level and fly ash content be increased to 200 or more pounds per cubic yard. They anticipated that this change could be made without impairing the permeability of the concrete and would still maintain the other desirable qualities of the LVM mix. WJE, Inc recommended that further tests be done to verify this conclusion. This LVM alteration is labeled WJE, Inc mix design and is mix number 2 in this study. The quantities can be found in Table3.2.

Based on the findings of the literature review, concrete products were found that were not used in practice when the LVM mix was first developed. New mix designs

were formulated for the purposes of this research based on previous successes of the relatively new products. Metakaolin is a product that is currently being developed and is used as a supplementary cementitious material much like silica fume. The report findings listed in the literature review proved metakaolin to be a viable material for use in concrete floating bridges. It was also recommended that additional research on this product would be valuable. Two mixes, one with 5 percent ordinary Portland Cement (OPC) replacement and one with 10 percent OPC replacement were designed. These replacement values were selected so that nearly direct comparisons could be made to the WJE, Inc mix, which was designed with 5 percent OPC replacement with silica fume, and the LVM mix, which was designed with about 8 percent OPC replacement with silica fume. The mix designs incorporating metakaolin are numbers 3 and 4 and can be seen in Table 3.3 and Table 3.4, respectively.

A concrete waterproofing admixture that has been of interest to many developers is Everdure Caltite. Traditional means of creating a waterproof concrete structure has been the use of external membranes or surface treatments. As was mentioned previously, silica fume and metakaolin are also effective in reducing the permeability of concrete, but in a different way. Caltite was incorporated into two of the mix designs tested in this study. The first mix utilized the LVM mix design quantities, with some of the mix water replaced with equal parts of the Everdure Caltite. The replacement quantity was consistent with the recommended Caltite to concrete ratio or 6 gallons of Caltite for every cubic yards of concrete. This mix design can be seen in Table 3.6. The second Caltite mix design, and the final mix incorporated into this study, was studied for its properties, as the other mixes were, but was intended to be a cost saving mix. The mix design would

be the same as the LVM, though it would not contain silica fume. The concrete quantities for this mix can are shown in Table 3.7. The cementitious material quantity is slightly less than the LVM parent mix. It was anticipated that this mix design would produce concrete strength in excess of the required 6500 psi. Workability properties would be similar to the LVM and the level of chloride ion penetration would be acceptable as well due to the presence of Caltite. The Caltite quantity was as before, 6 gallons per cubic yard of concrete.

This research necessitated the casting of nine concrete test cylinders for each mix design to be studied. Seven of the cylinders were standard 6 by 12 inch specimens, and two of the cylinders were standard 4 by 8 inch specimens. Three of the seven 6 by 12 inch cylinders were needed to obtain an average ultimate compressive strength value for each mix design. The remaining four cylinders were used for the creep tests: two cylinders for the total strain measurements and two companion cylinders for the shrinkage measurements. The two 4 by 8 inch specimens were required for the chloride ion penetration tests. All the cylinders were cast in vertical, one-time-use plastic molds.

The course and fine aggregate used in the concrete of the LVM floating bridge had the gradations listed in Table 3.7. Coarse and fine aggregates used in this research were from Glacier Northwest in Dupont, Washington. This is the anticipated stockpile that will be used for the actual concrete used in the floating bridge construction and had gradations very similar to that of the original LVM mix. The quantities were entered into an aggregate spreadsheet to determine the effectiveness of the gradations and the results were plotted on a gradation power chart to graphically display the results. The spreadsheet format can be seen in Table 3.8.

The ordinary Portland cement used in the original LVM mix design and required was OPC Type II. According to the Portland Cement Association, type II Portland cement generates less heat at a slower rate and has a moderate resistance to sulfate attack. A lower heat of hydration is beneficial in large structures to avoid shrinkage cracking. Resistance to sulfate attack in a harsh environment is critical for the durability of hardened concrete.

As a result of conclusions reached from the literature review, a relatively new superplasticizer was selected for use in this research. Polycarboxylic-ether based superplasticizers produce concrete with more desirable concrete workability characteristics than the older lignosulfonate, naphthalene, or melamine based superplasticizers. The superplasticizer used in all mixes tested was Glenium 3000. Based on the effectiveness of this product, it was determined that no normal range water reducer would be necessary in LVM mix or any of the new mix designs.

Table 3.1 – Mix #1 LVM Mix Design, Reference Mix Design

Concrete Constituent	mix proportions lbs / 1 yd^3
Course Aggregate	1770
Fine Aggregate	1295
Portland Cement Type II	624
Silica Fume (AASHTO M307)	50
Fly Ash (AASHTO M295)	100
Water (Total)	255
Water Reducer (ASTM C494)	none
Superplasticizer (ASTM C494)	5.5 floz/cwt
w/c ratio=	0.329
slump =	8.0"

Table 3.2 – Mix #2 1st Alteration - WJE, Inc. Report Recommendation

Concrete Constituent	mix proportions per 1 yd^3
Course Aggregate	1770 lb
Fine Aggregate	1295
Portland Cement Type II	540
Silica Fume (AASHTO M307)	35
Fly Ash (AASHTO M295)	200
Water (Total)	255
Water Reducer (ASTM C494)	none
Superplasticizer (ASTM C494)	4.3floz/cwt
Caltite	none
w/c ratio=	0.329
slump =	7.5"

Table 3.3 – Mix # 3 - 2nd Alteration - Metakaolin - 5% OPC Replacement

Concrete Constituent	mix proportions per 1 yd^3
Course Aggregate	1770 lb
Fine Aggregate	1295
Portland Cement Type II	636.3
Silica Fume (AASHTO M307)	none
Fly Ash (AASHTO M295)	100
Metakaolin	38.75
Water (Total)	255
Water Reducer (ASTM C494)	none
Superplasticizer (ASTM C494)	5.5floz/cwt
Caltite	none
w/c ratio=	0.329
slump =	9.0"

Table 3.4 – Mix # 4 - 3rd Alteration - Metakaolin - 10% OPC Replacement

Concrete Constituent	mix proportions per 1 yd^3
Course Aggregate	1770 lb
Fine Aggregate	1295
Portland Cement Type II	597.5
Silica Fume (AASHTO M307)	none
Fly Ash (AASHTO M295)	100
Metakaolin	77.5
Water (Total)	255
Water Reducer (ASTM C494)	none
Superplasticizer (ASTM C494)	7.0floz/cwt
Caltite	none
w/c ratio=	0.329
slump =	8.5"

Table 3.5 – Mix # 5 - LVM Mix Design #2 - Reference Mix Design

Concrete Constituent	mix proportions per 1 yd^3
Course Aggregate	1770 lb
Fine Aggregate	1295
Portland Cement Type II	624
Silica Fume (AASHTO M307)	50
Fly Ash (AASHTO M295)	100
Water (Total)	258.66
Water Reducer (ASTM C494)	none
Superplasticizer (ASTM C494)	5.5floz/cwt
Caltite	none
w/c ratio=	0.334
slump =	8.5"

Table 3.6 – Mix # 6 - 4th Alteration - LVM Mix with Caltite Admixture

Concrete Constituent	mix proportions per 1 yd^3
Course Aggregate	1770 lb
Fine Aggregate	1295
Portland Cement Type II	624
Silica Fume (AASHTO M307)	50
Fly Ash (AASHTO M295)	100
Water (Total)	222.12
Water Reducer (ASTM C494)	none
Superplasticizer (ASTM C494)	5.5floz/cwt
Caltite	6 gallons
w/c ratio=	0.351
slump =	8.5"

Table 3.7 – Mix # 7 - 5th Alteration - Caltite Mix Design

Concrete Constituent	mix proportions per 1 yd^3
Course Aggregate	1770 lb
Fine Aggregate	1295
Portland Cement Type II	624
Silica Fume (AASHTO M307)	none
Fly Ash (AASHTO M295)	100
Water (Total)	154.64
Water Reducer (ASTM C494)	none
Superplasticizer (ASTM C494)	6.3floz/cwt
Caltite	6 gallons
w/c ratio=	0.282
slump =	9.0"

Table 3.8 - Aggregate Gradations

Course Aggregate		
Sieve Size	Percent Passing	Weight Passing (lbs)
5/8	100%	1770
1/2	97.40%	1724
3/8	82.80%	1466
1/4	32.00%	566
#4	5.30%	94
#6	1.00%	18
Total Weight		1770.0
Fine Aggregate		
Sieve Size	Percent Passing	Weight Passing (lbs)
#4	97.60%	1264
#8	76.10%	985
#16	55.30%	716
#30	35.60%	461
#50	13.30%	172
#100	2.70%	35
#200	0.70%	9
Total Weight		1295.0

Table 3.9 - Total Aggregate Blend Gradation

		BLEND REQUIRED - %							
		1-1/2" X 3/4"	3/4" X #4	1/2" X #4	3/8" X #4	Bldg-sand	Pavg-sand		
		0	0	58	0	42	0	100	
		ACCUMULATED PERCENT PASSING						BLENDED	
SIEVE SIZE		1-1/2" X 3/4"	3/4" X #4	1/2" X #4	3/8" X #4	Bldg-sand	Pavg-sand	AGG'S	
(us)	**(mm)**								
1-1/2"	37.500	100.00	100.00	100.00	100.00	100.00	100.00	100.00	%
1.0"	25.000	100.00	100.00	100.00	100.00	100.00	100.00	100.00	%
3/4"	19.000	100.00	92.10	100.00	100.00	100.00	100.00	100.00	%
1/2"	12.500	100.00	47.20	97.40	100.00	100.00	100.00	98.49	%
3/8"	9.500	100.00	23.50	82.80	89.80	100.00	100.00	90.02	%
#4	4.750	100.00	3.00	5.30	12.90	100.00	99.60	45.07	%
#8	2.360	100.00	0.00	1.00	1.60	91.30	75.00	38.93	%
#16	1.180	100.00	0.00	0.00	0.00	64.50	49.00	27.09	%
#30	0.600	100.00	0.00	0.00	0.00	38.20	31.00	16.04	%
#50	0.300	100.00	0.00	0.00	0.00	18.50	13.00	7.77	%
#100	0.150	100.00	0.00	0.00	0.00	7.70	4.00	3.23	%
#200	0.075	0.00	0.80	0.00	0.30	2.30	1.00	0.97	%
	(FM)	0.00	7.34	6.14	5.96	2.80	3.28	4.73	

To achieve the standard for end conditions of compressive strength and creep test cylinders, specimen end grinding, sawing, or capping must be performed. A high-strength gypsum mortar called Hydrostone was used as an end-capping compound. This material was obtained from Special Effects Supply Corporation, Salt Lake City, Utah. A mortar of high compressive strength was needed and although tests were not performed in this research, USG specifications listed the compressive strength at 10,000 psi for a 0.32 water to gypsum ratio (www.freemansupply.com). An ideal water/gypsum ratio was determined to be 0.25 for the purposes capping concrete cylinders. Large sheets of glass were used as a level surface to ensure the end-smoothness requirement standard. An

estimated set time of 17 to 20 minutes was beneficial when many cylinders had to be capped in a minimal amount of time. A picture a hardened gypsum end cap can be seen in Figure3.1.

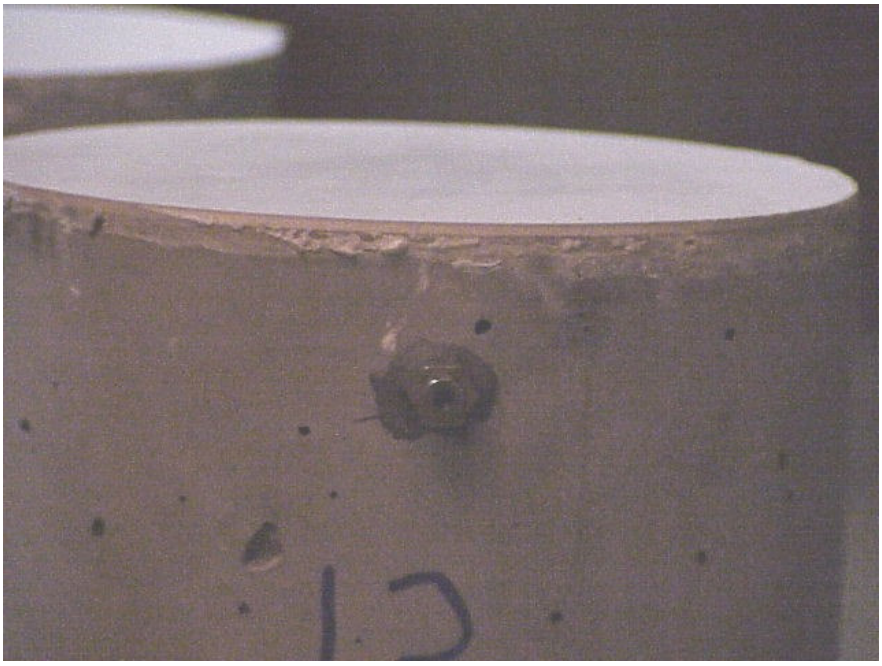

Figure 3.1 - Gypsum Cylinder End Cap

3.2 CREEP

Concrete used in floating bridges must be analyzed for its creep potential and there is need for important experimental investigations into appropriate mix designs for use in these types of bridges. For this research, creep frames had to first be designed and fabricated. A basic creep frame schematic pictured in Annual Book of ASTM Standards was used as a basis for the design. Other frame designs and configurations were considered, but this one was selected due to its simplicity and its efficiency. ASTM C512 provides a written description of the basic creep frame design. The standard

requires that the frame be capable of applying and maintaining the desired load on the specimen, despite any changes in the axial length of the specimen. The frame design is shown in Figure 3.2 and Figure 3.3.

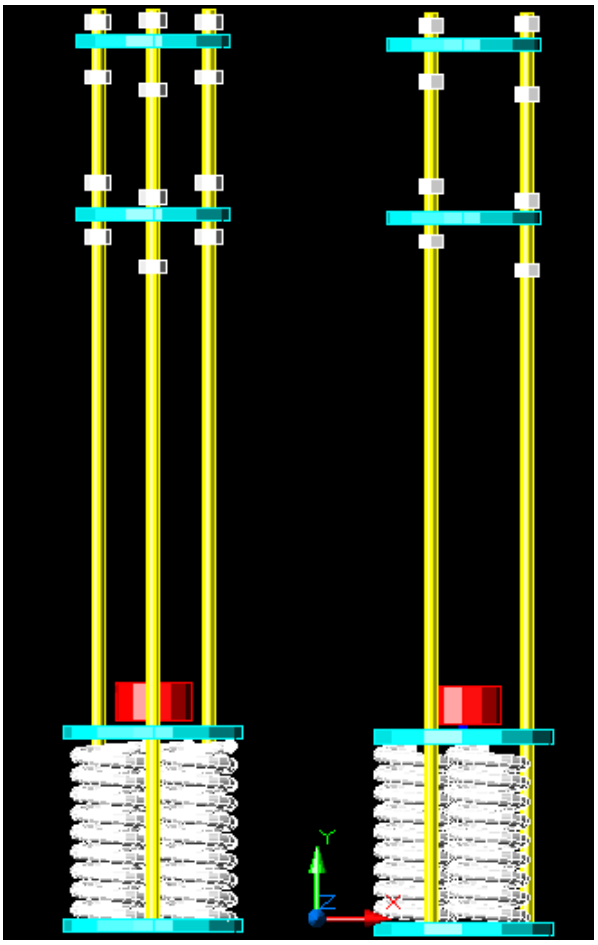

Figure 3.2 - CAD Drawing of Creep Frames

Figure 3.3 – Creep Frame

Creep frames must be designed with the strength of the concrete to be tested as the main parameter and all of the components in the frame including the compression springs, steel bar diameter and strength, and the plate sizes and strength are sized accordingly. Concrete mix designs used in recent floating bridge construction has had ultimate compressive strength values of up to 12,500 psi. An upper limit of 14,000 psi was selected for the concrete compressive and as the capacity of the creep frames. The ASTM standard calls for not more than 40% of the maximum compressive strength to be applied to the concrete cylinders in the creep test. Thus taking 40% of 14,000 psi, a value

for the maximum stress that the frame would have to restrain is determined. The stress value is converted to a force in pounds by multiplying its value by the end surface area of the six-inch diameter concrete cylinder. This value of approximately 160,000 pounds can be divided equally among the three rods. The tensile force in each rod is the force that will be applied to each compression spring

As stated previously, the springs were designed with a strength capacity of 53,000 pounds. For the purpose of the creep test, the springs also had to be designed with a very high stiffness so that the force would not change considerably due to a minute change in length. A suitable spring was designed using a high strength steel wire with a diameter of 2.125 in., an outside spring diameter of 9 5/8 in., 12 in. free height, 9 5/16 in. solid height, spring rate of 22,480 pounds per inch, and total compressed capacity of 60,000 pounds. See Figure 3.4 for a picture of the compression springs.

Figure 3.4 - Creep Frame Compression Springs

With the springs designed, the diameter of the steel base plate was sized by circumscribing three springs in a triangular pattern and this diameter value was minimized to reduce plate mass and cost. The three threaded, B7 steel reaction rods, diameter 1.125 inches, were then positioned in a triangular pattern similar to the springs and moved as close to the center of the plate as the springs and the concrete specimens would allow. This placement was important to reduce plate deformation, which could cause unwanted stress concentrations in the concrete. The upper jack plates were sized according to the bar placements and were minimized to reduce the weight and cost. The thickness of all of the plates was chosen to be 1.25 inches so that excessive deformation or yielding would not occur. See Figure 3.5 for plate dimensions. The localized stresses at the points of threaded rod insertion in the base plate were of particular interest so that pull out would not occur when the rods were tensioned.

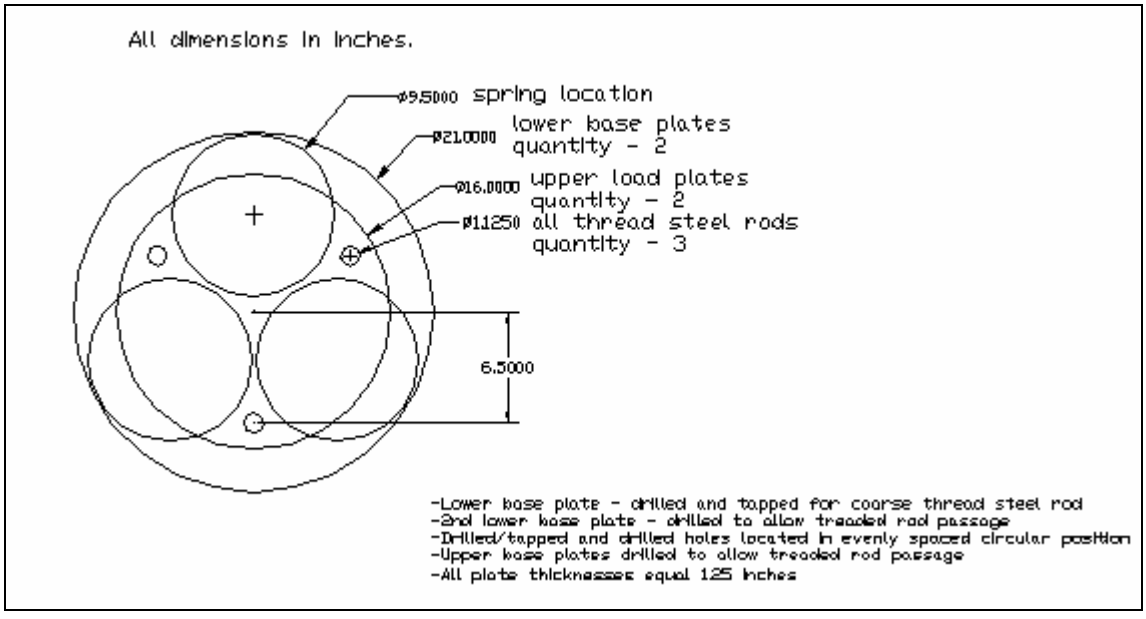

Figure 3.5 - Plate Dimensions

To ensure that stress concentrations in the concrete due to slight deviations from the vertical in load application, a ball and socket joint was fabricated to allow for specimen rotation. This joint consisted of a high strength steel ball bearing with a diameter of .625 inches and a steel plate 2 inches thick with a diameter of 6 inches in order to match the diameter of the specimens. Another plate of equal size, with no socket, was made and placed on top of the specimens to eliminate stress concentrations due to the bending of the lower jack plate. In order to ensure an even stress distribution transfer from the load plates to the concrete specimens the flat surfaces of the end platens were machined to within the smoothness tolerance listed in ASTM C39 of less than 0.002 inch deviations from plane.

With the design of the creep frame completed, focus was shifted to load application and load measurement. A 60-ton load jack was sufficient to produce a load corresponding to the design concrete compressive strength. A hand pump and load jack system was acquired for the purposes of this test. The hand pump was equipped with a calibrated dial gage which one could read the applied load to within certain accuracy. The pump and jack system was calibrated using the Satec Model 400 QC Prism-1007 hydraulic compression machine located in the concrete lab in Albrook Hall. This manner of load measurement using the dial gage was determined to be a good measure of applied load. To provide an approximate check of applied load and load loss due to concrete creep, a strain gage was attached to one of the steel reaction rods in each frame. The strain gage was connected to a portable strain meter displaying strains in the steel rod, from which stresses could then be calculated using approximated rod areas and material

properties. The tensile stress in the rods was then transferred directly to the axial compressive stress in the concrete cylinders. Young's Modulus for the steel rods was assumed to be $29(10)^3$ ksi and was approximately verified using the dial gage on the load jack. The strain gage placement and orientations can be seen in Figure 3.6.

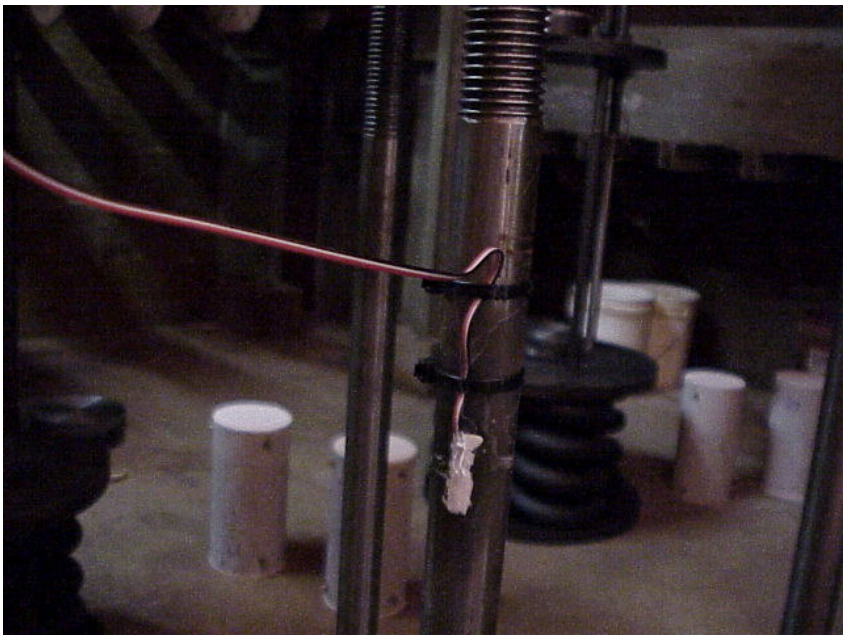

Figure 3.6 - Reference Strain Gage

ASTM C512 calls for concrete cylinders with a diameter of 6 inches and a height of 12 inches. There are different ways in which strains in the cylinders can be measured, but only 2 methods are typically practiced. The first method involves an internal strain gage that is cast within the concrete specimen at the time of batching. A horizontal concrete mold is used and the gage is positioned in a perfectly longitudinal manner within the center of the mold. Concrete is then placed and consolidated around the gage. This method can be accurate, but it is very difficult to position the strain gage and horizontal

molds are less common and more expensive than the typical vertical concrete cylinder mold.

The second method used for measuring creep and shrinkage strains is the installment of external gage points on longitudinal planes on the surface of the cylinder and measuring and recording strains by hand. This method is the one selected to determine the creep strain in this research. Three planes spaced 120 degrees apart around the circumference of the cylinder were used so that an average strain could be calculated for each specimen. A standard gage length of 10 inches is marked on each plane, and 3/8 inch diameter, ½ inch deep holes were drilled using a mill press and a masonry bit. The drilling process can be seen in Figure 3.7. Brass gage points were glued into these holes using a strong, waterproof adhesive called JB Weld. With a known initial gage length, any decrease in length of the cylinders could be measured using a hand-held mechanical extensometer / compressometer.

Figure 3.7 - Drilling of holes for gage points

The mechanical comparator must be accurate to the nearest ten-thousandths of an inch, which is necessary for the small results expected. A multi position strain gauge was acquired from ELE International to measure the strain deformations in the creep specimens. This is a handheld device designed for measuring relative displacement between the set gage lengths. Due to the length of most creep tests, the device selected for measuring strain must be durable and stable enough to maintain accurate readings throughout the length of the tests. The type of strain gage used in this research is considered stable because it can be calibrated using a constant length standard bar before every measurement. The gage length of 10 inches mentioned previously was recommended by Carreira and Burg (Creep and Shrinkage – Structural Design Effects) and was used in this research. This gage length is the longest span that can be used without me echanical comparator

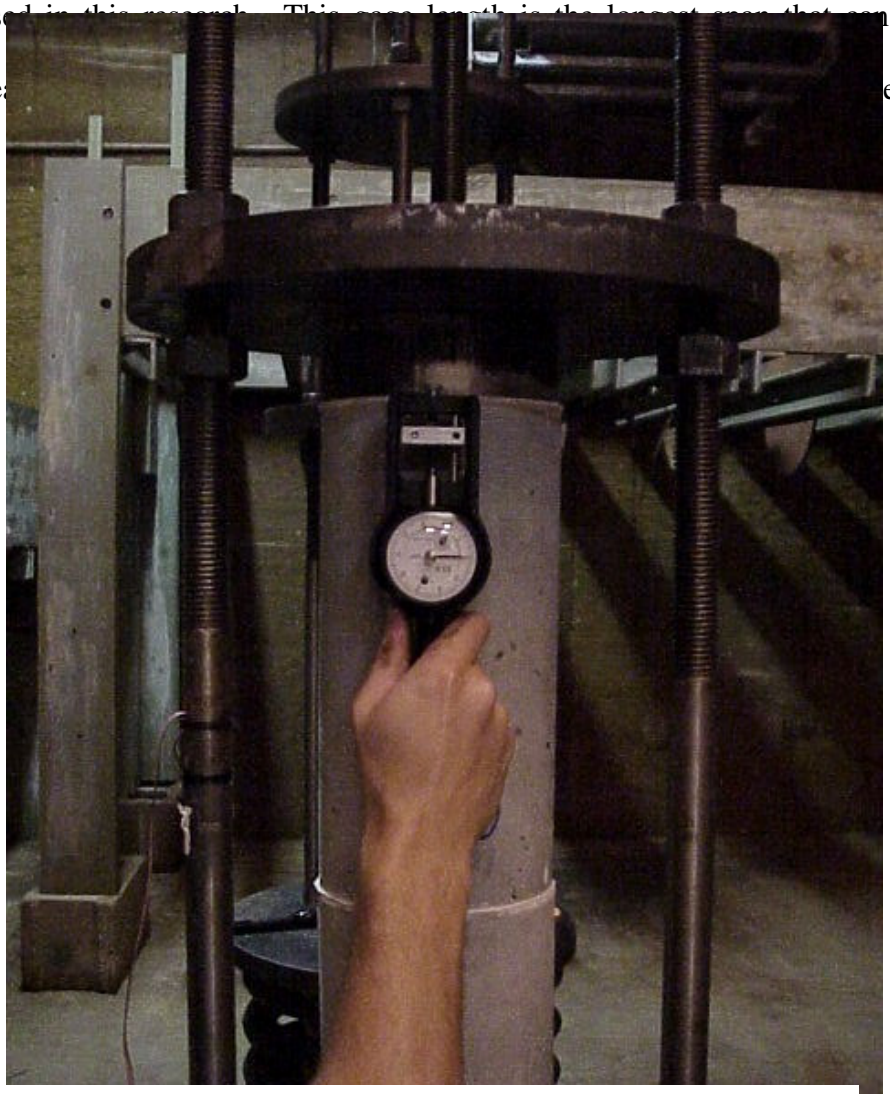

Figure 3.8 - Creep strain measurement

ASTM C512 was used as the basis for the creep test standards. However, some complications leading up to the testing portion of the experiment lead to some deviations from the standard. Concrete curing lasted longer than the recommended standard time of 28 days. Due to problems in the preparations for the creep tests, a delay in the start date was necessary to ensure successful strain measurements. The second phase of concrete mix batching was done 2 days following the 28th day curing for the first phase of batching, so the delay occurred in both phases of testing. Due to the delays in testing, curing conditions varied between the two phases of creep tests. The concrete cylinders in the first phase were cured in a water bath of standard temperature from age 24 hours to 26 days. On the 26th day of curing, the cylinders were removed from the water bath and holes were drilled and gage points were glued in place. End caps were fashioned at this point as well. The test cylinders were then placed in the controlled environment chamber in which the creep frames were to be located. The cylinders remained in the chamber until the 61st day of curing on which the creep tests commenced. During the testing period, the temperature and humidity could not be held constant due to problems with the chamber control system. The continuous data recorder was out of commission, so only daily temperature and humidity readings are reported in Table 3.10.

The concrete cylinders in the second phase were cured in a water bath of standard temperature from age 24 hours to 57 days. At this time, the cylinders were removed from the water bath and holes were drilled, gage points were glued in place, and end caps were fashioned. The cylinders were then placed in the controlled environment chamber and remained unloaded until the 61st day of curing, at which the creep tests commenced. Temperature and humidity data that was recorded for both phases are listed in Table 3.10.

The load applied to the concrete cylinders was readjusted periodically throughout the creep test. This was done in order to maintain a constant stress state in the cylinders. ASTM C512 requires that the load be adjusted if a change of 2% occurs from the correct value.

Table 3.10 - Temperature and Humidity History

	Phase 1		Phase 2	
Test Day	Temperature (Fahrenheit)	Humidity (%)	Temperature (Fahrenheit)	Humidity (%)
1	73.5	52.0	73.4	54.0
2	73.5	52.0	73.4	54.0
3	76.5	49.0	73.4	54.0
4	82.0	45.0	73.4	54.0
5	73.5	52.0	73.4	54.0
6	67.0	56.0	73.4	54.0
7	-	-	73.4	54.0
8	69.3	57.0	-	-
9	70.5	59.0	-	-
14	77.0	47.0	73.2	52.0
21	71.0	57.0	83.2	48.0
28	72.3	56.0	84.0	44.0

3.3 SHRINKAGE

Two 6x12 inch concrete specimens were cast from each mix design and were to be used to measure concrete shrinkage. The shrinkage specimens were cured along side their creep specimen counterparts and were subject to the same environmental conditions for the duration of the creep test as were listed previously. The specimens remained unloaded during the creep test. Strains in these specimens were measured in the same

manner as that of the creep specimens. Holes were drilled for brass gage points at ten inch spacing, and strains were measured using the multi position strain gauge from ELE International.

3.4 COMPRESSIVE STRENGTH

Structural requirements of floating bridges built in recent years have specified a minimum compressive strength of 6500psi. This was one of the criteria set by a previous study on concrete for floating bridges and was satisfied and far surpassed in previous tests of the LVM mix design. It has been documented and noted in the literature review that the creep potential of concrete is reduced with the increase of compressive strength. This is a benefit of having concrete with a compressive strength in excess of the design strength. While maintaining a compressive strength of 6500 psi provides adequate strength, higher strength concrete can easily be proportioned. The benefits produced in other performance criteria as a result of this increased strength are almost essential.

The method for testing the compressive strength of concrete was taken from ASTM C39. For each of the seven mix designs, three 6"x12" replicate cylinders were made and cured according to ASTM C192. The specimens were immersion cured in a saturated-lime water bath at 73.4 ± 3°F for 27 days and compressive strength tests were performed on the 28^{th} day of curing. The concrete mixes all had a relatively high design compressive strength and therefore had to be end-capped for testing, in order to achieve consistent results, rather than testing with standard neoprene pads and platens. Concrete cylinders were capped with Hydrostone as described previously. The specimens were tested for compressive strength using a hydraulic operated machine from SATEC, Model

400 QC Prism-1007, Grove City, PA. The longitudinal axis of the specimen was properly aligned with the thrust of the spherically seated block. A constant rate of loading was maintained throughout, within the tolerances of the testing machine, and the rate was within the limits provided in ASTM C39 of 20 to 50 psi per second. Ultimate compressive stress was recorded, in addition to the type of fracture observed.

3.5 CHLORIDE ION PENETRATION

Durable concrete is defined as having has the ability to withstand external effects, which may be mechanical, physical, or chemical, with minimal damage. Low permeability is key to long-term durability of concrete. Low permeability in high performance concrete provides protection against: damage due to freezing and thawing, alkali-aggregate reactivity, carbonation, acid attack, chemical resistance, sulfate attack, seawater exposures, etc. The Hood Canal is an extremely corrosive environment and care must be taken to ensure that any structural steel within the concrete is protected from chloride acid attack.

For this test, two 4 by 8 inch cylinders were cast from each mix design. The cylinders were removed from the molds after 24 hours curing under a plastic tent with wet burlap. The tent was used to maintain a relatively constant temperature and humidity of 68 degrees Fahrenheit and 60 %, respectively for the first 24 hours of curing. Upon removal from the molds, the specimens were partially cured by submersion in lime water followed by curing in a moisture cabinet until the 28th day of curing. The first phase of three mixes was cured for 22 days in the lime water before the specimens were placed in the standard cure moisture cabinet. The four mixes in the second phase were water cured

for 6 days before the transfer to the moisture cabinet. Tests for Chloride ion penetration were completed by WSDOT and were performed according to ASTM C 1202.

The experimental methods documented in this chapter are thorough and accurate. All of the deviations from standard testing methods have been listed and explained. Further analysis of the effects of these deviations from standard will be included in upcoming chapters.

CHAPTER 4: EXPERIMENTAL RESULTS AND ANALYSIS

The Federal Highway Administration provides classifications for high performance concrete (HPC) with different performance characteristics. Grades of HPC are listed from 1 to 4, 1 having the lowest performance in each of the criteria. It should be noted that HPC grade 1 is still a high performance concrete and performs "better" than normal concrete. The information is shown below in its original format in Table 4.1.

Table 4.1 - HPC Performance Grades (Table 1.2 - Definition of HPC according to Federal Highway Administration, Goodspeed, et al. 1996)

Performance Characteristics	Standard test method	FHWA HPC performance grade			
		1	2	3	4
Freeze-thaw durability (X = relative dynamic modulus of elasticity after 300 cycles)	AASHTO T 161 ASTM C 666 Procedure A	60%≤X<80%	80%≤X		
Scaling resistance (X = visual rating of the surface after after 50 cycles)	ASTM C 672	X=4, 5	X=2, 3	X=0, 1	
Abrasion resistance (X = avg. depth of wear in mm)	ASTM C 944	2.0>X≥1.0	1.0>X≥0.5	0.5>X	
Chloride penetration (X = coulombs	AASHTO T 277 ASTM C 1202	3000≥X>2000	2000≥X>800	800≥X	
Strength (X = compressive strength)	AASHTO T 2 ASTM C 39	41≤X<55 MPa (6≤X<8 ksi)	55≤X<69 MPa (8≤X<10 ksi)	69≤X<97 MPa (10≤X<14 ksi)	97 MPa≤X (14 ksi≤X)
Elasticity (X = modulus)	ASTM C 469	28≤X<40 GPa (4≤X<6x10^{6}psi)	40≤X<50 GPa (6≤X<7.5x10^{6}psi)	50 GPa≤X< (7.5x10^{6}psi≤X)	
Shrinkage (X = microstrain)	ASTM C 157	800>X≥600	600>X≥400	400>X	
Specific creep (X = microstrain per MPa)	ASTM C 512	75≥X>60/MPa (0.52≥X>0.41/psi	60≥X>45/MPa (0.41≥X>0.31/psi	45≥X>30/MPa (0.31≥X>0.21/psi	30/MPa≥X (0.21/psi≥X

4.1 CONCRETE MIX DESIGNS

The seven mix designs tested in this research were listed previously in Chapter 3 and can be seen again here in Table 4.2 for reference convenience. All the mix designs performed well in the batching process. The workability characteristics were comparable. Superplasticizer was added to each mix at a predetermined quantity, and then adjusted to achieve the desired slump at or between 8 and 9 inches. There was no indication of aggregate and cement paste segregation with any of the mix designs. Segregation was watched for and is an important problem to avoid in floating bridge pontoons due to the deep walls into which this concrete is to be placed. The freeze thaw characteristic of concrete is not a major issue in the Hood Canal region, so air content was not measured at the time of batching.

Table 4.2 - Concrete Mix Design Quantities

Mi							
Course Aggregate (lb)	1770	1770	1770	1770	1770	1770	1770
Fine Aggregate (lb)	1295	1295	1295	1295	1295	1295	1295
Portland Cement Type II (lb)	624	540	636.3	597.5	624	624	624
Silica Fume (AASHTO M307) (lb)	50	35	none	none	50	50	none
Fly Ash (AASHTO M295) (lb)	100	200	100	100	100	100	100
Metakaolin (Highly Reactive) (lb)	none	none	38.75	77.5	none	none	none
Water (lb)	255	255	255	255	258.7	222.12	154.64
Caltite - Waterproofing Admixture	none	none	none	none	none	49.86	49.86
W/C ratio	0.329	0.329	0.329	0.329	0.334	0.351	0.282
Water Reducer (ASTM C494)	none	none	none	none	none	none	none
Superplasticizer (ASTM C494)	5.5 floz/cwt	4.3floz/cwt	5.5floz/cwt	7.0floz/cwt	5.5floz/cwt	5.5floz/cwt	6.3floz/cwt
Slump (inches)	8.0	7.5	9.0	8.5	8.5	8.5	9.0

Caltite -> 6 gallons/yd^3 All Values Based per Cubic Yard

4.2 CREEP

Measuring deformations to the precision necessary for accurate creep and shrinkage results is an intricate task. The accuracy required by ASTM C512 is one ten-thousandths of an inch. The specimen preparation procedure must be performed with care. Gage points should be perpendicular with the axis of the cylindrical specimen and should be parallel with each other so that the mechanical comparator can be used effectively. Drilling of the holes and gluing the points into the correct position is critical for useful results. If the gage points are not lined up correctly as previously described, accurate measurements can still be collected. To collect strain data, the same person should take all of the measurements and the mechanical comparator must be held at the same orientation with respect to the specimen and gage points each time a reading is taken.

Creep potential of concrete is valuable information for knowing if the concrete to be used in construction is commensurate with the loadings to be applied throughout the design life of a structure. As was described in detail in the Chapter 1, creep is present in floating bridge pontoons and must be accounted for. Although creep deformation will continue throughout the life of a structure, it is essential that predictions of long term creep could be made based on short term data. Typically, creep tests are carried out for 180 days or up to one year or more. The expected creep strain after this time is much less than that which would occur during the testing duration. As was stated in the literature, (Brooks and Neville 1978) required creep accuracies for a given concrete application should be assessed so that appropriate test duration could be selected. Short term, 28 day tests were selected for this research. Such data can be used to observe concrete creep

potential at 28 days, and to extrapolate long-term results using empirical relationships. The extrapolation equations and expected error developed by Brooks and Neville (1978) are provided here in a revised form:

Basic creep- $c_t=c_{28}*0.50t^{0.21}$; $M_{bc}\approx16\%$

Total creep- $c_t=c_{28}[-6.19+2.15\ln(t)]^{1/2.64}$; $M_{tc}\approx19\%$

Shrinkage- $s_t = s_{28} + 100(3.61\log_e(t) - 12.05)^{0.5}$

$M_{sh}\approx14\%$

Measured and calculated creep quantities are shown in Table 4.3. The table lists for each mix number, the applied stress, the instantaneous elastic deformation, the calculated Young's Modulus, measured 28-day creep, the 28-day creep coefficient, 28-day specific creep, and long-term estimated creep strains. A graphical depiction for comparison of the 28-day measured specific creep values and the long-term extrapolated values, less the initial elastic strain, is shown in Figure 4.1. Other graphs displaying the measured deformation of each mix design can be seen in Figures 4.2 through 4.8. For visual clarity, actual measured data points are included in the graphs, and trend lines have been sketched over the points to model the data curves. The results are graphed in micro-strain versus time in days. The total strain was measured from the specimens under load in the creep frames. Shrinkage strains were measured from the companion cylinders cured at the same conditions as the creep specimens. The values for creep plus initial elastic strain have been calculated by subtracting the shrinkage strains from the total

strain measured. Initial elastic deformation is included in "creep strain" curves in the individual mix deformation graphs.

Table 4.3 - Creep Comparison

The axial stress applied to the specimens was approximately 25 % of the 28-day ultimate compressive strength. The dial gage accuracy for the applied load reading was reported by the manufacturer to be ±1% of the maximum number on the gage ring scale. For this particular application, the accuracy is equal to ±1% of 65 tons, or .65 tons.

The instantaneous elastic deformation is is the measured strain immediatly after the load is applied to the specimens. This strain is almost entirely recoverable when the load is removed. This portion of the total load induced strain is not considered creep and therefore, not included in the reported creep strain results. This property was described by Neville, Dilger and Brooks (1983). The modulus of elasticity of the concrete is calculated by dividing the applied stress by the instantaneous elastic strain. This Young's modulus is the initial value for the hardened concrete. As the concrete undergoes long term deformation under applied load, the modulus of elasticity is reduced. The values reported here in Table 4.3 are comparable to values seen in other research. In a study performed by Cascade Testing in Seattle, a MOE for a mix similar in composition to the LVM mix design was reported as 6.27(x10^6) psi. This is the same as the valued

$$\frac{c_t}{c_{28}} = (-6.19 + 2.15 * \log_e(t))^{\frac{1}{2.64}}$$

calculated for mix design #5. The MOE reported for a mix similar in composition to the Caltite mix design was reported as 6.77(x10^6) psi, indicating a 1% difference from the value calculated in this research of 6.84(x10^6) psi.

The 28-day creep is the actual measured strain for each concrete mix. The deflection was measured in inches for each gage length on both specimens for a given mix design. Each deflection measurement was divided by its respective gage length in inches to obtain a strain value. These strain values were then averaged for each mix design to obtain the value listed in Table 4.3. A routine check of strain similarity between creep cylinders can be made by observing the measured data. For mix #1, average total strain for cylinder 1 was recorded as 0.00088 in/in, and the average total strain for cylinder 2 was 0.00088 in/in. This produced an average of 0.00088 in/in with a standard deviation of 0.0. The standard deviation for the measured total strain data for mix 3 is 0.000014.

The results The 28-day creep coefficient is the ratio between the measured creep value at 28 days and the instantaneous elastic strain. It is important to note that creep strains are relative, based on the stress applied to the specimens. A constant ratio between applied and ultimate compressive stress has been used in this research. Normalization to comparable data is done by dividing the strain in the cylinders by the stress applied, resulting in the specific creep values presented in the Table 4.3. Specific creep is reported in units of microstrain per psi and is used when comparing creep potential of different mix designs. Extrapolated specific creep values for times of 180 days, 1 year and 5 years are also reported and listed in Table 4.3. The long term data was

calculated using the 28 day specific creep data and the equation previously reported from Brooks and Neville (1978).

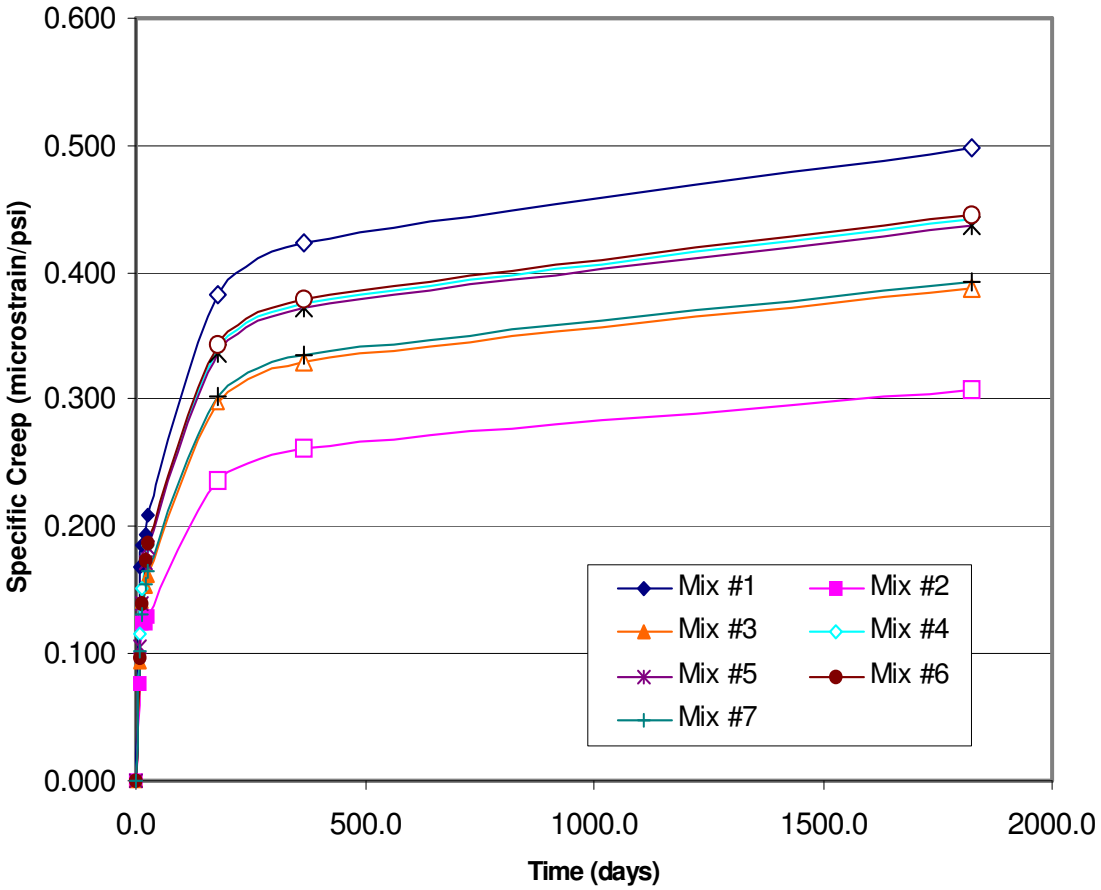

Figure 4.1 – Specific Creep Comparison – Estimated Strain Results to 5-Years

Dilger and Wang (2000) made the observation that creep strains for a high performance concrete mix are approximately 1.8 to 2.4 times the initial instantaneous elastic strain after a long time. This principle is fairly consistent with the mixes tested in this research. For one year extrapolated data, the creep coefficient ranges from 2.16 for mix #6 to 2.67 for mix #4.

Mix #2 had the lowest measured value for specific creep. A value of 0.128 micro-strain at 28 days was 22% lower than Mix #3, which had the next lowest specific creep results. It has been noted that mix #2 had the highest quantity of fly ash of all the mixes tested. Brooks (1999) found that fly ash was shown to result in lower ultimate creep values with an increase in cement replacement percentage of fly ash. This is because fly ash concrete continues to develop strength over a long period, unlike silica fume, which leads to faster development of ultimate compressive strength. Brooks (2000) also found that total creep decreases for low levels of silica fume. Both the higher level of fly ash and the lower level of silica fume in mix #2 helped produce the concrete with the lowest creep potential researched in this study.

Mix #7 had low specific creep, with a 28-day value of 0.165 micro-strain. This could be attributed to the relatively low water-to-cementitious ratio of 0.28 (Burg et.al. 1994). This particular mix had low cement paste content with respect to the other concretes. A decrease in cement paste content tends to produce concrete with decreased creep (Zia, 1993). Furthermore, high aggregate content is known to restrain creep deformations. It is unknown whether the Caltite lead to the reduction in creep as compared to the baseline mix. Referring to mix #6, the Caltite inclusion into the concrete

did not appear to considerably affect creep of the LVM mix. Similar values for creep were obtained for mix #6 as were for the LVM.

The LVM mix designs, #'s 1 and 5, produced creep values of slightly differing magnitude. Both extrapolated creep values at 180 days are classified as Grade 2 according to Figure 4.1. The values are resulting from concretes with different curing conditions and from a test that is difficult to repeat and achieve duplicate results.

Metakaolin modified concrete was similar to silica fume modified concrete in its creep potential. Mix #4 creep deformation, 0.340 micro-strain, was nearly equivalent to the creep of its counterpart, the LVM number 2, at 0.336 micro-strain at 180 days. Mix #3 performed better in creep than did mix #4. This was not expected since results observed in the literature claimed that creep of metakaolin modified concrete decreased with the increased inclusion quantity of metakaolin in the mix (Brooks et.al. 2001). The effect of the curing conditions may have affected the creep potential of the concrete. The loss of internal relative humidity from cement hydration as well as water loss to the ambient environment as the concrete cured in the testing chamber could have led to lower total creep in mix #3, compared to that of mix #4 (Dilger et.al 2000).

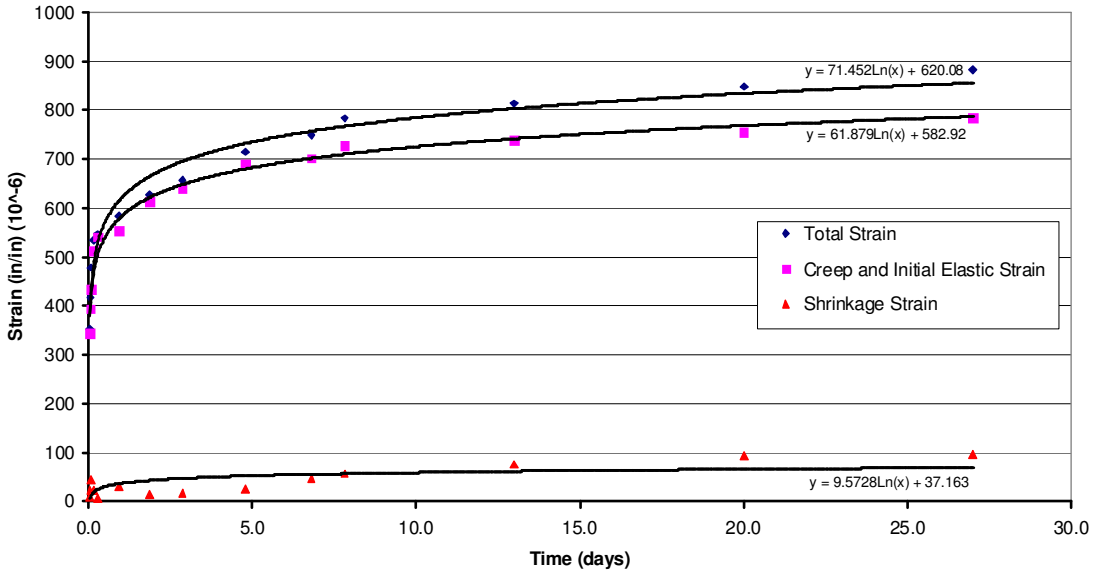

Figure 4.2 - LVM Mix Design Strain

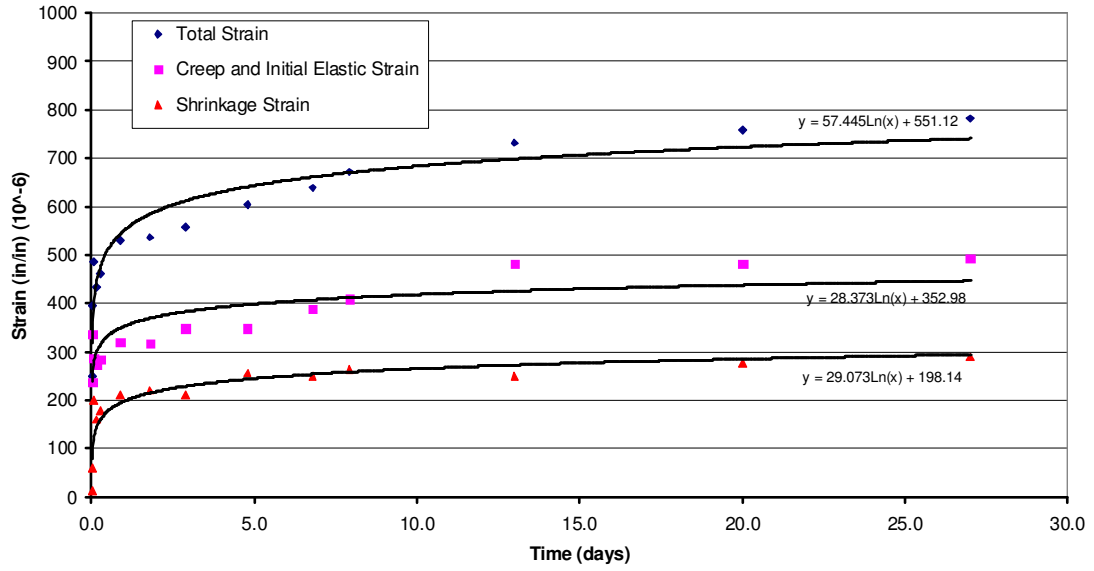

Figure 4.3 – WJE Inc. Mix Design Strain

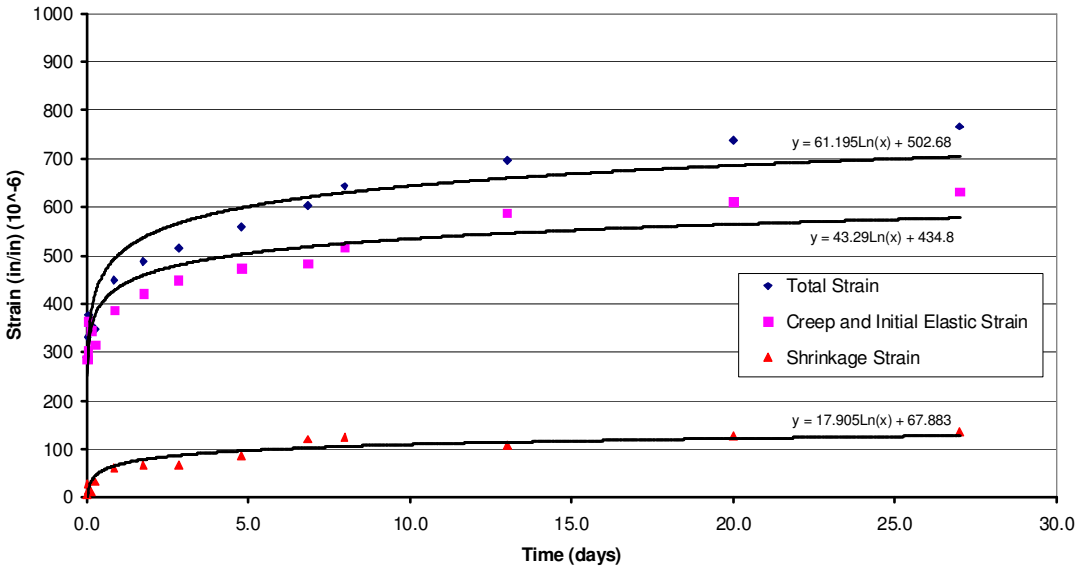

Figure 4.4 – 5% Metakaolin Mix Design Strain

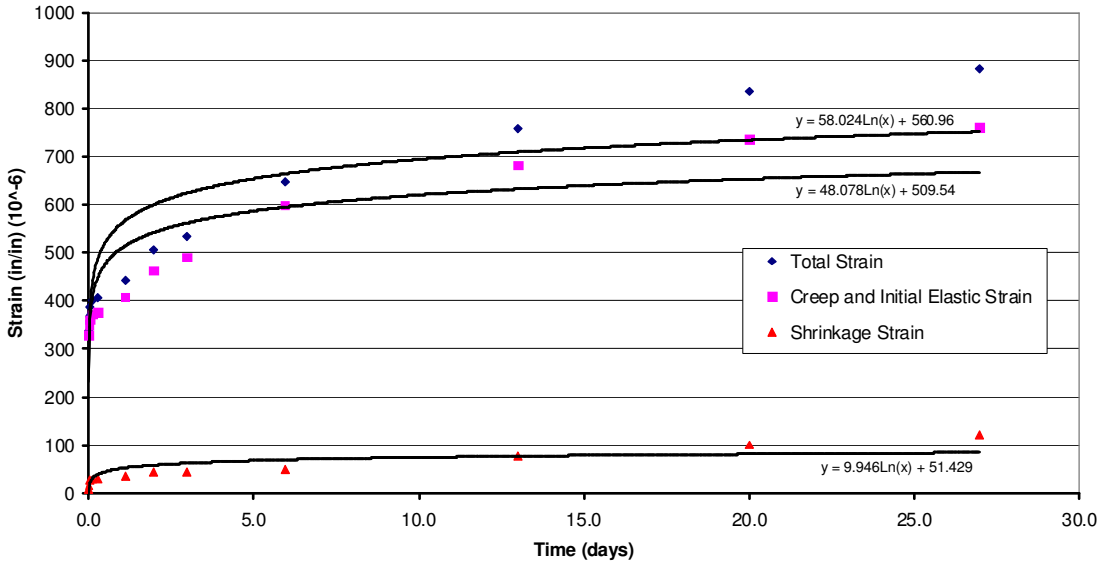

Figure 4.5 – 10% Metakaolin Mix Design Strain

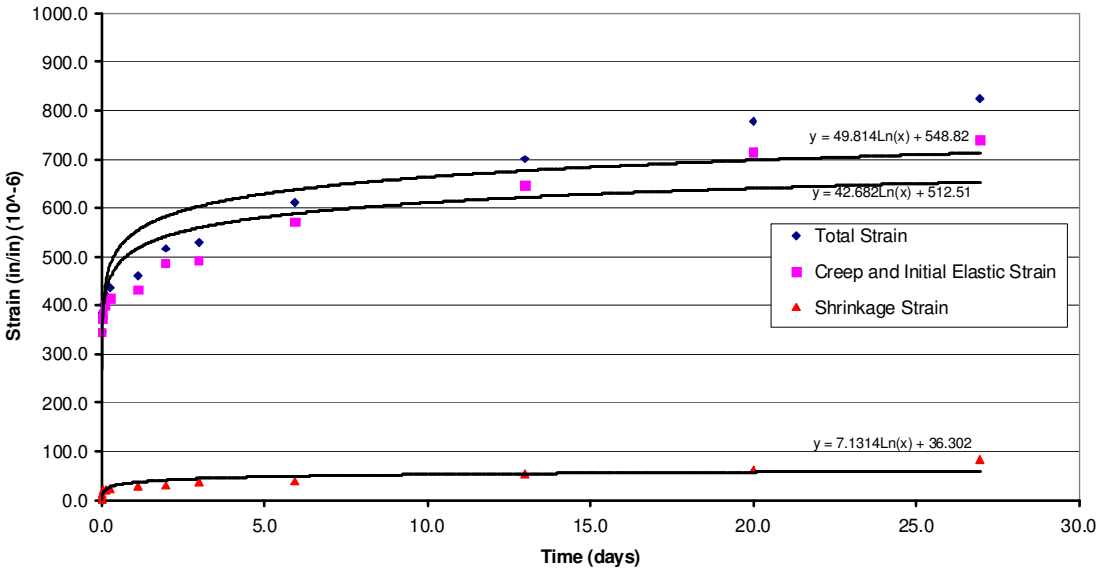

Figure 4.6 – LVM (#2) Mix Design Strain

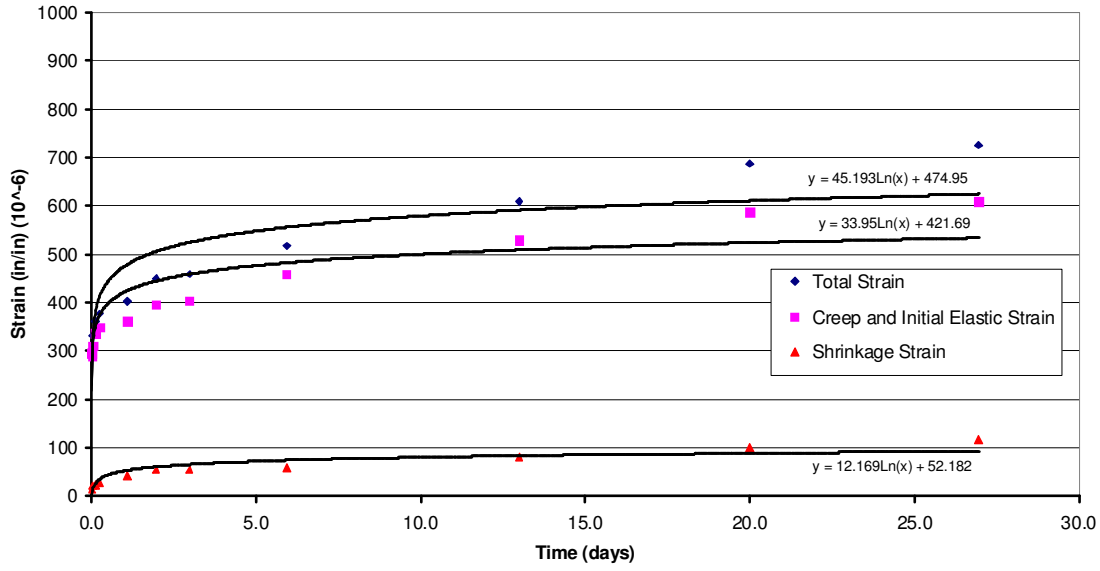

Figure 4.7 – LVM Mix w/ Caltite Waterproofing Admixture Mix Design Strain

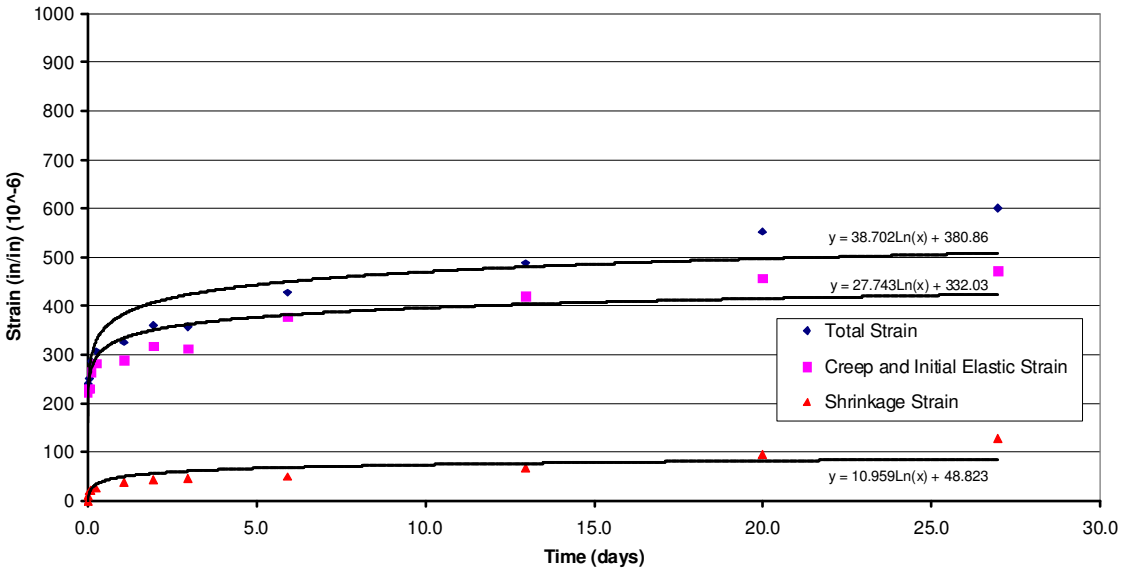

Figure 4.8 – Caltite Mix Design Strain

4.3 SHRINKAGE

The engineers that designed the Lacey V. Murrow Bridge specifications placed a limit on the maximum allowable shrinkage strains in the pontoons. The length change of hardened concrete, tested according to AASHTO T160 or ASTM C 157, was required to be less than 400 millionths (micro-strain) at 28 days. As was discussed previously, shrinkage strain must be kept to a minimum so that shrinkage cracking does not occur and allow water to penetrate into the pontoon cells.

The shrinkage testing method provided by ASTM C 157 was not used in this research. Obtaining shrinkage strains in a similar manor as the strains due to creep was desirable for direct comparisons and calculations. This method is prescribed by ASTM C 512 where necessary information requirements for creep are specified. It should be noted that due to the creep testing procedure described previously, measurements for shrinkage strains were not taken until the time the creep cylinders were subject to loading. This being the case, actual data reported for shrinkage are not true 28-day values. The curing conditions prior to strain measurements and age at testing have been described and should be noted when reviewing the shrinkage results. The 28-day measured shrinkage strain can be seen in Table 4.4.

Values observed for shrinkage strain are all classified as Grade 3 concrete strains according to FWHA, with mix #2 as the one exception, which is classified as Performance Grade 2. All mixes had shrinkage results well below the required limit of 400 millionths at 28 days. The LVM mix design, both numbers 1 and 5, performed quite well and had the lowest shrinkage strains observed here. As was expected, mixes containing silica fume experienced slightly lower shrinkage than the mixes containing

similar quantities of metakaolin, at early ages. (Calderone, Gruber, Burg 1994) This was observed in the comparison of the LVM to mix #4. In addition, shrinkage strains showed a decrease as the OPC replacement quantity by metakaolin increased (Ding, Li 2002). Caltite did not significantly affect shrinkage of the LVM mix, however a slight increase was observed.

With the exception of mix #2, all mix designs performed as expected in shrinkage. Mix design #2 had the highest shrinkage strain measured in this research. This occurrence is possibly because more water still existed in the concrete cylinders. The higher water content is due to the continuing of hydration over a longer period because of the high fly ash content. More water in the concrete would allow for more drying shrinkage as the concrete attempts to reach hygral equilibrium with the ambient environment. These results, however, are larger than expected when considering the curing conditions that the test specimens experienced prior to strain measurements.

Table 4.4 – Shrinkage Strains

Mix #	Modulus of Elasticity (10^6) (s/e_i) psi	28 Day Shrinkage (microstrain) (s_{28})	Estimated Long Term Shrinkage (microstrain) c_t=180 days	Estimated Long Term Shrinkage (microstrain) c_t=365 days	Estimated Long Term Shrinkage (microstrain) c_t=1825 days
1	6.76	96.7	355.5	400.8	484.8
2	8.41	289.5	548.3	593.6	677.5
3	7.30	135.0	393.7	439.1	523.0
4	7.01	121.8	380.6	425.9	509.8
5	6.27	83.4	342.2	387.5	471.4
6	5.69	116.7	375.5	420.9	504.8
7	6.84	128.6	387.3	432.7	516.6

$$s_t = s_{28} + 100(3.61\log_e(t) - 12.05)^{0.5}$$

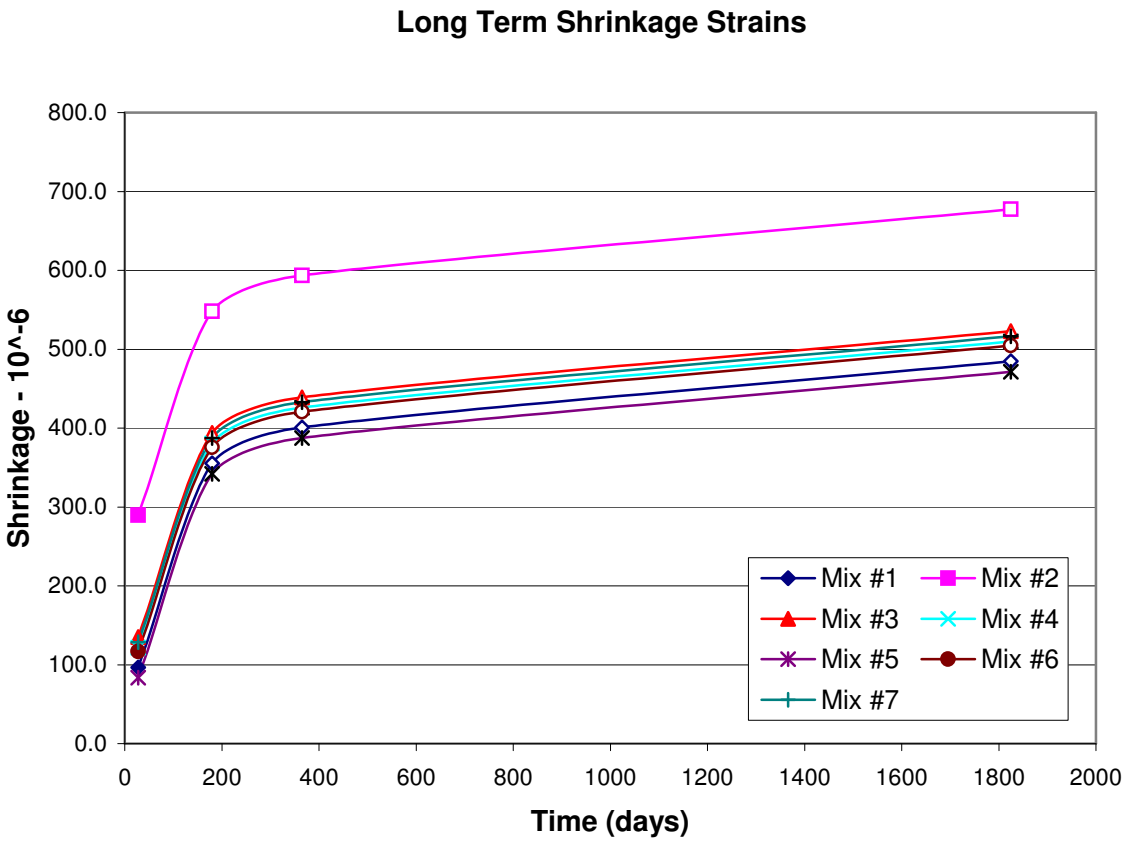

Figure 4.9 – Long Term Shrinkage Strains, Extrapolated from 28-day Data

4.4 COMPRESSIVE STRENGTH

The results for 28-day compressive strength can be seen in Table 4.5. The testing protocol followed to obtain strength data is prescribed by ASTM C39, as listed in Section 3.4 of this report. Three cylinders were cast and cured for each mix design and tested in axial compression on the 28th day. Standard deviations for the mean compressive strength are listed in Table 4.5 and are all within the requirement of 7.8% set forth in ASTM C39.

Mix design 4 produced the highest compressive strength with an average ultimate value of 9206.7 psi. The LVM mix design, numbers 1 and 5 with an average of the two average ultimate values of 8788.4 psi was the next highest value obtained in this research. The results of these two mixes are consistent with previous research findings mentioned in the literature review chapter of this report. Concrete compressive strength is greater with the inclusion of metakaolin than that of concrete with silica fume with similar OPC replacement values. The results of mix numbers 2 and 3 are also consistent with past metakaolin and silica fume comparison studies. Mix number 2 was proportioned with 4.5% OPC replacement with silica fume and mix number 3 had 5% OPC replacement with metakaolin. Mix number 3 demonstrated a higher ultimate compressive strength than number 2 by 7.5%.

The first mix incorporating Caltite, mix number 6, had a compressive strength of 6890 psi, which was lower than its parent mix design, the LVM, with an average compressive strength of 8788 psi. These results were consistent with past results from a similar study by Cascade Testing in Seattle, Washington where a control mix and a similar mix having water replaced by equal part Caltite were tested. The 28-day

compressive strength of the control mix was 12310 psi and that of the Caltite mix was 9980 psi. The reduction in compressive strength seen in this previous study of about 19.0 percent is similar to the results of this research of 21.6 percent. The Caltite was used as a water replacement and accounted for as water in the water-to-cementitious material ratio. The water-to-cementitious ratio was larger for this mix than the other mix designs tested in this study. This larger ratio may have been the cause for the lower strength, as past results have shown (Carette and Malhotra,1992). In addition, Caltite may not contribute to the hydration process in the same manor as water does. Due to the removal of water and replacement with Caltite, it could be speculated that similar hydration may not have been possible, which could produce concrete with reduced strength.

Mix design 7 had a 28-day compressive strength of 6233.3 psi. As previous results demonstrated, greater compressive strengths result from the inclusion of finer supplementary cementitious materials such as silica fume or metakaolin (Calderone, Gruber, Burg, 1994). The lower strength was expected due to the lack of these fines in the mix design. Mix number 7 had the lowest strength of all of the mix designs tested, and was just slightly lower than the required compressive strength of 6500 psi set forth in the concrete specifications.

Table 4.5 – 28-Day Compressive Strength

Mix Design	Cylinder #	28 day Compressive Strength (psi)	Standard Deviation	Average 28- Day Compressive Strength (psi)
1	1 2 3	8910 8650 8570	177.8	8710
2	1 2 3	8140 8200 8150	32.1	8163.3
3	1 2 3	8820 8780 8720	50.3	8773.3
4	1 2 3	9340 9080 9200	130.1	9206.7
5	1 2 3	8870 8820 8910	45.1	8866.7
6	1 2 3	7010 6800 6860	108.2	6890
7	1 2 3	6100 6350 6250	125.8	6233.3

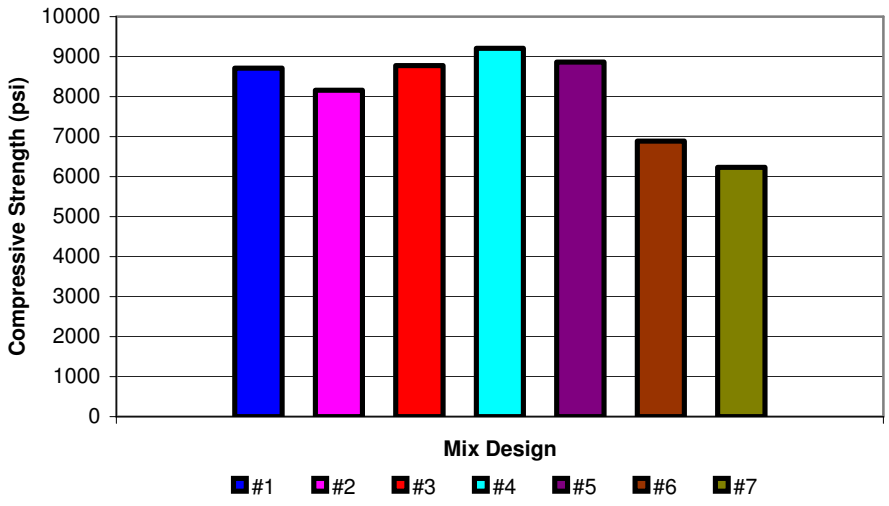

Figure 4.10 – 28-Day Compressive Strength

4.5 CHLORIDE ION PENETRATION

ASTM C 1202 prescribes the testing method for determining the chloride penetration resistance in of the concrete mixes. Two 4 by 8 standard cylinders were cast for each mix to execute this test, as was stated in Section 3.5. Test results for the 28-day cure chloride ion penetration tests can be seen in Table 4.6.

First, it should be noted that based on the creation of the LVM mix design, a chloride permeability resistance adequacy standard was set at a maximum of 1000 coulombs passed at 56 day cure. Results for 56-day cure chloride permeability were not determined in this research due to lack of test cylinders. This is a slight drawback since the results cannot be compared directly to the permeability requirement set forth as a basis for acceptability. However, trends can be noted using the 28-day data and the results can be compared with those from prior studies to determine the adequacy of chloride ion penetration resistance.

The lowest penetration result was mix number 5, the second phase LVM mix design. The low level of charge passed, 1158 coulombs, was consistent with previous LVM mix design permeability results. Lwin, Bruesch, and Evans (2001) reported test results from initial LVM mix design development studies. Permeability results reported were 1,198 coulombs at 28 days. This value was reduced to 790 coulombs at 56 days and then further reduced to 584 coulombs at 90 days. At the time of the LVM construction, 113 permeability tests were performed on the LVM concrete and the results were reported in the Concrete for Lacey V. Murrow Bridge Pontoons (1993), a WSDOT document. The results for 28, 56 and 90-day tests had averages of 1327, 785, and 577 coulombs, respectively. The decrease in permeability is due to the further hydration of

the concrete with time and the resulting infilling of the porosity. This typical characteristic of concrete can be assumed to act in a similar manor for all of the mixes studied in this research. Thus, it can be assumed that all of the permeability values would decrease as the cure time increased. Boddy, Hooton and Gruber (2001) demonstrated such property in a study in which long-term chloride penetration resistance of concrete containing high reactivity metakaolin was explored.

The addition of Caltite to the LVM mix to form mix design #6 increased the chloride penetration at 28 days to 1337 coulombs. This amounted to a 15% increase in permeability, though this mix design was the second most resistant to chloride ion penetration in this research.

Mix design number 4, the metakaolin mix with 10% OPC replacement had chloride permeability of 1682.5 coulombs. According to past studies, metakaolin concrete has a similar, but slightly lower resistance to chloride ion penetration than does silica fume concrete during early stages. Ding and Li (2002) found that for all OPC replacement values, silica fume is more effective in providing improved chloride resistance of concrete than metakaolin, but both were considerably better than their control mix with no fine supplementary cementitious materials. Ding and Li reported though, that after 90 days of observation, the silica fume and metakaolin 15% replacement concretes displayed equal resistance results. This is a testament to the nearly 100% reactivity of the metakaolin and the further hydration that results over time. Due to the results trend reported by Ding and Li, as well as conclusions reached by Boddy, Hooton and Gruber (2001), it could be speculated that the permeability of the 10%

metakaolin modified concrete would reduce to below 1000 coulombs at 56 days, and further reduction would occur by 90 days.

The conclusions to the aforementioned study by Ding and Li were not repeated here when comparing mix number 2, the WJE Inc. mix recommendation containing 5% silica fume, to mix number 3, which contained 5% metakaolin as OPC replacement. Mix numbers 2 and 3 had chloride resistance results of 2380 and 1938.5 coulombs, respectively. At 28 days, the metakaolin modified concrete showed greater resistance to chloride penetration than did the fly ash and silica fume concrete. It should be noted that the water to cementitious ratio was the same for both mixes, but the fly ash quantities differed greatly between the two. Due to its reaction with OPC hydration and its small size compared to OPC, it was shown that fly ash typically decreases concrete permeability (Aitcin 1998), but this has not been displayed here in this early age test. The curing conditions for these two mixes, as described in the Experimental Methods chapter of this report, were alike, so the metakaolin mix simply outperformed the WJE Inc mix in resistance to chloride ion penetration. It should be assumed that the permeability of these mixes would decrease drastically by the 56^{th} day of curing, possibly reducing the amount of coulombs passed by half. In a previous study (Ozyildirim,1998) examining the permeability of a concrete mix similar in proportion to mix 2, the number of coulombs passed reduced from 1454 at 28 days to 490 at 90 days.

Mix design number 7 had the largest chloride ion penetration at 2858 coulombs at 28 days. This is classified by ASTM C1202 as moderate. Due to the lack of a fine supplementary cementitious material, such as silica fume or metakaolin, the porosity of this mix was greater than the other mixes. It should be noted that a previous 58-day

chloride ion permeability test on a mix similar in composition to mix 7 produced an average result of 895 coulombs (CTL 1999)

Table 4.6 – Rapid Chloride Permeability Test Results - 28 day

Mix Design	Cylinder #	Charge Passed (Coulombs)	Average Coulombs	28 – Day Chloride Ion Penetrability
1	8	1598	1629*	Low
	9	1660		
2	17	2340	2380	Moderate
	18	2420		
3	26	1917	1938.5	Low
	27	1960		
4	35	1648	1682.5	Low
	36	1717		
5	44	1183	1158*	Low
	45	1133		
6	53	1340	1337	Low
	54	1334		
7	62	2916	2858	Moderate
	63	2800		

Table 4.7 – Permeability Classifications

Chloride Ion Penetrability Based on Charge Passed

Charge Passed (coulombs)	Chloride Ion Penetrability
>4,000	High
2,000-4,000	Moderate
1,000-2,000	Low
100-1,000	Very Low
<100	Negligible

(ASTM C 1202 – 97)

CHAPTER 5: SUMMARY AND CONCLUSIONS

This research provides a comparative study of several concrete mix designs for use in floating bridges for the purpose of improvements in existing practices. The Lacey V. Murrow (LVM) mix design is used as a baseline mix and alterations are made to that design to improved the concrete performance.

The concrete mixes were studied for their fresh and hardened properties including the 28-day compressive strength, chloride ion permeability, creep and shrinkage. For purposes of comparison and determination of a better mix design, it is advantageous to have a reference mix. Results are tabulated in Table 5.1 and should be referred to when reviewing the conclusions reached.

Results of this research reiterates that the LVM mix design is a quality, high performance concrete mix. The LVM has performed well in all the categories tested, and has only slightly been improved in some areas by certain mix alterations. Though the mix design was developed in 1991, it remains a mix that is quite suitable for use in concrete floating bridges. Bridge designers must evaluate the importance of minor improvements in the LVM concrete performance for the benefits in the application.

Table 5.1 – Mix Design Test Results

Mix Design	Average 28 day Compressive Strength (psi)	Average Coulombs	Chloride Ion Penetrability	Predicted 180-Day Specific Creep (microstrain/psi)	Predicted 180-Day Shrinkage (microstrain)
Baseline	8788	1394	Low	0.359	349
2	8163	2380	Moderate	0.236	548
3	8773	1939	Low	0.297	394
4	9207	1683	Low	0.340	381
6	6890	1337	Low	0.343	376
7	6233	2858	Moderate	0.303	387

Mix design number 2 is a modified LVM mix, with decreased silica fume and increased fly ash contents. The workability was acceptable and the fresh concrete could attain similar slump to the LVM of 7.5 inches with a lesser amount of superplasticizer. There was no indication of segregation. The 28-day compressive strength was 7.1% lower, the permeability was classified as moderate, the 180-day specific creep decreased by 34.3%, and the 180-day shrinkage was 57.2% greater than the baseline mix.

Mix design number 3 consists of high reactivity metakaolin at 5% OPC replacement. Fly ash content was the same as the LVM and no silica fume was included. The fresh concrete showed excellent performance with a slump of 9 inches when using an equal amount of superplasticizer as the LVM mix. Compressive strength was only slightly less by 1.7%, permeability was low, creep was reduced by 17.3%, and shrinkage increased by 12.9%.

Mix design number 4 contains 10% high reactivity metakaolin as a supplementary cementitious material. Fly ash content was the same as the LVM and no silica fume was used. An 8.5-inch slump was measured with 7.0 fluid oz/cwt. The compressive strength showed an increase over the LVM by 4.8%, permeability was low, 180-day specific creep was reduced by 5.3%, and shrinkage increased by 9.1%.

Mix design number 6 contains the same quantities of cementitious materials and superplasticizer as the baseline design, with a portion of the water replaced by Everdure Caltite waterproofing admixture. Workability was excellent with the fresh concrete attaining a slump of 8.5 inches. The compressive strength was decreased by 21.6%, chloride ion permeability was low, creep was lower by 4.5%, and shrinkage was greater than the LVM by 7.7%.

Mix design number 7 contains similar aggregate quantities as the LVM, as well as equivalent amounts of OPC and fly ash. Silica fume is not used in this mix. Everdure Caltite is added in place of equal parts mix water. The concrete attained a slump of 9.0 inches using 6.3 fluid oz/cwt of superplasticizer. The 28-day compressive strength was 6233.3 psi, showing a reduction in strength of 29.1%. The chloride ion permeability was moderate, 180-day specific creep was 15.6% lower than the baseline mix, and shrinkage increased by 11.0%.

General conclusions from the results of this research have been realized. The reduction of silica fume and increase of fly ash proved successful in attaining required specification properties. LVM concrete properties were improved by the inclusion of high-reactivity metakaolin in some cases. Caltite waterproofing admixture reduced chloride ion permeability in the LVM mix, but decreased 28-day compressive strength. Concrete with insufficient compressive strength was created with the removal of silica fume and the inclusion of Caltite.

The results and conclusions reached are reliable and can serve a valuable tool in the selection of concrete for use in floating bridges. As is the case with any concrete mix, tests must be performed to ensure the suitability for a given application. This research could be viewed as a first step in the selection and testing of a concrete mix. However, prior to implementing a particular mix, an engineer may need to perform additional tests to ensure compliance with desired performance criteria. Large-scale wall and slab sections representative of the bridge pontoons in which the concrete is to be used should also be tested to ensure satisfactory constructability performance. Such studies are critical for the successful implementation of a given concrete mix in floating bridges.

REFERENCES

1. "Concrete for Lacey V. Murrow Bridge Pontoons," (1993). Wiss, Janney, Elstner Associates, Inc. WJE No. 912145

2. "Results of ASTM C666 Rapid Freezing and Thawing, AASHTO T277 Rapid Chloride Permeability, and AASHTO T259/260 90 Day Chloride Solution Ponding of Specimens From Nine Concrete Mixes," (1999). Construction Technology Laboratory, Skokie, Illinois

3. Aitcin, P.C. (1998). *High Performance Concrete*. London. E & FN Spon.

4. Brooks, J. J. (2000). "Elasticity, Creep and Shrinkage of Concretes Containing Admixtures," *ACI Special Publication 194*, pp283-360

5. Brooks, J. J. (1999). "How Admixtures Affect Shrinkage and Creep," *Concrete International*, April

6. Brooks, J. J. and Johari, M.A. Megat. (2001). "The Affect of Metakaolin on Creep and Shrinkage of Concrete," *Cement and Concrete Research*

7. Brooks, J. J. and Neville, A. (1992). "Creep and Shrinkage of Concrete As Affected by Admixtures and Cement Replacement Materials," *ACI Special Publication 135-2*, pp19-36

8. Brooks, J. J. and Neville, A.M. (1975). "Estimating Long-term Creep and Shrinkage from Short-term Tests," *Magazine of Concrete Research*. Vol 27 No. 90; March, pp. 3-12

9. Brooks, J. J. and Neville, A.M. (1978). "Estimating Long-term Creep and Shrinkage from Short-term Tests," *Magazine of Concrete Research*. Vol 30 No. 103; pp. 51-61

10. Burg, R.G. and Ost, B.W. (1994). "Engineering Properties of Commercially Available High Strength Concretes," *Research and Development Bulletin - RD 104*, Portland Cement Association, Skokie, Illinois, USA

11. Calderone, M. A., Gruber, K. A., and Burg, R. G. (1994). "High Reactivity Metakaolin: A New Generation Admixture," *Concrete International*, Nov, pp 37-40

12. Carreira, D.J. and Burg, R.G. (2000). "Testing for Concrete Creep and Shrinkage," *ACI Special Publication 194*, pp381-420

13. Carrette, G.G., Bilodeah, A., Chevrier, R.L., and Malhotra, V.M. (1993). "Mechanical Properties of Concrete Incorporating High Volumes of Fly Ash from Sources in the U.S.," *ACI Materials Journal*, Nov-Dec, Vol. 90 No.6, pp.535-544

14. Carrette, G.G.and Malhotra, V.M. (1992). "Long-Term Strength Development of Silica Fume Concrete", *Proceedings, Canmet/ACI 4th International Conference on Fly Ash, Silica Fume, Slag and Natural Pozzolans in Concrete*, Istanbul, ACI SP-132, vol. 2, ed. V.M. Malhotra, American Concrete Institute, Farmington Hills, Mich., pp. 1651-1671

15. Collins, T.M. (1989). "Proportioning High-Strength Concrete to Control Creep and Shrinkage," *ACI Materials Journal*, Nov-Dec, Vol 86, No. 6, pp.576-580

16. Dhir, R. K. and Dyer, T. D. (1999). *Modern Concrete Materials*. Thomas Telford Publishing, London

17. Dilger, W.H. and Wang, C. (2000). "Creep and Shrinkage of High Performance Concrete," *ACI Special Publication 194*. pp 361-371

18. Ding, J.T. and Li, Z. (2002). "Effects of Metakaolin and Silica Fume on Properties of Concrete," *ACI Materials Journal* V. 99, No. 4, July-August. pp 393-398

19. Dusenberry, D. O. (1993). "What Sank the Lacey Murrow*?,*" *Civil Engineering* (New York), v. 63, n. 11, Nov. p 54-57.

20. Feng, N.Q., Chan, S.Y.N., He, Z.S. and Tsang, M.K.C. (1997). "Shale Ash Concrete," *Cement and Concrete Research*, Vol. 27 No. 2, pp. 279-291

21. Firth, C. R. (1993). "What Sank the Lacey Murrow? The Contractor's Case," *Civil Engineering* (New York), v. 63, n. 11, Nov. p 58-59.

22. Gloyd, Charles S., (1988) "Concrete Floating Bridges," *Concrete International*, May

23. Goodspeed, C. H., Vanikar, S. and Cook, R. A. (1996). *Concrete International*, Vol 18, Issue 2, February

24. Jianyong, Li and Yan, Y. (2001). "A Study on Creep and Drying Shrinkage of HPC," *Cement and Concrete Research 31*, pp 1203-1206

25. Khatri, R. P. (1995). "Effect of Different Supplementary Cementitious Materials on Mechanical Properties of HPC," *Cement and Concrete Research*, Vol. 25, No. 1

26. Lwin, M. Myint (1999). Chapter 22 - Floating Bridges. *Bridge Engineering Handbook*, CRC Press, LLC

27. Lwin, M. Myint, (1989). "Design of the Third Lake Washington Floating Bridge," *Concrete International*, Feb. p 50-53.

28. Lwin, M. Myint, Bruesch, Alan W. and Evans, Charles F. (2001). "High Performance Concrete for a Floating Bridge," *Fourth International Bridge Engineering Conference*; pp. 155-162

29. Lwin, M. Myint, Gloyd, Charles S. (1984). "Rebuilding the Hood Canal Floating Bridge," *Concrete International*, June, p 30-35.

30. Lwin, M. Myint. (1993). "Floating Bridges – Solution to a Difficult Terrain," *Transportation Facilities through Difficult Terrain*, Wu & Barrett. Balkema, Rotterdam, ISBN 90 5410 3434

31. Memon, A.H., Radin, S.S., Zain,M.F.M. and Trothier, Jean-Francois. (2002). "Effects of Mineral and Chemical Admixtures on High Strength Concrete in Seawater," *Cement and Concrete Research 32*, pp 373-377

32. Neville, A.M., Dilger, W.H. and Brooks, J.J. (1983). *Creep of Plain and Structural Concrete*, Longman Inc; New York.

33. Nichols, C. C., (1964). "Construction and Performance of Hood Canal Floating Bridge," *Symposium of Concrete Construction in Aqueous Environments*. *ACI Publication SP-8*, P. 97-106. ACI

34. Ozyildirim, C. (1998). "Fabricating and Testing Low-Permeability Concrete for Transportation Structures," VTRC 99-R6, Virginia Transportation Research Council, FHA, August

35. Paulson, K.A., Nilson, A.H., Hover, K.C. (1991). "Long-Term Deflection of High-Strength Concrete Beams," *ACI Materials Journal*, Mar-Apr, Vol 88, No. 2, pp. 197-206

36. Persson, Bertil. (2001). "A Comparison between Mechanical Properties of Self-Compacting Concrete and the Corresponding Properties of Normal Concrete," *Cement and Concrete Research 31*, p 193-198, USA

37. Ramachandran, V.S. (1995). *Concrete Admixtures Handbook, 2nd Edition*; Noyes Publications; Park Ridge, New Jersey, USA

38. Sicker, A. and Huhn, M. (1997). "The Influence of Admixtures on the Rheological Properties of Mortars," Helm Lacer No. 2

39. Xu, Yunsheng and Chung, D. D. L. (2000). "Improving Silica Fume Cement by Using Silane," *Cement and Concrete Research*

40. Yamamoto, T. (1990). "Creep and Shrinkage of High-Strength Reinforced Concrete Columns," *Transactions of the Japan Concrete Institute*, Vol. 12, pp. 101-106

41. Zia, P., Ahmad, S.H., Leming, M.L., Schemmel, J.J. and Elliott, R.P. (1993). "Mechanical Behavior of High Performance Concretes, Volume 5: Very High Strength Concrete," *Strategic Highway Research Program*, *National Research Council*, Washington, D.C., xi, 101pp. (SHRP-C-365)

42. Zia, P., Leming, M.L., Ahmad, S.H., Schemmel, J.J., Elliott, R.P., and Naaman, A.E. (1993). "Mechanical Behavior of High Performance Concretes, Volume 1: Summary Report." *Strategic Highway Resesarch Program, National Research Council,* Washington, D.C., xi 98, pp. SHRP-C-361.

CHAPTER 6: LITERATURE REVIEW

This literature review focuses on three main topics. The first one is the history of floating bridges with special attention to the Hood Canal Floating Bridge. The second topic is on mix designs used on past floating bridges in the state of Washington. Finally, the third topic is on concrete experiments that addressed leakage tests through cracked concrete elements, waterstop testing and compaction level tests for concrete construction joints.

6.1 FLOATING BRIDGE HISTORY

Floating bridges have been an important element of the transportation system for the Puget Sound and Seattle, Washington area for over 60 years. Lwin (1993b) stated that floating bridges have been constructed to cross wide bodies of water where the depth of water is very great or the soil bottom is too soft making conventional bridges too expensive. Lwin et al. (1984) discussed a relative cost analysis performed during the replacement of the west half of the Hood Canal Floating Bridge in the early 1980's. The relative cost of the floating bridge replacement was at least two-and-a-half times less expensive than a conventional fixed bridge. Lwin (1993b) stated that experience has shown prestressed concrete bridges are an economical, durable and low maintenance bridge solution.

6.2 HOOD CANAL DESIGN AND CONSTRUCTION

The west half of the Hood Canal Floating Bridge sank under high winds in 1979. Lwin et al. (1984) speculated that the failure could have been caused by dynamic loading due to wind and waves, slippage of the anchors, ponding of water on the pontoon decks

or water entering inside the pontoons. The west half was rebuilt and completed in 1982. The undamaged east half was left unchanged at the time.

Typical pontoon dimensions of the east half of the Hood Canal Bridge were described by Henley et al. (1997) as having widths of 50ft, heights of 14.3ft and pontoon drafts of 9.2ft with post-tensioning only in the longitudinal direction. Nichols (1964) discussed the construction process involved in pouring the pontoons for the bridge's east half. Concrete was poured through metal chutes to limit segregation. The maximum concrete drop height from the end of the chutes was limited to five feet and was allowed to spill out into the bottom slab area. The concrete was consolidated about 1 to 2 hours after placement by allowing vibrators to sink of their own weight in the partially stiffened mass.

Henley et al. (1997) discussed the dimension changes made to the Hood Canal Bridge's west half following the rebuilding after the 1979 storm. Typical dimensions of pontoons for the west half of the bridge have widths of 60ft, heights of 18ft and pontoon drafts of 12ft. The pontoons are post-tensioned transversely, vertically and longitudinally. Lwin et al. (1984) described the construction of the west half of the floating bridge following the storm. The pontoons used for the replacement west half were divided into compartments 20ft wide by 30ft long. A 28day compressive strength of 6500psi was required. Coarse aggregate was limited to ¾ inch nominal maximum size. Non-air entrained concrete was used. Pontoons consisted of "C" and "T" shaped precast segments that were assembled by joining precast segments with cast-in-place concrete. Pontoons were assembled in graving docks and floated to the site.

6.3 MIX DESIGN

The mix design used for the Lacey V. Murrow Floating Bridge in 1991 has performed well in the field and will be used for the Hood Canal East Half Replacement Project. Lwin et al. (1995) stated that the LVM mix was designed towards water-tightness and durability because of their importance in the long-term performance of a floating structure exposed to water and severe environmental conditions. The LVM mix design is shown in Table 7.1. The report by Wiss, Janney, Elstner Associates, Inc. (1993) found that water-tightness and durability are achieved through low water-cement ratios and through the use of dense cement paste between aggregates.

Table 7.1 LVM Mix Design (after Lwin et al. 1995).

Weights per cubic yard (saturated, surface-dry)	
Concrete Constituent	lbs.
Type II Portland cement	624
Silica fume (AASHTO M307)	50
Fly ash (AASHTO M295)	100
Paving sand	1295
Coarse aggregate	1770
Water	255
Water Reducing Agent (ASTM C494), ounces	25
Superplasticizer (ASTM C494), ounces	131
Air entrainment:	none
Water/cement ratio	0.33
Slump, in	7

The report also found that the maximum water-cement ratio to limit concrete permeability should be 0.33. The required LVM mix strength was 6500psi and was easily achieved. Non-air entrained concrete was used for the pontoons because of the mild climate. A maximum coarse aggregate size of a ½ inch was specified but a 3/8-inch

aggregate was ultimately used because of availability. To improve bond across the construction joint the surface of the hardening concrete was water-blasted to expose the aggregate. The roughening of the surface was reported to enhance the chemical adhesion and mechanical interlock across the joint. Lwin et al. (1995) stated that a slump of seven to nine inches was used for the mix and produced a flowable concrete that provided good workability.

The LVM mix was designed after failure of the first Lacey V. Murrow Bridge in 1990. Lwin et al. (1994) described that the new mix was made using high performance silica fume concrete to assure low permeability and shrinkage, thereby reducing the risk of another failure. To further lessen the danger of failure individual cells were isolated from adjacent cells to reduce the risk of flooding multiple cells in the event of a leak. As another safety precaution Lwin (1993a) stated that individual cells were monitored by sensors installed in each watertight compartment for early detection and warning of water entry. An alarm would sound in the event of a leak notifying personnel to start the bilge pumps. All the aforementioned safety improvements in addition to others were implemented based on recommendations of a Blue Ribbon Panel, established after the sinking of the Lacey V. Murrow Bridge in 1990.

6.4 WATER LEAKAGE TESTS THROUGH CRACKED CONCRETE ELEMENTS

Dusenberry et al. (1993) performed tests on water flow rate through a cracked reinforced concrete element. The dimensions of the concrete test sections were predetermined as was the placement of reinforcement within the test specimen. The

reinforced specimens were cast monolithically and allowed to cure for seven days before being physically cracked using hydraulic jacks.

A hydraulic head of 2.13m was applied to the crack face. The pressure was applied to the specimen through a pressure chamber attached to the top surface of the specimen. The pressure was maintained by an elevated reservoir with a continuous water supply and overflow tube as shown in Figure 7.1. Water flow rate through the crack was measured by recording the weight of collected water in a tarred pan placed beneath the specimen over a measured time period.

Dusenberry et al. found that the equation Q = T * dh/dl where T is transmissity and dh/dl is the hydraulic gradient through the wall thickness for smooth planar cracks with parallel surfaces can be modified by an adjustment factor for non-smooth surfaces. The adjustment factor reduces flow through new cracks smaller than 0.5mm and is partly caused by roughness within the crack. The adjustment factor C is expressed as,

$C = K(1-b_0/b)^3$ where K = 0.118, b_0 = 0.013mm and b is crack width in millimeters.

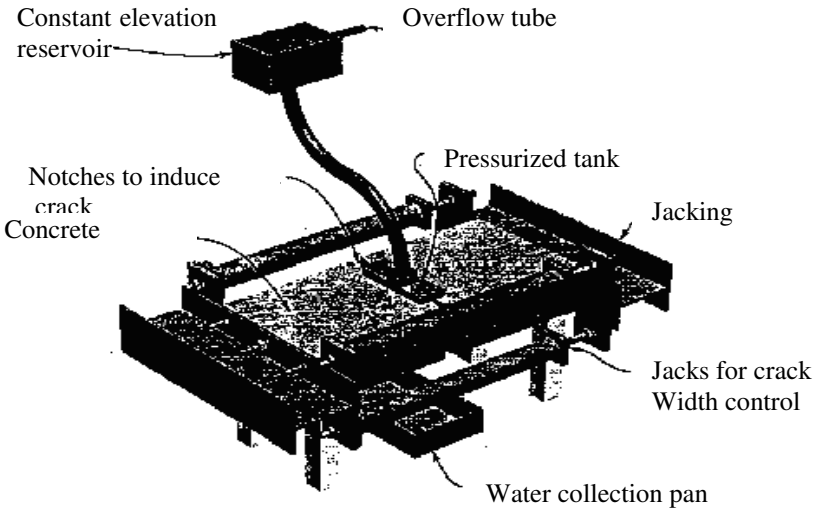

Figure 7.1 - Test configuration (after Dusenberry et al. 1993).

Rashed et al. (2000) presented the results of the experimental phase of a research program into the behavior and design of partially prestressed concrete water containment structures. Typical wall sections were 250mm (9.84in) thick. The wall sections were cracked using hydraulic jacks. A 300 by 1000mm plexi-glass chamber was fixed to the top of the concrete specimen as shown in Figure 7.2 and filled with pressurized water from a cylindrical steel container. Air pressure equivalent to 8-10m head of water was applied to the water through the pressure regulator. A pressure of 70kPa (10.15psi) was applied on the joint.

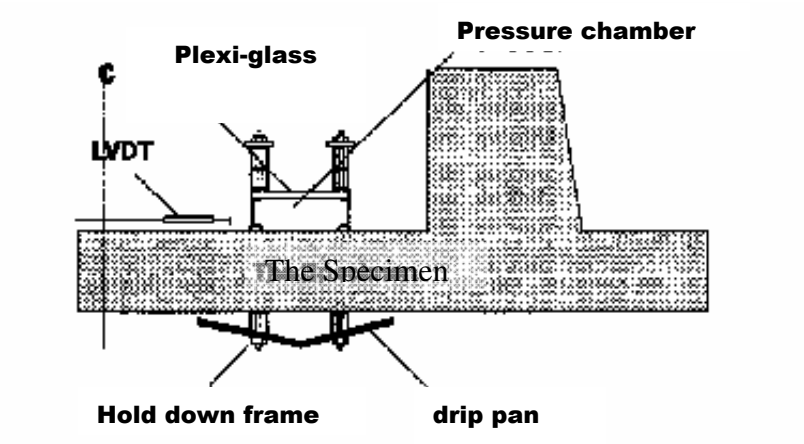

Figure 7.2 - Leakage test setup (after Rashed et al. 2000).

Water was collected from the underside of the joint and transferred to a graduated cylinder. The volume of water collected was recorded manually together with the corresponding time. Additionally, the leakage rate was recorded using load cells located beneath the pressurized water container that measured the decreasing container water weight. The weight of water lost was recorded electronically along with the corresponding time.

Under a constant pressure of 70kPa specimens were subjected to a hydraulic jacking force until leakage occurred. Leakage began for an average crack width of 0.1mm from the north side and 0.03mm from the south side of the specimen in only a few minutes. Once leakage occurred jacking was stopped and water loss measurements were taken until water penetration stopped at which point the jacking force was increased and the process continued. Leakage rates were initially low and decreased with time. For through cracks with effective widths less than 0.15mm, the cracks leaked initially and then self-sealed. Cracks with wider effective widths flowed continuously.

Clear (1985) performed tests to observe autogenous healing in concrete specimens. Autogenous healing of concrete reduces the flow of water through a crack at rates primarily affected by the width of the crack. Initial reduction in flow is due primarily to blockage of the flow path by loose particles already in the crack that is later enhanced by precipitation of calcium carbonate.

Site observations were performed on an existing water reservoir three-and-a-half months old. Moisture was collected from two existing cracks in the walls of the reservoir using aluminum gutters. Flow rates were determined by recording the time necessary to collect a measured volume of water. Flow was recorded during the filling of the reservoir and for the following two weeks when the cracks were subject to a constant head of water. After the maximum water level in the tanks was reached the flow rates decreased with time at an ever-decreasing rate.

A lab experiment was also performed to observe autogenous healing in a $150mm^3$ concrete block. The block was cracked two days after casting through the use of jacking bolts embedded in the concrete. The specimen was jacked until surface widths of 0.1, 0.2

or 0.3mm were observed. A hydraulic gradient of 22.5 was selected for the program to represent a severe case (height of fluid column/thickness of wall) and was obtained using a constant-head water tank attached to the entrance of the specimen. An elevation head of 3.37m of water was maintained. Water passing through the crack was collected and the time recorded to determine flow as shown in Figure 7.3. After seven days of flow, each crack specimen was dismantled so that material within the crack could be examined.

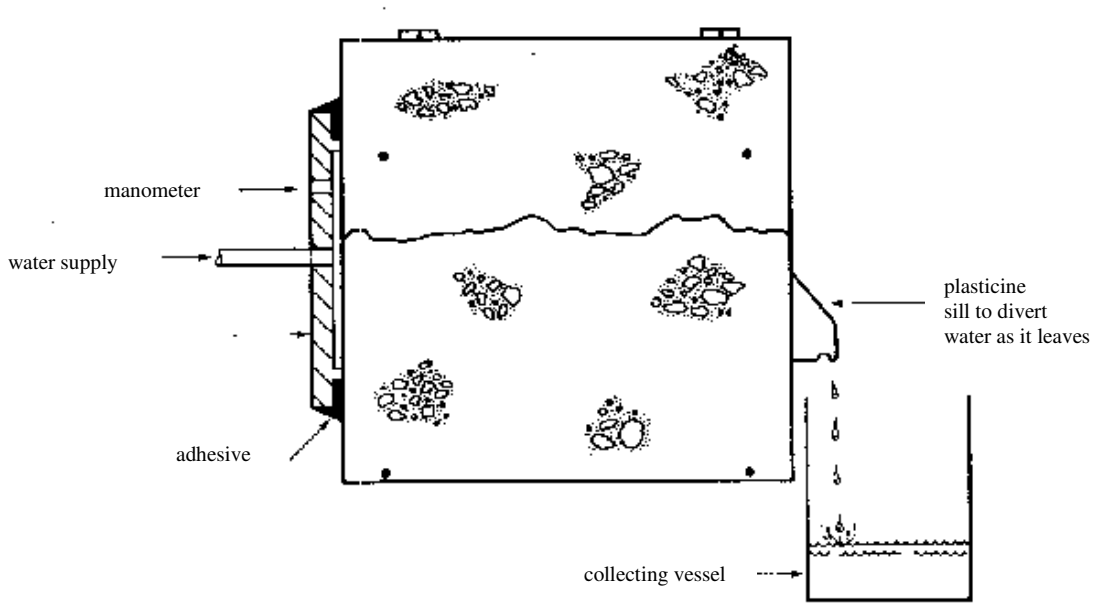

Figure 7.3 - Cross-section of testing experiment (after Clear 1985).

The leakage of water through cracks in concrete is mainly proportional to the effective width of the crack. The smaller the initial effective width, the faster the crack will seal. The healing mechanism is a combination of mechanical blocking and chemical precipitation of calcium carbonate. Results revealed that filling the reservoir slowly could significantly reduce the total loss of water from the reservoir.

6.5 MOIST CURING AND PERMEABILITY

Tan et al. (1995) performed tests on 100mm by 100mm cube specimens of concrete aged two months to determine the desirable moist curing conditions necessary to limit permeability. The testing faces were brushed before a water pressure was applied to the face of the tested specimens as shown in Figure 2.4. Pressure heads of 0.3, 0.5, and 0.7 MPa were applied for the 1st, 2nd, 3rd day respectively. Specimens were split at the conclusion of testing to determine their penetrating fronts. Tests revealed that specimens cured in water for two days did not show significant differences in permeability as those cured in water for six days. Only specimens soaked for 28 days showed significant drops in concrete permeability. In all cases, the silica fume concrete had a much higher resistance to water penetration than the specimens without.

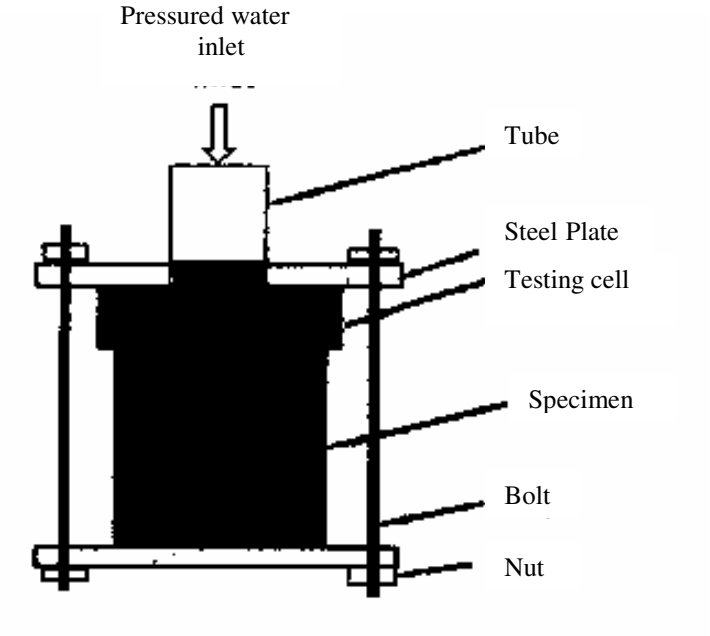

Figure 7.4 - Test setup for water penetration test (after Tan et al. 1996).

6.6 WATERSTOP TESTING

Tatro et al. (1988) summarized techniques for replacing damaged waterstops, primarily in dams. Waterstop failures are generally attributed to excessive movement of the joint which ruptures the waterstop, honeycomb areas adjacent to the waterstop resulting from poorly consolidated concrete, contamination of the waterstop surface which prevents bond to the concrete, punctures of the waterstop or complete omission during construction and breaks in the waterstop due to inadequate or non-existing splices. The life of a waterstop is related to the relative movement across the joint. As the movement increases the life of the waterstop decreases.

Wallis' (1992) paper looks into efforts to decrease or eliminate water penetration through underground tunnel walls. Water penetration can cause safety hazards through freezing and unsightly stains. Wallis (1992) reported that water will always find a path around obstacles and creating an impermeable barrier (waterproofing membrane) between water source and protected environment is most cost effective and secure method of ensuring a watertight underground structure.

Kishel (1989) performed tests to study the cost effectiveness of providing a lining at contraction joints between concrete slabs that make up the lining of a canal. The linings are often waterstops or sealants applied to the joint to limit water leakage. Seepage rate tests were performed on an unlined concrete canal in Arizona. Information was also available for two canals located within 100 miles of the test site that were lined with polyvinyl chloride strips or elastomeric sealant.

Evaporation of water from the canal was determined through the use of a class A Weather Service evaporation pan that was installed next to the pan in a secure area. The

seepage rate for the unlined canal was calculated as 0.036ft^3/ft^2/day. The seepage rate for the two canals with linings was found to range between 0.0110-0.090ft^3/ft^2/day. The open jointed canal rates were within the range of the sealed joint canal. The value of water saved over a 20- or 30- year payback period would be less than the cost of sealing at present cost levels. Observed rates indicate a lack of economic justification for providing contraction joint sealing.

6.7 COMPACTION LEVEL FOR CONCRETE CONSTRUCTION JOINTS

Liou (1996) described tests to determine the effects of construction joints in the Kawasaki man-made island in the center of Tokyo Bay. The island was so extensive that the concrete for the basemat-of the island would have to be completed in several pours. The tests were designed to simulate the worst conditions that could be experienced in the field. They wanted to determine the best placing schedule and compaction level for the concrete to produce the best joint. The joint was evaluated in terms of compressive strength tests of cylinders and when testing initial vibration, slump tests were also performed.

The concrete used in the tests was too flowable to allow meaningful conventional slump data to be gathered. The worst-case condition experienced in the field was for a joint that formed a 45-degree angle. Liou (1996) found that compaction of concrete layers seems to have a beneficial effect on the compressive strength of the large-sized concrete specimen (150mm diameter, 300mm high). Tests showed that placement delay times longer than four hours seemed to have a slight detrimental effect on the strength. Also, the initial vibration of the concrete delays the hardening process in the concrete and prolongs its workability over time.

Loiu (1996) reported that the level of compaction was simulated by either striking a concrete layer with a standard stick a predetermined number of times or by introducing a small vibrator into the concrete layer. A test specimen that simulated a medium compaction level in the field received 10 stick strikes in each of the two casting layers of concrete; while a test specimen that simulates maximum compaction level in the field received 25 stick strikes per layer. When a vibrator was used it was carefully introduced into the sample at several equally spaced points for a total vibrational duration of 40 seconds. This helped to obtain uniform compaction and to avoid segregation in the sample. Results showed that vibration provided by a small vibrator generally had a better effect than vibration provided by using a striking rod.

6.8 SUMMARY

The literature review has revealed that limited research is available on joints in floating bridges. The main reasoning for this limited information is due to the fact that only a limited number of floating bridges exist in the world. It is evident from this limited literature that there have been two approaches to deal with water penetration through concrete joints. The first one is the use of special material added to the joint that act as water stoppers or barriers to water flow. The chemical composition, placement and application processes of these materials vary significantly. The second approach is to allow the rough surfaces of concrete joints to act as barriers for the flow. The experimental plan in the remaining parts of this thesis investigates the effectiveness of these two approaches in reducing or eliminating water infiltrations through joints in floating bridges.

CHAPTER 7: MATERIALS AND TESTING METHODS

7.1 MIX DESIGN SPECIFICATIONS

The mix design for the reconstruction of the Lacey V. Murrow Floating Bridge across Lake Washington was used for this project. The mix was chosen based on its water-tightness, durability and low permeability. The mix was modified to use only a superplasticizer, Glenium 3000 NS instead of the normal and high-range water reducers. The materials needed to produce the test specimens were shipped from mixing plants around the state to Washington State University. Table 8.1 contains the mix design chosen for the laboratory experiments. The final mix prepared at Washington State University is described in Table 8.2.

7.2 TEST SPECIMENS

Specimen dimensions were chosen after studying a typical joint in the Hood Canal Floating Bridge. The joint had a thickness of 18 inches with a 3/4in deep by 9-inch long keyway centered within the joint as shown in Figure 8.1. Test specimen dimensions were reduced because of space and weight considerations. Specimens needed to be small enough to construct and store within a tight work area and be light enough to allow easy handling. Smaller dimensions produced a worst-case scenario because the wall thickness, and therefore the distance water must travel through the joint would be far greater in the field.

Specimens were 8 inches thick, 16 inches long and 12 inches tall. A construction joint was placed halfway up the height and contained a 1/2in deep by 3-inch wide keyway centered in the specimen's depth. Two thin steel plate’s 1/8in thick, 8 inches

wide and 16 inches long were bonded to the freshly poured concrete at the top and bottom of the 12in tall specimen. Figure 8.2 shows the dimensions and layout of a typical specimen. The plates were designed to help hold the freshly poured concrete in place and distribute the pressure applied to two 7/8in steel bars embedded into the concrete. The steel bars were attached to nuts welded to the bottom steel plate. Two one-inch diameter openings in the top steel plate were provided to allow the bars to slide through. Schematics of the steel plates are shown in Figure 8.3.

The steel bars were spaced 8 inches on-center at the center of the specimen's thickness. The bars were threaded over the bottom one-inch of length to allow threading into nuts welded to the bottom plate. Threading was provided over the top 19 inches of the 30in bar length to allow threading of a nut. Figure 8.4 shows a picture of the steel bars and lower plate.

Specimens were cast within forms built for the experiment. The forms were connected together to make the necessary dimensions. Two sets of forms were created for each specimen. The first set was 6 inches tall while the second set was 12 inches tall. The 6-inch forms created a box placed over the lower steel plate. The two 7/8in steel bars were connected into the plate and a one-inch diameter PVC tube was placed around the steel bars. The tube separated the concrete from the steel reducing the chances of small stress cracks near the steel. The tubes were cut just long enough to measure 12 inches when added to the height of the nuts they rested on. Figure 8.5 shows the placement of forms around the steel bars and the location of the PVC tubes covering the steel bars.

Six 10in long carriage bolts were embedded into the specimen's face. The bolts were applied in a circular pattern with the construction joint located in the center. The bolts were needed to attach a pipe with flanged fitting to the face of the specimen. The pipe supplies a water pressure to the face of the specimen. Holes were drilled into the forms in the locations of the flange's boltholes. The carriage bolts were embedded halfway into a specimen's depth with a 1/2in flat washer glued to each bolt to provide additional pullout resistance.

Concrete compaction and smoothing completed the construction of the initial concrete pour. A hand trowel was used to smooth the surface of the joint and to create the keyway shown in Figure 8.6. The 6-inch specimens were placed near wet burlap and covered for 24 hours to cure. After the 24-hour period ended specimens were removed from the 6-inch forms and the 12in forms were fastened in place.

The final pour of concrete was 48-hours after the completion of the initial pour. The concrete was compacted and smoothed by hand trowel. The top steel plate was fitted over the 7/8in steel bars and firmly pressed down onto the freshly poured concrete. Specimens were placed beside wet burlap and covered for 24-hours to cure. After 24 hours specimens were removed from the forms creating a finished specimen as shown in Figure 8.7.

Two 60ton hollow plunger cylinders were used in unison to tension the 7/8in steel bars of each specimen simultaneously. A nut was threaded the full 18 inches onto the steel bars. The nuts were threaded until hand-tight against the steel plate. A steel spacer was then placed over the bars to provide room for tightening the nuts after jacking. The hydraulic cylinders were placed over the bars to rest on the spacer. A one-inch thick steel

bar with two one-inch circular openings was placed over the cylinders. Finally a nut was threaded down the 7/8in bars to the one-inch thick steel bar. The post-tensioning setup is shown in Figure 8.8.

The nuts were tightened against the one-inch thick steel bar before the hydraulic cylinders were loaded. A hand pump with pressure gauge was used to load the cylinders. The two cylinders were attached to the hand pump by a pressure T that applied an equal pressure to both cylinders. The cylinders were loaded slowly forcing the one-inch steel bar and top nuts upward applying tension to the 7/8in steel bars. The system was loaded to a 3000psi gauge pressure reading on the hand pump before the bottom nuts were tightened and the pressure was released from the cylinders. The top nuts, one-inch thick steel bar, hydraulic cylinders and steel spacer were then removed from the specimen. The process was repeated with all post-tensioned specimens. Loading of each specimen took a few minutes to complete.

Each post-tensioned bar was assumed to apply a pressure to the concrete over a confined area 3 inches in diameter. The thin steel plate resting on the specimens was too thin to effectively distribute the applied pressure after the force was transferred from the cylinders to the steel bars. The pressure applied to the concrete by the jacking force was calculated as 5402.78psi by the equation:

$$P = (P_j * A_{hc} * N) / A_e \quad (8.1)$$

where:

P = pressure applied to the specimen (psi),

P_j = pressure supplied by hand pump to cylinders (3000psi),

A_{hc} = effective area of one hydraulic cylinder (12.73in^2),

N = number of cylinders (2),

A_e = area of concrete effected by one hydraulic cylinder (assumed 3in diameter effective area =7.07in^2).

The 5402.78psi pressure applied to the concrete is much higher than that seen in the field. The pressure applied to the joint in the field is about 450psi at the joint. This was determined based on a 180kip force applied by tendons spaced 2ft on-center. The original pressure supplied by the hand pump was determined assuming that the force applied to the specimens would be applied over the entire surface of the specimens. The pressure this would have applied to the specimens assuming losses totaling 25% from the jacking system was 447psi. The plates located at the top and bottom of the specimens were too thin to effectively distribute the pressure throughout the specimen, hence the high-pressure concentration.

The increased compressive stress around the steel bars should not affect the results. The increased stress was over a very small area that increased the stress in that area but should not have significantly increased the stress in the surrounding areas. This increased stress would affect water penetration through the joint within this elevated compression area but should not affect the surrounding areas of the joint. The majority of the joint was unaffected by the increased compressive stress and would have functioned normally.

Table 8.1 Mix Design

Weights per cubic yard (saturated, surface-dry)	
Concrete Constituent	lbs.
Type II Portland cement	624
Silica fume (AASHTO M307)	50
Fly ash (AASHTO M295)	100
Paving sand	1295
Coarse aggregate	1770
Water	255
Water Reducing Agent (ASTM C494), ounces	none
Superplasticizer (Glenium 3000 NS), floz/cwt	4-12
Air entrainment:	none
Water/cement ratio	0.33
Slump, in	7-9
Compressive Strength, f'c, psi	6500

Table 8.2 Final Mix Design

Weights per cubic yard (saturated, surface-dry)	
Concrete Constituent	lbs.
Type II Portland cement	624
Silica fume (AASHTO M307)	50
Fly ash (AASHTO M295)	100
Paving sand	1295
Coarse aggregate	1770
Water	255
Water Reducing Agent (ASTM C494), ounces	none
Superplasticizer (Glenium 3000 NS), floz/cwt	5.50
Air entrainment:	none
Water/cement ratio	0.33
Slump, in	8
Compressive Strength, f'c, psi	8788

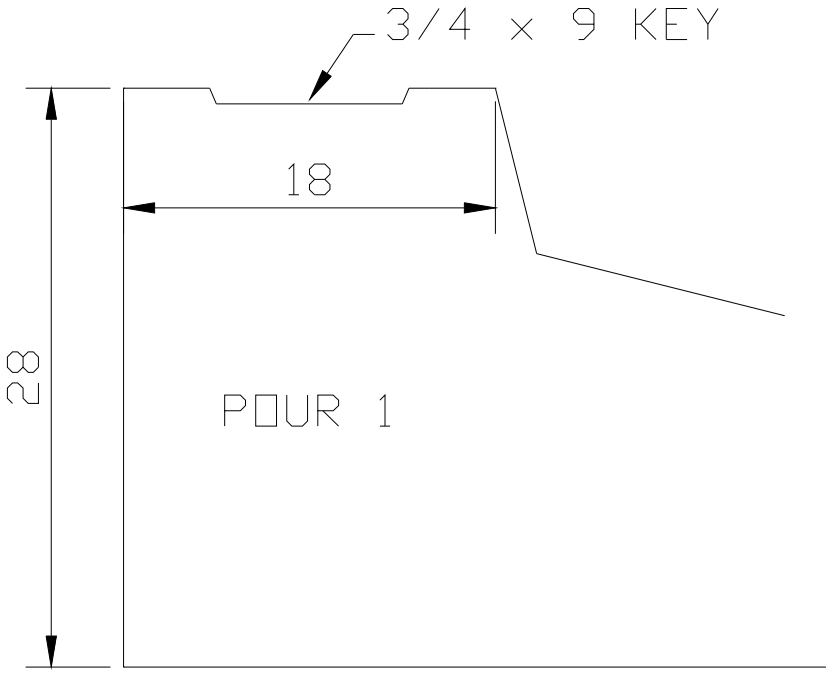

Figure 8.1 - Keyway dimensions in field (after Hood Canal Retrofit and East-half Replacment Construction Plans: SEC C-C).

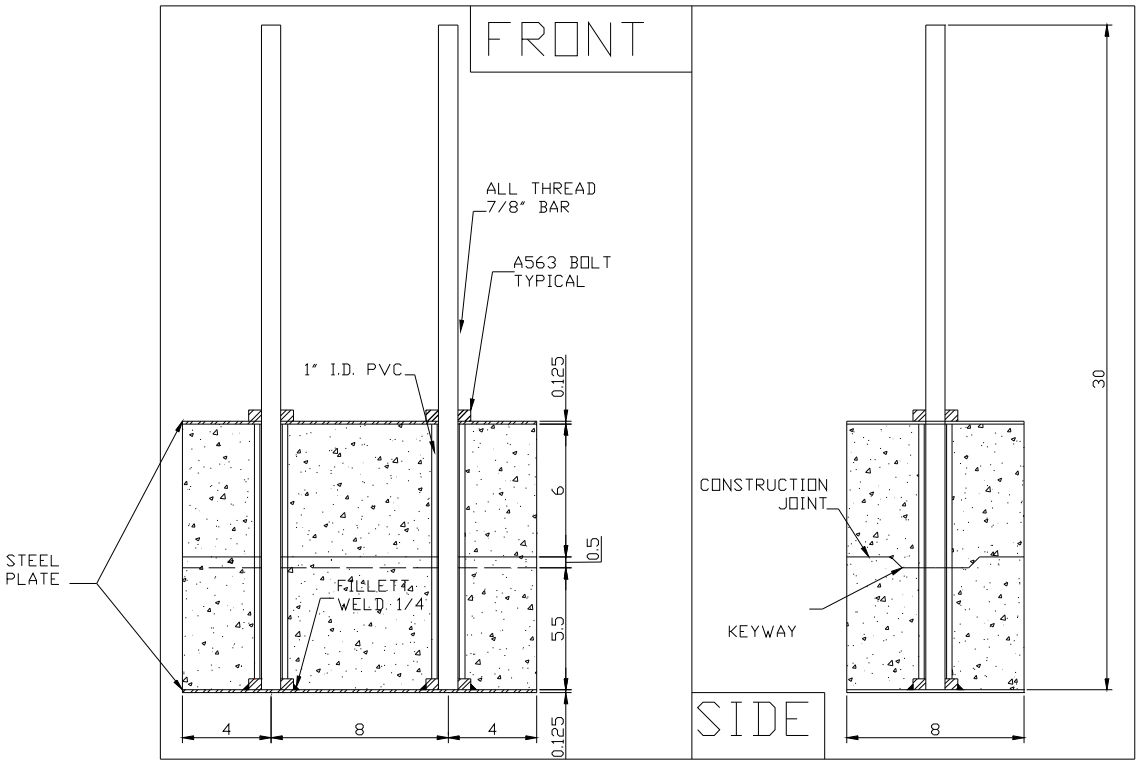

Figure 8.2 - Test specimen dimensions.

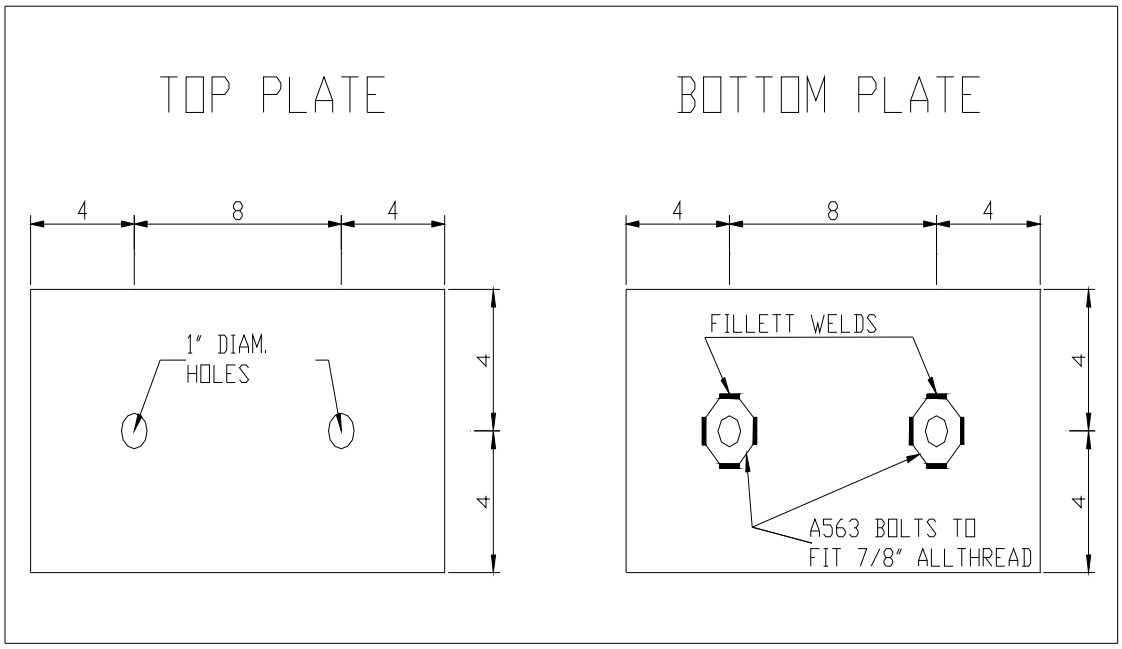

Figure 8.3 - Dimension specifications for the steel plates.

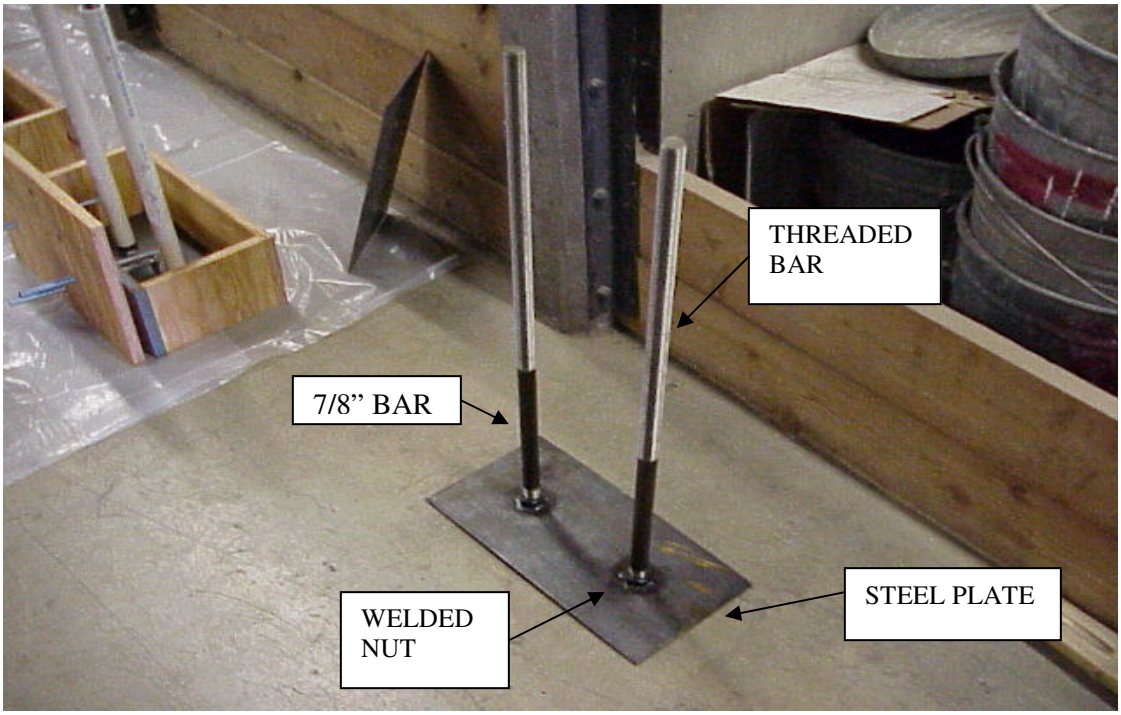

Figure 8.4 - Steel Bars 7/8in diameter screwed into bottom plate.

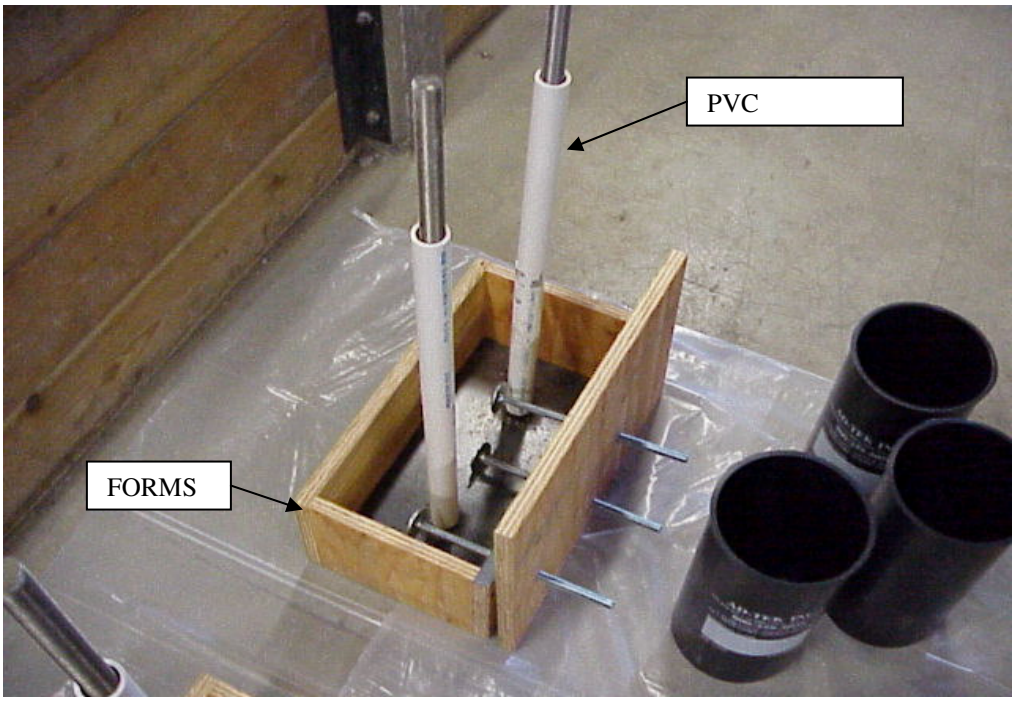

Figure 8.5 - Construction setup for initial concrete pour.

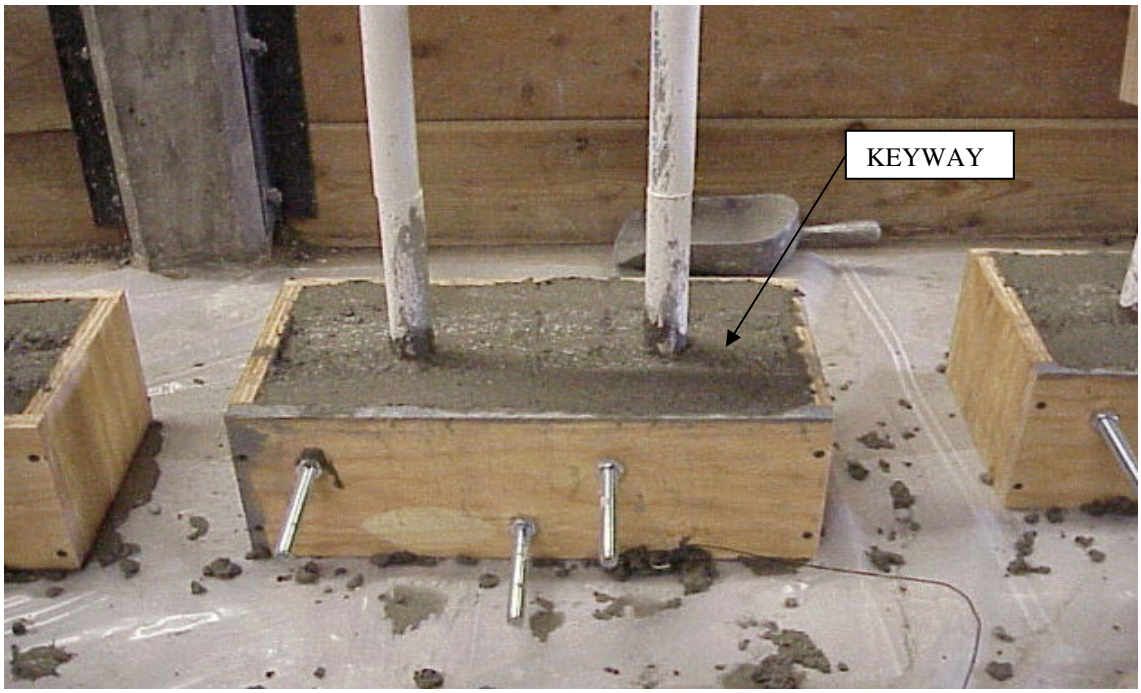

Figure 8.6 - Completed keyway of initial pour.

Figure 8.7 - Completed test specimens.

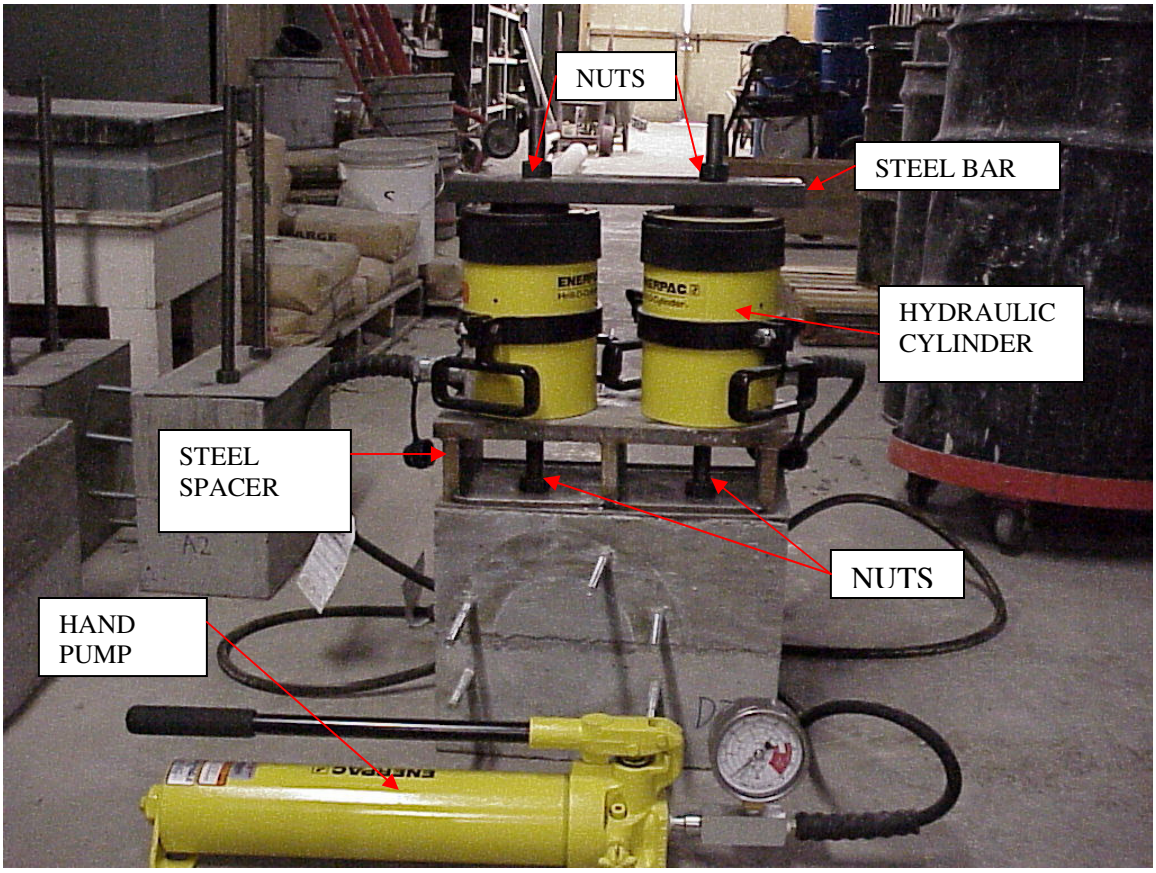

Figure 8.8 - Hydraulic cylinder setup for post-tensioning the specimens.

7.3 PRODUCTS AND CONSTRUCTION METHODS TESTED

Products chosen for testing were determined based on manufacturer's recommendations and available product data sheets. Tested products included waterstops designed to prevent water penetration by forming a preventive barrier within the joint and a cement coating designed to prevent water penetration by forming a barrier outside the joint. The chosen products are listed in Table 8.3.

The construction methods chosen for laboratory testing were based on recommendations from the Washington State Department of Transportation (WSDOT 2001) and companies within the concrete industry. The different methods were designed to decrease water leakage at the joint by either; improving bond across the joint, increasing the surface area that water must follow to pass through the joint or by improving compaction at the joint. The construction methods chosen are listed in Table 8.4.

Table 8.3 - Products tested in experiments.

Product	Company	Advantages	Placement
MC-2010MN (Waterstop)	Adeka Ultra Seal USA	expands upon contact with water, forms water barrier	within keyway on negative pressure side of 7/8in steel bars
Synko-flex (Waterstop)	Henry	adhesive waterstop, bonds to freshly poured concrete during curing, forms water barrier	within keyway on negative pressure side of 7/8in steel bars
Waterstop-RX 101TRH	CETCO	expands upon contact with water, forms water barrier	within keyway on negative pressure side of 7/8in steel bars
Tegraproof (Coating)	ChemRex	slurry coat, seals wall-floor joints	brush applied to external face of specimen in direct contact with water pressure

Table 8.4 - Construction methods tested in experiments.

Construction Method	Procedure	Advantages	Placement
Mortar/slurry	3 parts sand to 1 part cement plus water **(WSDOT 2001)**	greater compaction at joint	first two inches of final pour
Preco HI-V	Retarder (Master Builders), brush applied to joint surface	exposes aggregate at joint, improves bond strength	freshly poured joint surface of initial pour
Raking Method	0.5in deep grooves 1.5 inches on-center (perpendicular to water flow)	lengthens water path through joint	freshly poured joint surface of initial pour

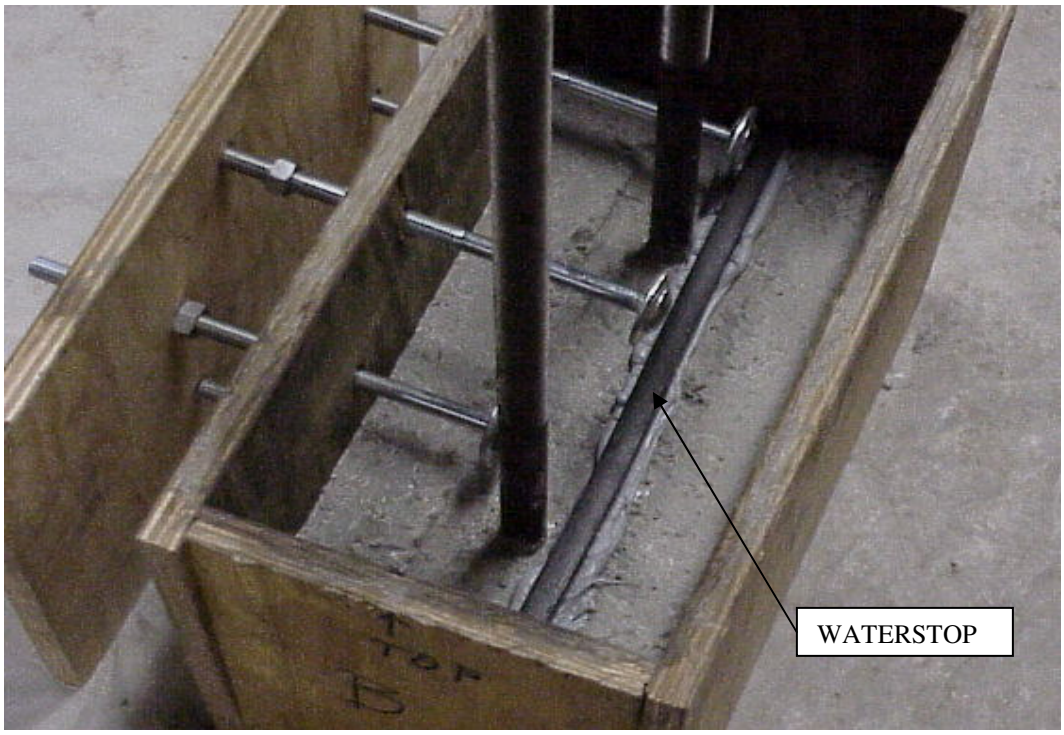

Figure 8.9 - Waterstop placement within construction joint of specimen.

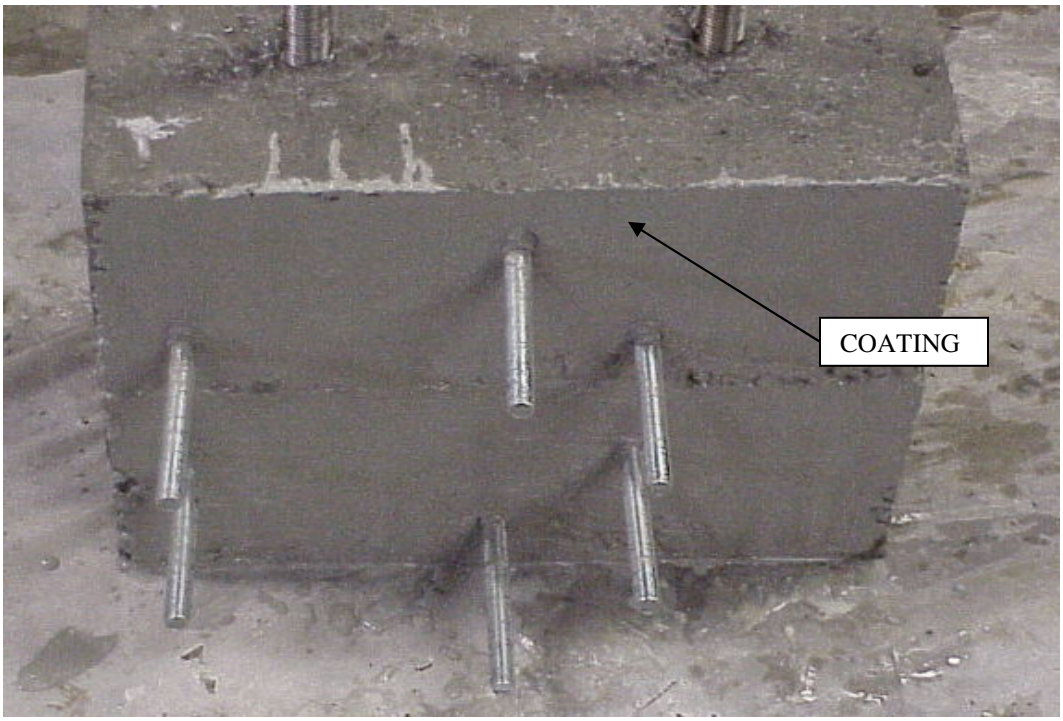

Figure 8.10 - Tegraproof coating placed on exterior joint face.

Figure 8.11 - Mortar/slurry grout over initial two-inch depth of the second pour.

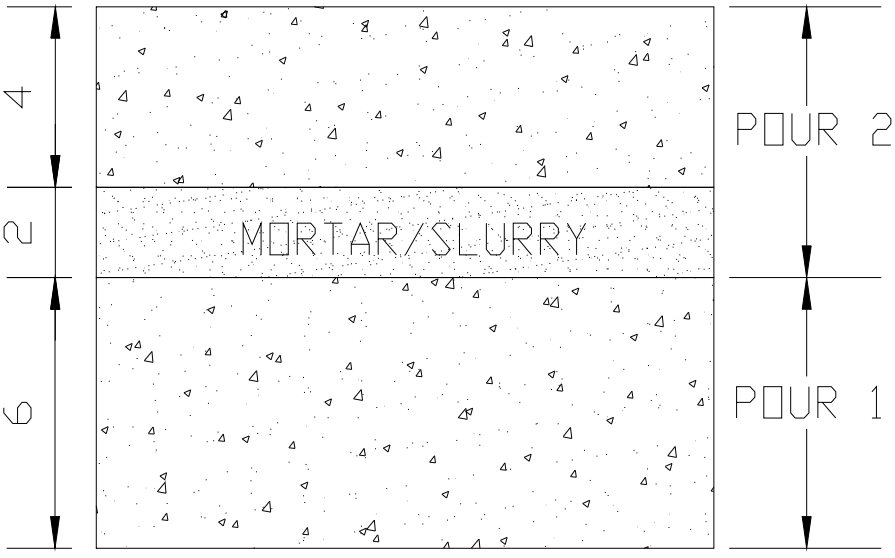

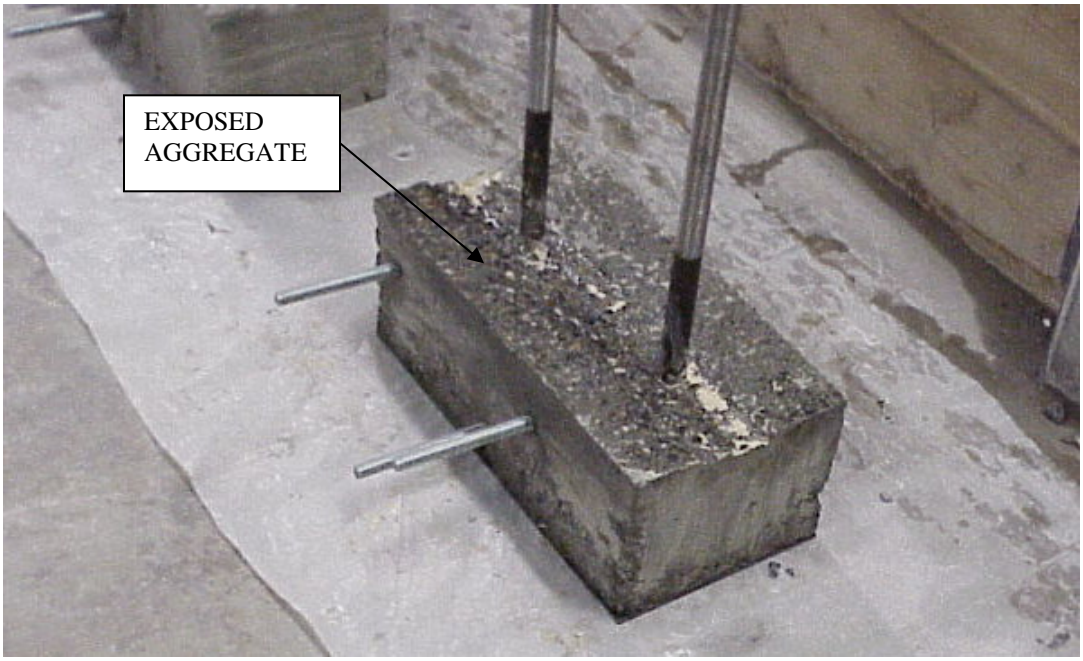

Figure 8.12 - Exposed aggregate along surface of joint caused by Preco HI-V.

7.4 EXPERIMENT 1

Experiment one involved exposing specimens to a constant water pressure similar to that experienced in the field. A typical pontoon for the Hood Canal Floating Bridge has a draft of 13ft. The horizontal construction joint studied was located 28in from the base of the pontoon creating a joint 128 inches or 10.67 feet below the water line. The water elevation of 128 inches corresponds to a pressure on the joint of 19.44psi. The pressure was determined by the equation:

$$P = \gamma h + P_0 \qquad \text{(Young et al. 1997))} \qquad (8.2)$$

where:

P = pressure on joint (psi),

γ = specific weight of fluid (salt water 64lb/ft^3 (Young et al. (1997))

h = water elevation height (in)

P_0 = atmospheric pressure (assumed 14.7psi (Young et al. (1997))

The 19.44psi pressure was supplied to the system by means of an elevated water reservoir with water elevation 128 inches above the surface of the specimens. The reservoir consisted of an 18in diameter PVC cap fastened to the ceiling. Water entered the reservoir through a constant inflow tube attached to the bottom of the cap. Water was supplied from a second reservoir located at the ground surface by a small 1/30hp centrifugal pump located on the ground. A tube was attached to the side of the elevated reservoir 128in above the surface of the specimens. The tube served as an overflow pipe for the upper reservoir and returned any excess water to the lower reservoir. The lower reservoir consisted of a plastic 55-gallon barrel filled with salt water from the Hood

Canal Floating Bridge. The system created was self-maintained and could be left unmonitored overnight.

Six flexible tubes were connected to the bottom of the elevated reservoir. The six tubes ran to different specimens. The tubes were connected to a 6-inch PVC cap glued to an 18in long PVC pipe. The PVC pipe was glued to the inside of a flanged fitting with eight bolthole openings. The PVC pipe was bolted to the side of the concrete specimens with the pipe centered on the joint.

The flanged fittings glued to the six-inch PVC pipe were connected to the concrete specimens by 10in long carriage bolts embedded into the concrete. Additional pullout resistance was supplied by gluing 1/2in flat washers to the carriage bolts. Six carriage bolts were embedded into each specimen because of limited spacing. A neoprene gasket was placed beneath the flanged fitting to prevent water leakage at the interface between the flange and concrete. The test setup is shown in Figure 8.13.

The system was designed to test up to six specimens simultaneously. Fewer specimens could be tested because 1/2in ball valves were connected to each specimen setup above the 6-inch cap. The valves could be closed to prevent water flow from tubes unconnected to specimens. The valves also allowed lines to be closed once leakage occurred to prevent pressure loss from the system.

A 3/8in bleed-hole was drilled into the 6-inch PVC cap. The bleed-hole allowed air to escape the system when water was being added. Once water began escaping through the bleed-hole the valve was closed and a 3/8in bolt with Teflon tape covering the threads was tightened in the opening. The ball valve was then reopened to finish filling the system with water. Specimens were shaken to remove any additional air

trapped beneath the six-inch PVC cap. Air bubbles were allowed to escape through the top of the reservoir. The pressure system connection to the test specimens is shown in Figure 8.14.

Hood Canal water was used for the experiment to ensure pressures similar to those experienced in the field. The supplied pressure was equivalent to the 19.44psi experienced in the field because the same fluid was used in the laboratory and the water elevation was held at 128 inches above the specimen. Any atmospheric pressure differences were ignored.

Specimens were placed on their sides in the testing apparatus to allow the water pressure supplied by the 6-inch pipe to be applied vertically. Specimens were placed on two 3.5-inch square wood beams located 14 inches apart on-center. The beams rested on cinder blocks that raised the specimens two feet off the ground allowing a large funnel to be placed beneath the specimens. The funnels were 18in diameter barrel funnels positioned beneath the specimens to catch water escaping through the specimens. Additional room was provided for a visual inspection of the underside of the specimens and to provide space for a small water collection beaker. Two people were needed to lift specimens onto the setup. The water collection system located beneath the specimens is shown in Figure 8.15.

Stage 1

Stage one consisted of four specimens. The four specimens included two controls one with a construction joint and one without as well as two waterstops MC-2010MN and Synko-flex as shown in Table 8.5. The four specimens were post-tensioned nine days after the second concrete pour. Specimens were compacted by mechanical stinger

repeatedly lowered into the freshly poured concrete for 30 seconds. Specimens were tested for 15 days with monitoring every 24 hours to observe water leakage. The time corresponding to when leakage occurred was recorded.

Table 8.5 - Stage one specimens.

Stage 1		
Product	**Product Placement**	**Construction/Application**
Control (No Joint)	N.A.	specimens completed in one pour, mechanical vibration of concrete
Control (Construction Joint)	N.A.	specimens completed in two pours, mechanical vibration of concrete
MC-2010MN Waterstop	within keyway on negative pressure side of 7/8in steel bars	two concrete pours, mechanical vibration of concrete; applied continuous bead of P-201 paste to the joint and allowed to cure for 24 hours before pressing MC-2010MN into the paste.
Synko-flex Waterstop	within keyway on negative pressure side of 7/8in steel bars	two concrete pours, mechanical vibration of concrete; brush applied Synko-flex primer to surface and allowed to dry 3 hours. Peeled release paper from one side of Synko-flex strip and press firmly onto primed surface.

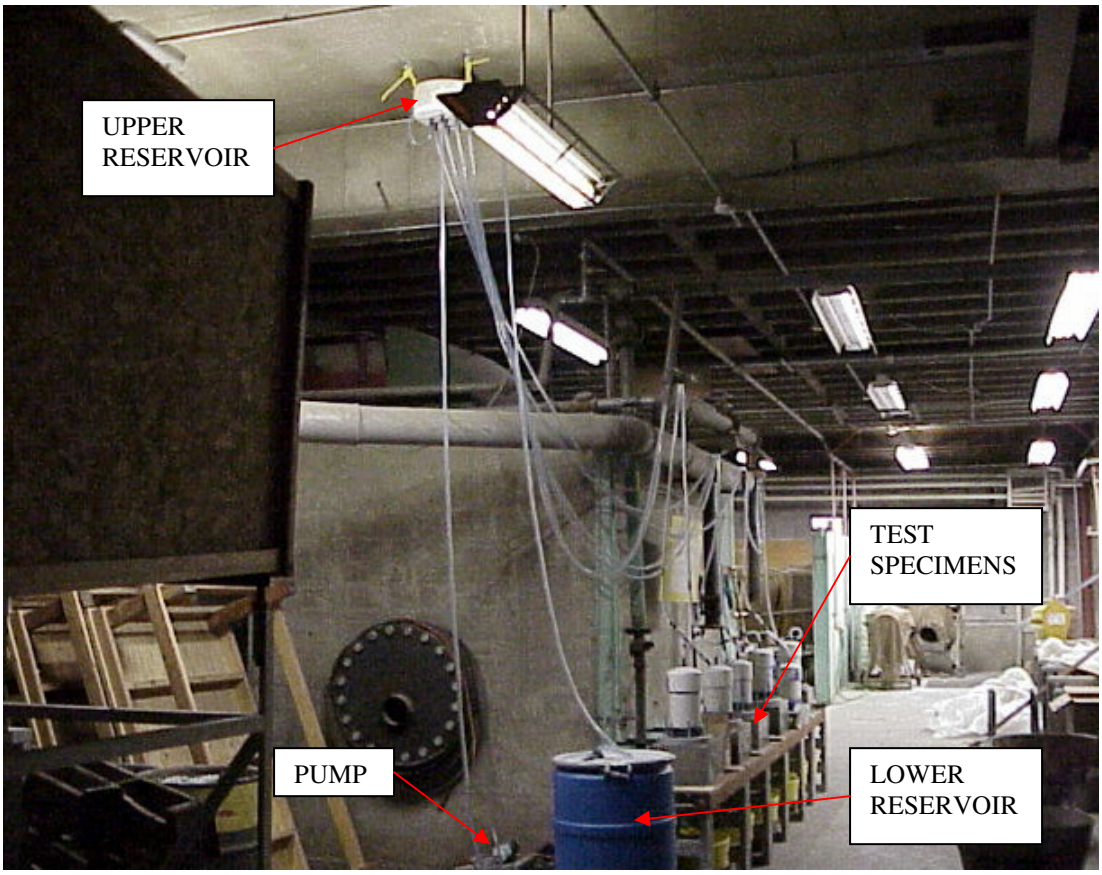

Figure 8.13 - Experimental setup of the first experiment.

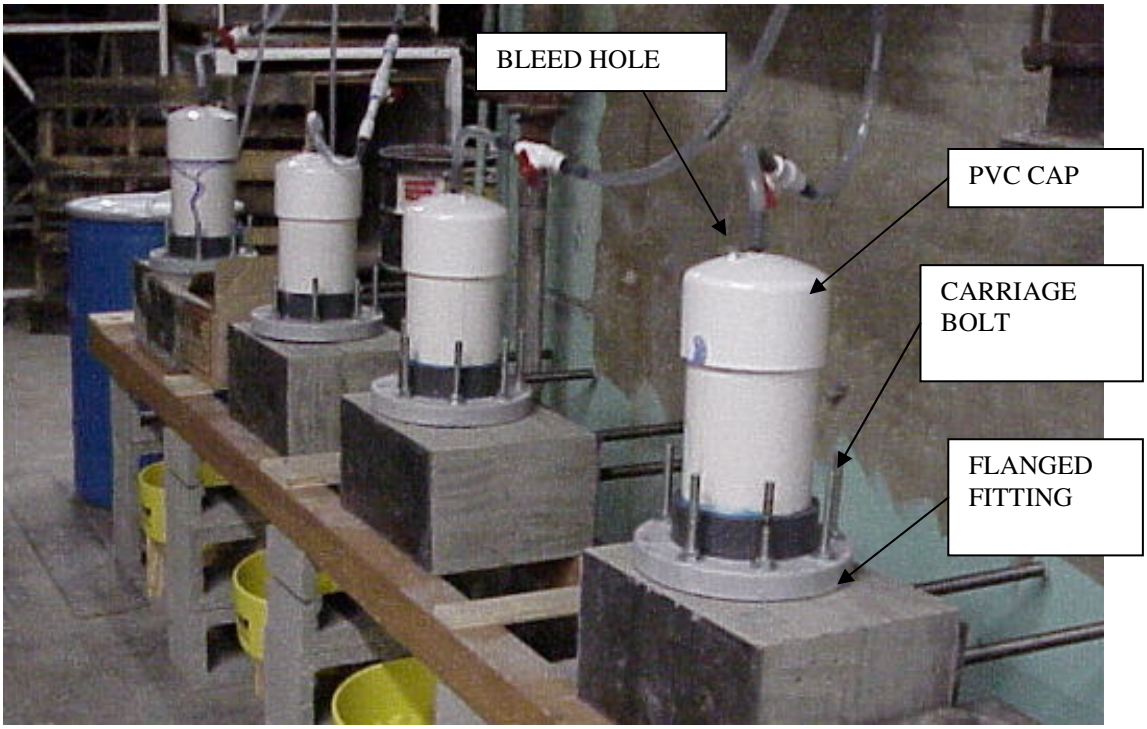

Figure 8.14 - Specimen connection to pressure system.

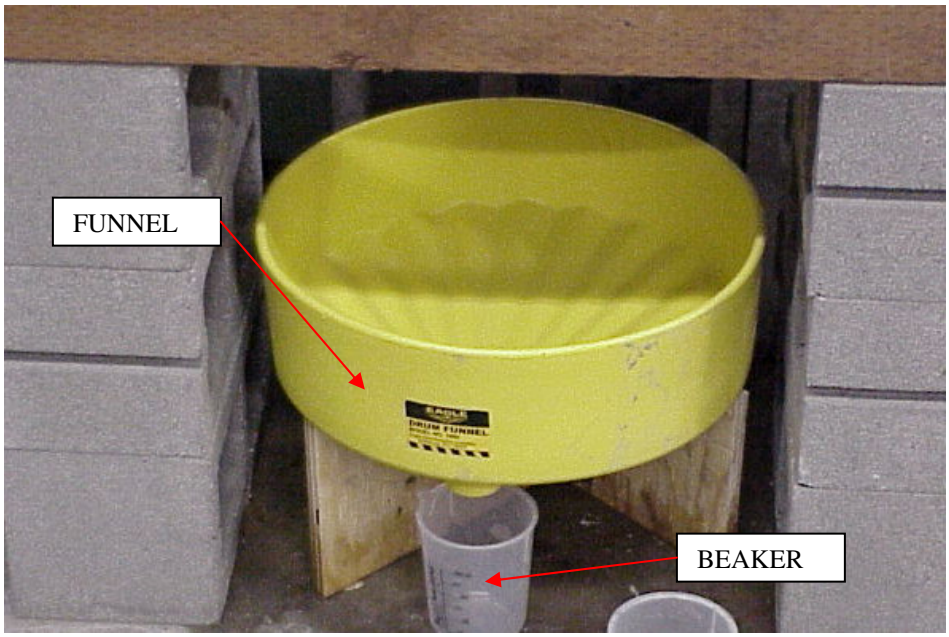

Figure 8.15 - Water collection system located beneath specimens.

7.5 EXPERIMENT 2

Experiment two involved placing a variable pressure on the system. The setup of experiment one was modified for use in experiment two. The pressure applied by the system needed to be significantly increased so the upper reservoir of experiment one was removed and an air pressure system was installed in its place.

Experiment one's testing setup was modified by removing the reservoirs and flexible tubing from the system. The experimental setup of the second experiment is shown in Figure 8.16. Air pressure was applied to the specimens by a 2-inch diameter galvanized steel pipe suspended above the specimens. Openings were placed every 18 inches along the galvanized pipe. A 2-foot long by 1/2in inner diameter clear plastic tube was securely fastened to the galvanized pipe as shown in Figure 8.17. Polyethylene hose with 1/2in outer diameter by 0.375in inner diameter was connected to the clear tubing and ran to the 1/2in ball valve of the original system. The polyethylene hose could hold a water pressure up to 123psi.

One end of the 2-inch diameter galvanized pipe was capped while the opposite end was connected to an air compressor by means of an air pressure hose. The hose was connected to a valve used as a shutoff for the system. The setup also included a pressure gauge and regulator used to increase and decrease pressure on the system as shown in Figure 8.18.

Water was added to the system after specimens were attached to the flanged fittings. The system was initially designed to allow water to be pumped into the galvanized pipe from the lower reservoir by means of a seventh connection to the galvanized pipe. Water was not pumped through the galvanized pipe because of the high

probability of corrosion. The valve connected to the seventh line was shut to prevent air leaks from the system through the open line. Water was poured into the system through funnels at the connections between the galvanized pipe and tubing.

The bleed-hole was used to release trapped air as the specimens were filled with water. After all air was removed from the line the water level was increased to a mark 4 feet above the surface of the specimens. The initial pressure on the specimens due to water elevation and atmospheric pressure was 16.48psi. Any air pressure added to the system was directly added to the initial pressure to obtain the total pressure on the system.

Air pressure on the system was increased until leakage occurred in all specimens. The valves were closed once leakage occurred to prevent pressure loss from the system. The leakage was recorded and used to determine the relative success of different products.

Stage 1

The specimens of stage one were re-tested using the variable air pressure system of experiment two. Stage one specimens were tested in experiment two, three months after initial casting. Air pressure on the system was initially zero and was increased every half hour to a maximum air pressure of 100psi.

Stage 2

Six specimens were cast in stage two constructions. The specimens consisted of the three waterstops; MC2010MN, Synko-flex and Waterstop-RX 101TRH as well as three specimens where the mortar/slurry was added over the first two inches of the second pour as shown in Table 8.6. The three waterstops were placed on the exposed

joint one-day after initial curing. Waterstops were placed 24 hours before submersion in tap water for five days. Specimens were then removed and allowed two days of drying before completion of the second pour of concrete.

Table 8.6 - Stage two specimens.

Stage 2		
Product	**Product Placement**	**Construction/Application**
MC-2010MN Waterstop	within keyway on negative pressure side of 7/8in steel bars	two concrete pours, mechanical vibration of concrete; applied continuous bead of P-201 paste to the joint and allowed to cure for 24 hours before pressing MC-2010MN into the paste.
Synko-flex Waterstop	within keyway on negative pressure side of 7/8in steel bars	two concrete pours, mechanical vibration of concrete; brush applied Synko-flex primer to surface and allowed to dry 3 hours. Peeled release paper from one side of Synko-flex strip and press firmly onto primed surface.
Waterstop-RX 101TRH	within keyway on negative pressure side of 7/8in steel bars	two concrete pours, mechanical vibration of concrete; brush applied WB-ADHESIVE to joint surface, allowed to dry for 20 minutes before waterstop pressed onto surface
Mortar/slurry over normal joint	applied to first two inches of second pour	two concrete pours, mechanical vibration of concrete, initial pour was normal. Mortar/slurry: 91lbs sand, 30lbs cement, 9.9lbs water and 5mL superplasticizer
Mortar/slurry applied over exposed aggregate surface caused by (Preco HI-V)	Preco HI-V retarder to joint surface, Mortar/slurry applied to first two inches of second pour	two concrete pours, mechanical vibration of concrete, initial pour had Preco HI-V applied to freshly poured surface for 24 hours before being washed off. Mortar/slurry: 91lbs sand, 30lbs cement, 9.9lbs water and 5mL superplasticizer
Mortar/slurry applied over raked joint surface	Grooves cut into joint surface of initial pour, Mortar/slurry applied to first two inches of second pour	two concrete pours, mechanical vibration of concrete, initial pour contained no keyway, grooves cut into freshly poured concrete. 1/2in deep by 1-1/2in on-center, Mortar/slurry: 91lbs sand, 30lbs cement, 9.9lbs water and 5mL superplasticizer

The mortar/slurry was placed at the time of the second pour of concrete. The mortar/slurry was applied to the first 2 inches of the second pour. Construction methods differed for the initial pour of concrete for each of the three specimens. One specimen consisted of a typical initial pour of concrete as described in section 8.2. The next two specimens were designed to increase the surface area along the joint of pour one, thereby improving bond strength and forcing water to follow a longer path to penetrate through the specimen. One specimen had Preco HI-V, a chemical retarder used to expose aggregate, applied to the freshly poured joint surface of pour one. The second specimen used a raking method to create grooves in the concrete surface perpendicular to the flow path of water through the specimen. No keyway was used with the raking method; instead grooves were cut in the flat joint surface by dragging a thick wire through the freshly poured concrete. The vertical grooves were a 1/2in deep and spaced an inch-and-a-half on-center.

The six specimens of experiment two were tested two-and-a-half months after the final concrete pour. The specimens were post-tensioned and tested on the same day. Specimens were compacted by mechanical stinger lowered into the freshly poured concrete for 30 seconds. Air pressure on the system was initially zero and was increased every half hour to a maximum air pressure of 100psi.

Stage *3*

Six specimens were tested in stage three. The six specimens included one control joint, the Tegraproof coating brush applied to the external surface of the specimen in direct contact with the water pressure and a 2-inch thick mortar/slurry placed over a normal initial concrete pour. Additional specimens included the Preco HI-V retarder

applied to the joint surface of the initial concrete pour, and two waterstops: MC2010-MN and Synko-flex as shown in Table 8.7. The specimens of stage three were tested 29 days after the final pour of stage three.

Table 8.7 - Stage three specimens.

Stage 3		
Product	**Product Placement**	**Construction/Application**
Control (Construction Joint)	N.A.	specimens completed in two pours, compacted by 10 stick-strikes
MC-2010MN Waterstop	within keyway on negative pressure side of 7/8in steel bars	two concrete pours, compacted by 10 stick-strikes; applied continuous bead of P-201 paste to the joint and allowed to cure for 24 hours before pressing MC-2010MN into the paste.
Synko-flex Waterstop	within keyway on negative pressure side of 7/8in steel bars	two concrete pours, compacted by 10 stick-strikes; brush applied Synko-flex primer to surface and allowed to dry 3 hours. Peeled release paper from one side of Synko-flex strip and press firmly onto primed surface.
Mortar/slurry over normal joint	applied to first two inches of second pour	two concrete pours, compacted by 10 stick-strikes, initial pour was normal. Mortar/slurry: 24lbs sand, 8lbs cement, 3.2lbs water
Preco HI-V Retarder	Preco HI-V retarder applied to joint surface to expose aggregate	two concrete pours, compacted by 10 stick-strikes, initial pour had Preco HI-V applied to freshly poured surface for 24 hours before being washed off.
Tegraproof Coating	applied to surface of specimen directly exposed to water pressure	two concrete pours, compacted by 10 stick-strikes, Tegraproof mix: 10lb Tegraproof, 3.41lb water; brush applied to wetted joint surface, surface kept moist for 48 hours

No PVC tubing was placed around the 7/8in bars because the specimens were not post-tensioned. Specimens were compacted by 10 stick-strikes of the slump rod during each pour to reduce compaction at the joint and represent poor compaction that could occur in the field during construction. The 1/8in steel plate placed on top of earlier specimens was not used because no post-tensioning occurred. A concrete filler/sealant

was applied to the surface of the joint to ensure that water leakage would occur only through the joint. The sealant was applied to the sides of the specimen and across the specimen face, except in the area in direct contact with the water pressure as shown in Figure 8.19. The back of the specimen was left uncovered to allow water penetration to occur through the specimen.

Figure 8.16 - Experimental setup of the second experiment.

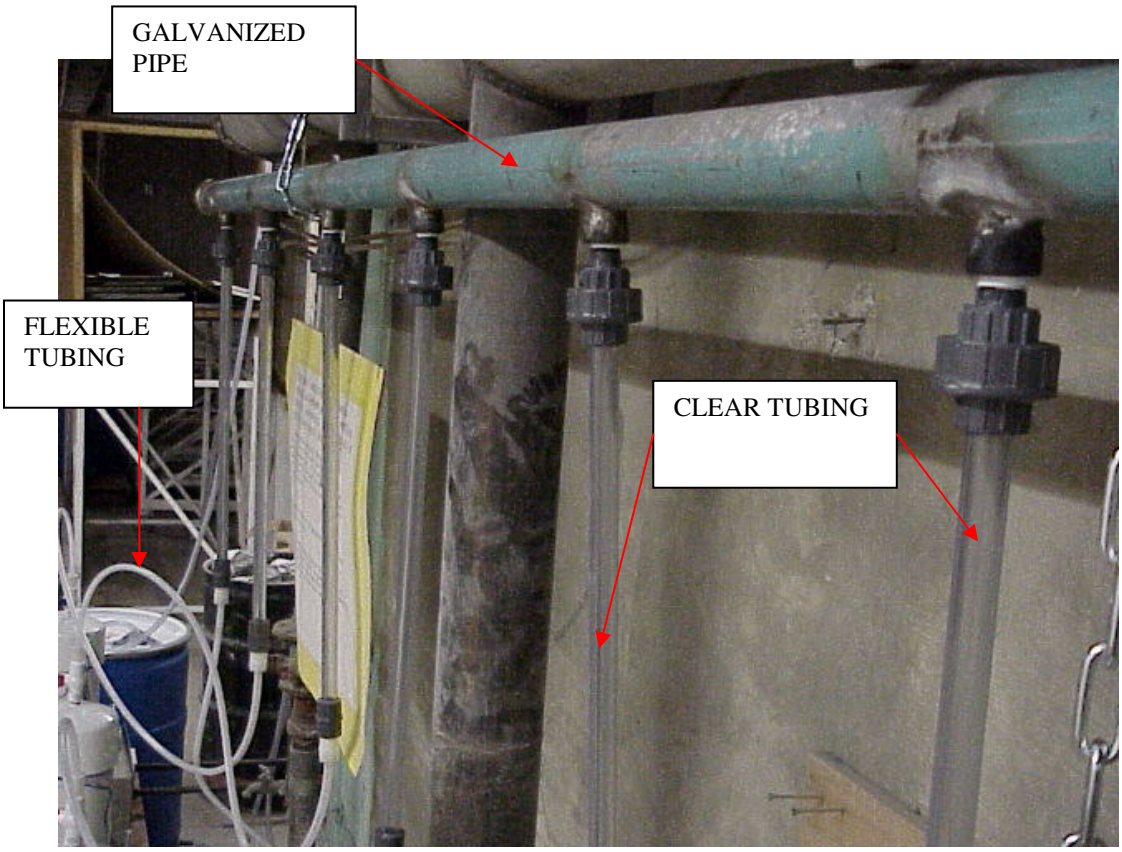

Figure 8.17 - Connection of clear plastic tubing to galvanized pipe.

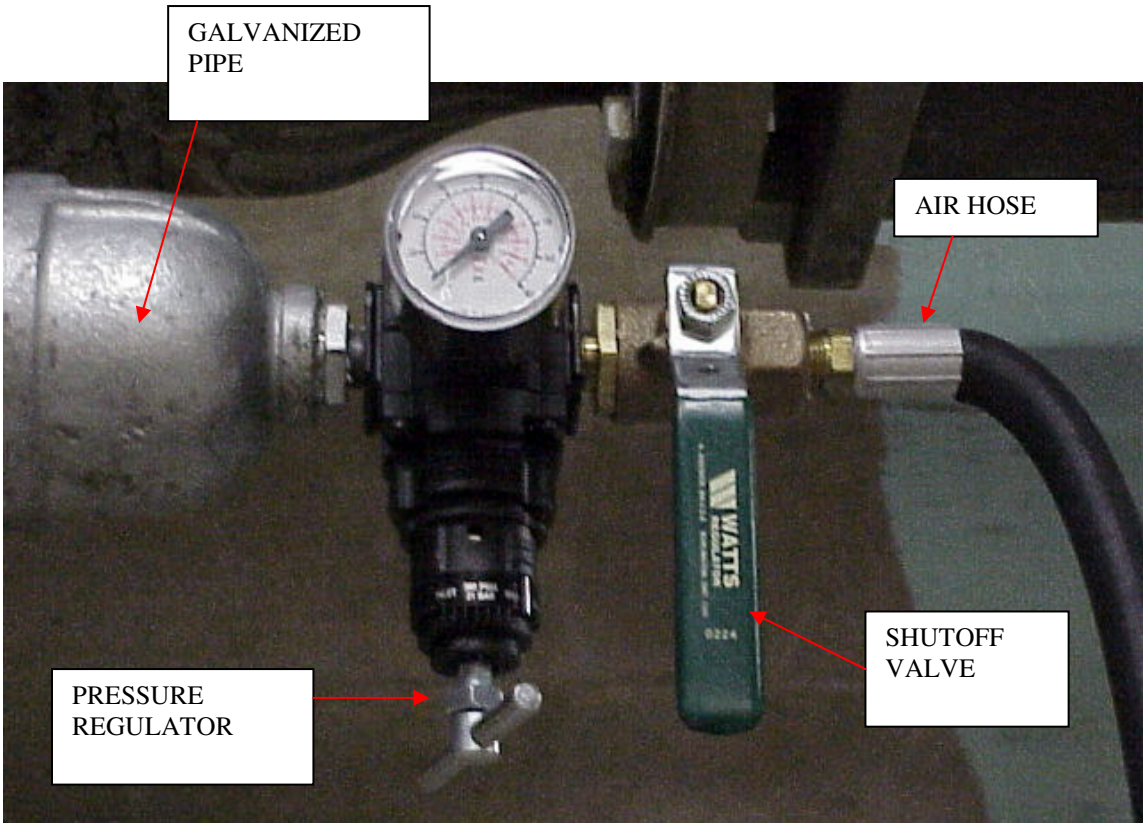

Figure 8.18 - Pressure regulator for air pressure system.

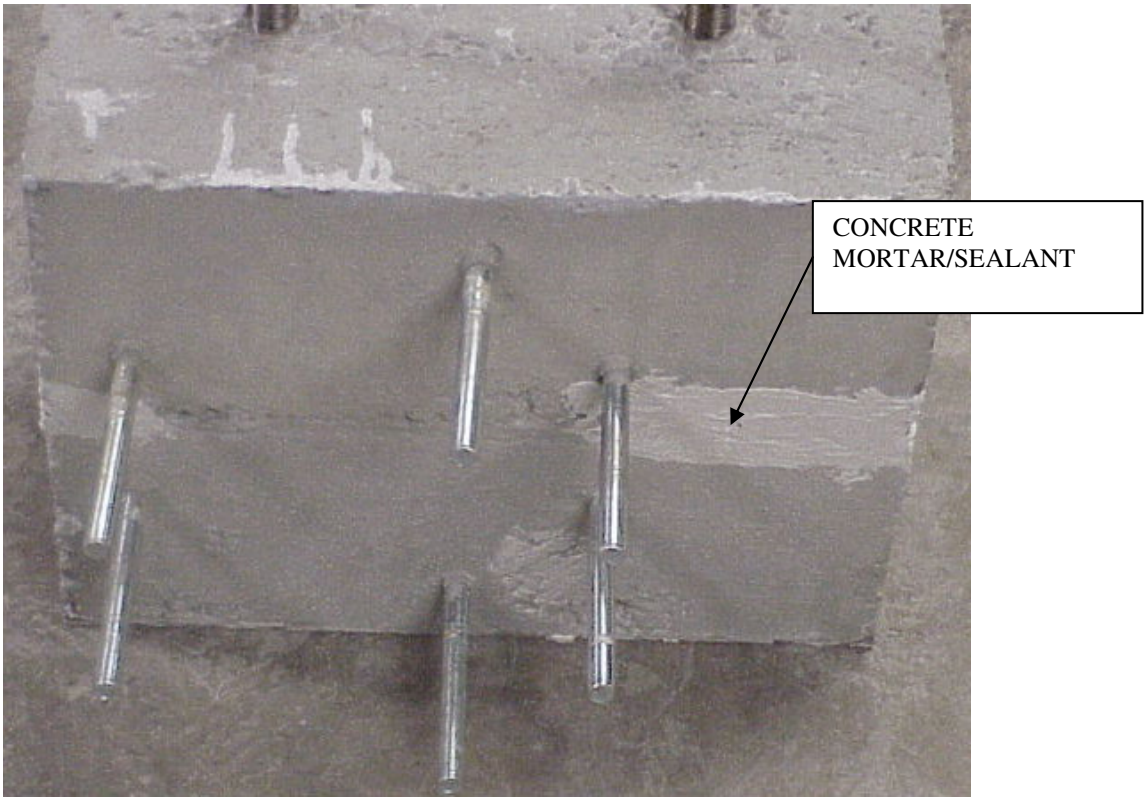

Figure 8.19 - Concrete filler and sealant applied to the construction joint of stage three specimens.

7.6 EXPERIMENT 3: WATERSTOP TESTING

The Washington State Department of Transportation (WSDOT) was concerned with premature expansion of the tested waterstops. An extended period of time could elapse between the pouring of the first and second pours of concrete in the field. Waterstops placed on the joint surface during the initial pour could be exposed to severe environmental conditions that might cause waterstop swelling. WSDOT wanted to ensure that for a worst case scenario (standing water on the waterstop) the waterstops would not expand excessively before the second pour of concrete. Excessive expansion of a waterstop before joint completion could lead to waterstop damage or failure.

Three samples of each waterstop tested in earlier experiments were cut into 200mm lengths for the experiment. One sample of each waterstop was placed in a plastic container filled with tap water. Samples were completely submerged beneath the surface of the water to simulate a submerged joint in the field. Waterstops that floated were placed beneath plastic strips anchored beneath the water surface. Figure 8.20 shows the experimental setup of experiment three.

Measurements of waterstop weight, length and thickness were taken at intervals. Measurements were taken at day 0, 1, 3, 5, 7, 10, 14, 15, 20, 28, 31, 36 and 42. Samples were removed from the containers and wrapped in paper towels to remove excess surface moisture from the specimens before weighing. After all measurements were recorded samples were re-submerged. Expansion rate determined by equation:

Expansion rate = (weight after soaking – weight before soaking) / weight before soaking.

Figure 8.20 - Testing setup of the third experiment.

CHAPTER 8: TEST RESULTS

8.1 MIX CHARACTERISTICS

The characteristics of the mix prepared at Washington State University were described in Table 8.2. All specimens were prepared as closely to the LVM mix design as possible. The amount of water reducer used per mix was slightly modified to create a more workable mix. Concrete compressive strength and slump were determined for six test cylinders made with the given mix. Slump tests and compressive strength tests were not performed for each concrete pour due to the similarity between pours.

8.2 EXPERIMENT 1 TEST RESULTS

Four 8x12x16 inch concrete specimens were tested in the first experiment according to methods described in section 8.3. The specimens tested in the first experiment were two controls, one with and one without a construction joint and two waterstops, the MC-2010MN product and the Synko-flex product. The specimens were exposed to a water pressure of 19.44psi for 15 days. Specimens were repeatedly checked over the initial two days of testing to observe leakage in the system. No leakage was observed during the first two days of testing. Observations were taken once every 24 hours for the remainder of the test. Testing was stopped after 15 days because no water leakage was observed through any specimen.

No leaks were observed from the pressure system connected to the specimens. The water elevation in the system was held constant throughout the duration of the test. The pump was able to transport water from the lower reservoir to the upper reservoir without interruption.

The four specimens tested prevented water penetration through the joint for a pressure of 19.44psi. The test was inconclusive in determining the effectiveness of a given product at preventing water penetration through the joint. All specimens prevented leakage including the control specimen containing a construction joint. The jointed control should have been the first specimen to leak out of all specimens tested. The inability to produce water leakage through the specimens showed that the pressure supplied by the system was inadequate for determining the most effective product or testing method for preventing water leakage.

The lack of water leakage from the test specimens at a pressure similar to those experienced in the field that cause leakage shows that construction methods in lab were better than those used in the field. The specimen joint had a much smaller thickness than that in the field but was not exposed to the excessive stresses experienced in the field due to wave and tidal fluctuations. A likely reason the specimens did not leak is improved concrete compaction in the lab. Nichols (1964) stated that concrete in the field was poured from significant heights over large areas before being vibrated. The lower drop height, reduced specimen size, better access to the joint and the use of the LVM mix in the lab all helped to improve joint construction, thereby reducing water penetration.

8.3 EXPERIMENT 2 TEST RESULTS

As discussed in Chapter 8, the setup of the first experiment was modified to apply a variable air pressure to the system as described in section 8.4. A variable air pressure system was used because the pressure that would cause leakage through the specimens was unknown. Air pressure could be slowly increased until leakage occurred through the joint. The initial water pressure on the system was 16.48psi. Air pressure applied to the

system would be added to the initial water pressure to compute the total pressure applied to the specimens.

Stage One

The four specimens tested in the first experiment were retested in the second experiment using the variable air pressure. Water levels within the clear plastic tubing connected to the galvanized pipe were monitored and water heights recorded to determine water volume decreases. Measurements were taken every half hour to determine decreases in water volume and to observe any water leakage from the system, both through the specimen and pressure system. Air pressures were increased every half-hour from an initial pressure of zero to a final pressure of 100psi. The 100psi air pressure was held on the system for 30 minutes before testing was completed.

Water volume decreases within the clear tubing at different air pressures are shown in Figure 9.1. The same water volume decreases are shown for total pressure changes in Figure 9.2. Measurements of water level changes were no longer recorded after they fell below the clear tubing. Water level changes were taken immediately before increasing the pressure. Decreases in water volume were seen in all four specimens tested. Water volume changes were no longer recorded once water leaks occurred within the pressure system of a specimen. The Synko-Flex waterstop specimen experienced a leak in the pressure system after 5psi air pressure was applied to the system. A leak was observed in the pressure system for the control specimen containing construction joint at 25psi air pressure. The specimens all had similar water volume changes when no leaks were observed in the pressure systems.

No water leakage was observed through the construction joint of the test specimens at any pressure. Testing was stopped after 100psi air pressure was held in the system for 30 minutes. Water leaks from the system did not significantly reduce air pressure in the system. Pressures close to six times that experienced in the field were applied to the joint without causing leakage. No leakage was observed through the specimen showing that construction methods used in lab were better than those used in the field. The specimens were too highly compacted to allow water leakage through the joint.

The MC-2010MN specimen had water volume decreases very similar to the joint-less control specimen even though one specimen contained a construction joint and one did not. Neither specimen experienced a significant leak from their pressure systems. The control specimen containing construction joint also had similar water volume decreases before a pressure system leak was observed at an air pressure of 20psi. The three specimens all had similar water elevation changes when there were no leaks in the pressure system. The likely reason was the high level of concrete compaction caused the second pour of concrete to completely bond to the initial concrete pour effectively closing the construction joint.

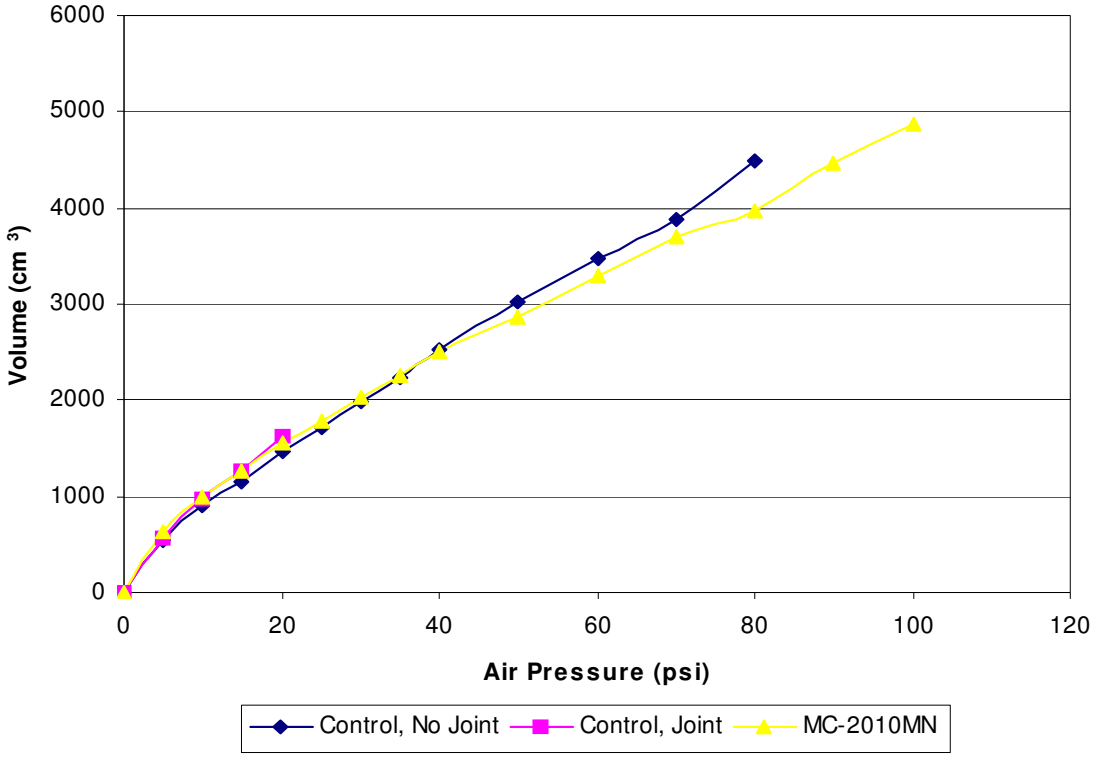

Figure 9.1 - Water volume changes versus air pressure applied to stage one specimens of the second experiment.

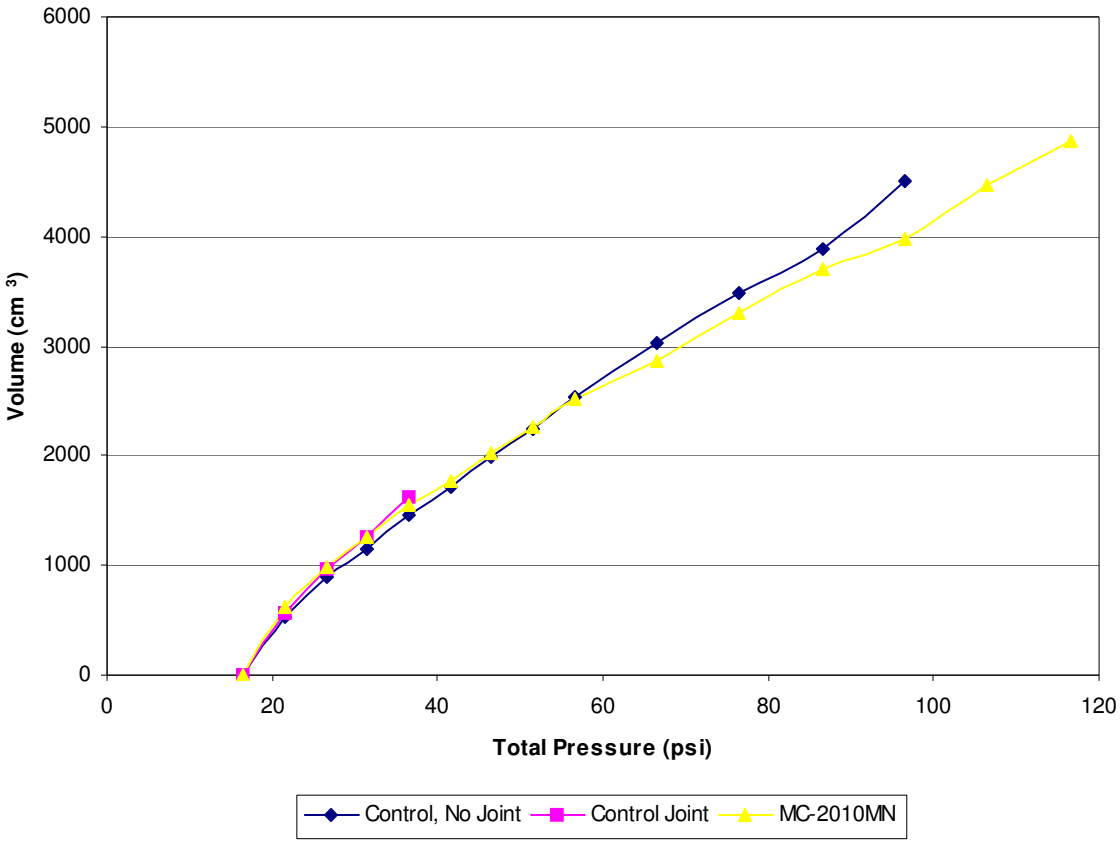

Figure 9.2 - Water volume changes versus total pressure on the system for stage one specimens of the second experiment.

Stage Two

Six specimens were constructed for stage two testing. The six specimens included the three waterstops; MC-2010MN, Synko-flex and Waterstop-RX 101TRH as well as three specimens where a mortar/slurry mixture was added over the first two inches of the second concrete pour to create the joint. The mortar/slurry was placed over a normal joint, over an exposed aggregate surface created by the Preco HI-V retarder and over a concrete surface that had been raked to form grooves in the concrete of the joint. The six specimens were completed before testing was finished for the first experiment. The specimens were constructed and compacted similarly to those of stage one.

The water elevation in each specimen setup was recorded. Air pressure in the system was increased 10psi every 10 minutes for the length of the test. Testing began with no air pressure on the system and concluded after 100psi was held on the system for 10 minutes. No leakage was observed through any specimens' construction joint.

Decreases in water volume within the clear plastic tubing were recorded immediately before air pressure was increased. All pressure systems other than the system connected to the Synko-flex product leaked immediately. The pressure applied in the previous experimental stage had caused leaks in the pressure systems that had not been effectively repaired. Leakage occurred at the connection between the 6-inch PVC cap and 6-inch pipe or at the interface between the pipe and flanged fitting. The Synko-flex specimen was connected to a pressure system unused in stage one testing.

Leakage was experienced almost immediately in five of the six specimens. Water volume changes were inaccurate for determining the effectiveness of different products at preventing water penetration through a construction joint for the five specimens that

experienced pressure system leaks. The Synko-flex product was connected to the only setup that contained no observable leaks from the pressure system.

Figure 9.3 shows a graph of the water volume decrease versus air pressure for the Synko-flex specimen of stage two along with the MC-2010MN specimen and control specimen with no construction joint of stage one. The three specimens have similar water volume decreases with increases in air pressure even though stage two pressures were increased more rapidly.

No leakage was observed through the construction joint of any specimen tested in stage two. Volume decreases in stage two testing are similar to stage one testing for specimens that experienced no leakage from the pressure system. All 10 specimens tested in stages one and two should have had similar water volume decreases to those of the control specimen without joint if no water losses occurred through the pressure system. Water loss through leaks in the pressure system was the predominant factor effecting water volume decreases.

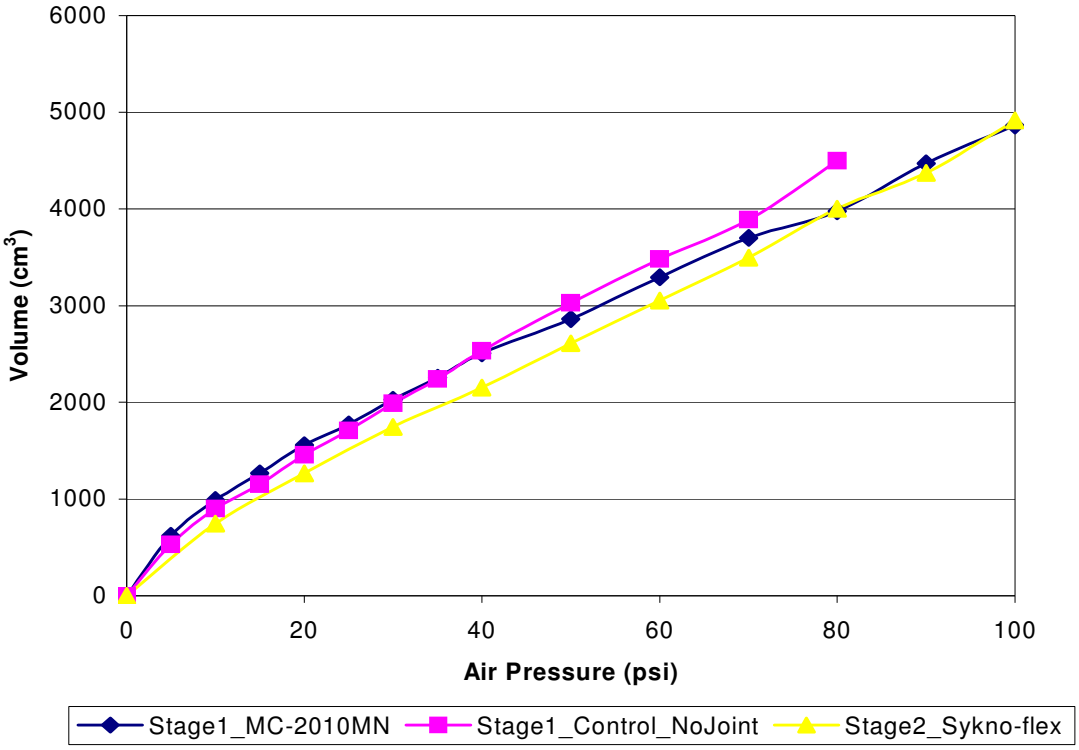

Figure 9.3 - Water volume changes versus air pressure for the three specimens of stages one and two that experienced no leakage from the pressure system.

Stage Three

The six specimens of stage three were constructed without mechanical vibration of the concrete. The specimens were compacted by 10 stick-strikes of the slump rod per specimen pour. The completed specimens contained significant honeycombing of the concrete within the first few inches of each pour. No post-tensioning of the concrete was performed. The six specimens tested included one control joint, the Tegraproof coating, the mortar/slurry over normal initial pour, the Preco HI-V retarder to expose aggregate along the joint, and two waterstops; MC-2010MN and Synko-flex.

Specimens were compacted without mechanical vibration and post-tensioning to investigate the influence of compaction on leakage. The high occurrence of honeycombing near the joint seemed likely to cause leakage through the construction joints of the specimens, even at low pressures. Specimens were placed on their sides and water was poured along the joint to determine whether specimens would leak without any air pressure being applied.

Four of the six specimens completed in stage three constructions leaked immediately when water was poured along the joint. Water leakage was fast enough to ensure that placing the four specimens within the testing setup was meaningless because water would leak at too high a rate to obtain meaningful results. The two specimens that did not immediately leak were the mortar/slurry mixture over a normal initial pour and the Tegraproof coating applied to the surface of the joint. The two specimens were placed in the pressure system and water was added through the connection between the galvanized pipe and clear plastic tubing. Water began leaking through the construction joints within several minutes.

Leakage occurred through the two specimens within minutes due to their prolonged exposure to the water added to the system. All six specimens initially had water poured over the joint to check for leakage but only four leaked immediately. The four specimens that immediately leaked had significant openings within the construction joint that allowed a clear path for water flow through the joint. The mortar/slurry specimen and Tegraproof specimen had smaller openings that caused water to take a less direct path to penetrate through the specimens. The mortar/slurry helped improve consolidation at the joint thereby limiting air voids at the joint and the Tegraproof coating helped to cover the face of the joint thereby impeding waters path through the joint. There was most likely a small hole that opened in the Tegraproof coating that allowed the leak to occur.

Both specimens leaked through the construction joint before any air pressure was added to the system. Water was continually added to the system until reaching the marks drawn on the clear tubing four feet above the surface of the specimens at which point measurements of water loss through the joint began being taken. Water that passed through the construction joint of the two specimens was collected and weighed to determine volume lost at varying times as shown in Figure 9.4. No pressure was applied to the system until leakage had stopped for 35 minutes in one of the specimens.

An air pressure of 10psi was applied to the system after leakage had stopped for 35 minutes for the Tegraproof coated specimen. Pressures were increased 10psi every hour for the remainder of the test. Testing was stopped after 30psi was held on the system for one hour.

The Tegraproof and mortar/slurry mixture specimens had similar water leakage amounts as shown in Figure 9.5. The graph shows total water lost immediately before air pressures were increased. The Tegraproof product had less initial leakage when no air pressure was on the system. The Tegraproof specimen healed itself more rapidly than the slurry coating and was completely healed for 35 minutes before pressure was applied to the system. When the 10psi air pressure was added the Tegraproof specimen quickly began leaking more excessively than the mortar/slurry specimen. As pressure was increased both the mortar/slurry and Tegraproof specimens leaked more excessively.

All six specimens tested in stage three leaked excessively before air pressure was applied to the system. Four of the six specimens leaked when water was poured over the construction joint. The two specimens that did not initially leak had either a surface coating that helped prevent water penetration or contained a mortar/slurry at the joint that improved consolidation at the joint. Both products leaked before any air pressure could be applied to the system showing that compaction levels in the lab were inadequate to allow the determination of the most effective product for limiting water penetration.

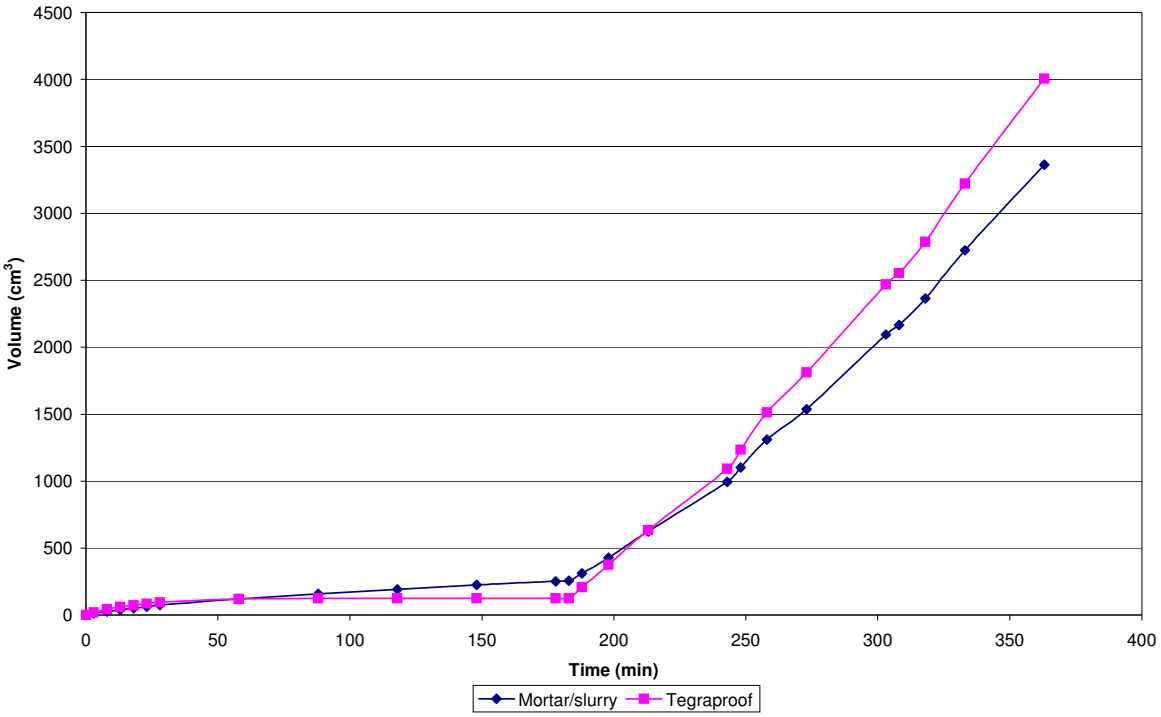

Figure 9.4 - Water volumes lost versus time for the stage three specimens tested.

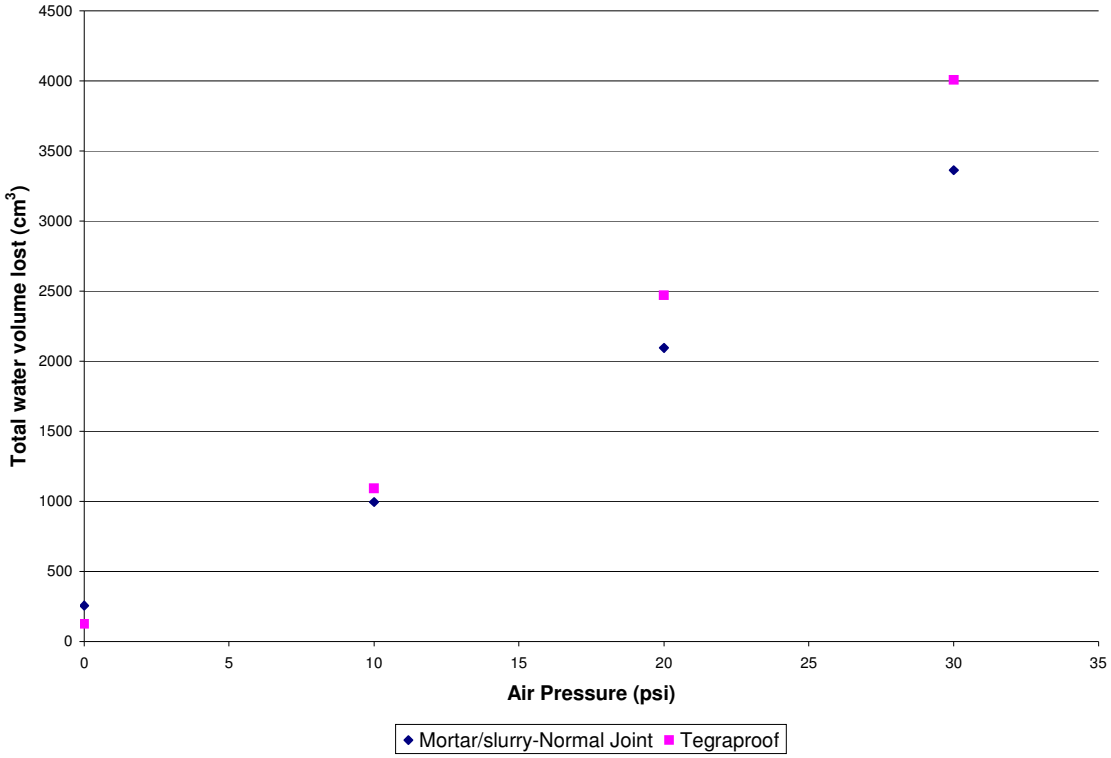

Figure 9.5 - Total water volume lost at a given air pressure for stage three specimens immediately before air pressure was increased.

8.4 THIRD EXPERIMENT: TEST RESULTS

The three waterstops tested in the third experiment performed very differently. Measurements of waterstop expansion and thickness increases were taken. Waterstops damaged during handling were removed from testing. Testing began with three samples of each waterstop.

The Waterstop-RX 101TRH product swelled almost immediately when placed in water. The Waterstop-RX products had expansion rates over 200 percent by day seven as shown in Figure 9.6. The Waterstop-RX products became difficult to handle once soaked and would easily break during handling. One sample was damaged after only one day of testing. The other two Waterstop-RX 101TRH samples became too difficult to handle by day seven.

The MC-2010MN product expanded much more slowly than the Waterstop-RX product. The product had an expansion rate over 100% close to day 20 as shown in Figure 9.7. The product was much easier to handle than the Waterstop-RX product. After day 30 expansion of the product slowed considerably.

The Synko-flex product expanded the least. The product was not designed to expand upon contact with water as test results showed. After 40 days of submersion in water the Synko-flex product had expanded less than two percent as shown in Figure 9.8.

The average expansion rates of the three different waterstops are shown in Figure 9.9. The figure clearly shows that the Synko-flex product expands the least of any of the three products while the Waterstop-RX product expanded the most. The average thickness increases of the three waterstops are shown in Figure 9.10. The thickness increases follow the general waterstop expansion rate increases.

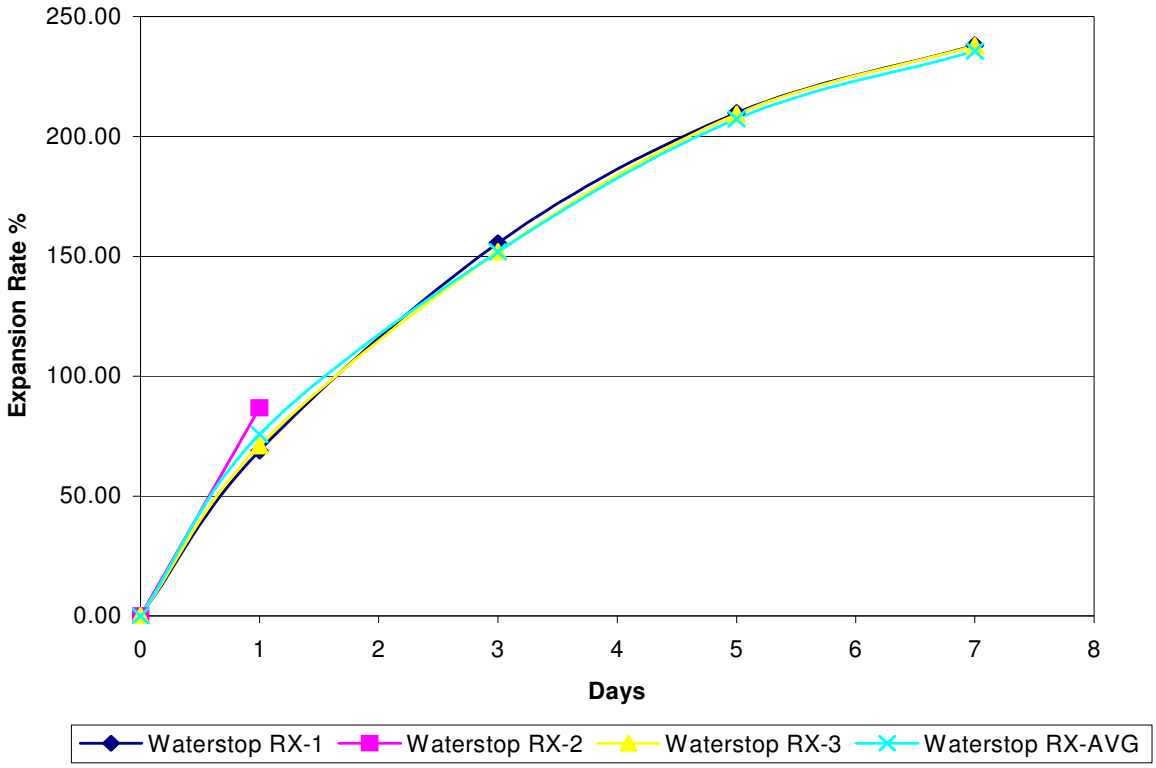

Figure 9.6 - Expansion rates of Waterstop-RX 101TRH samples in the third experiment.

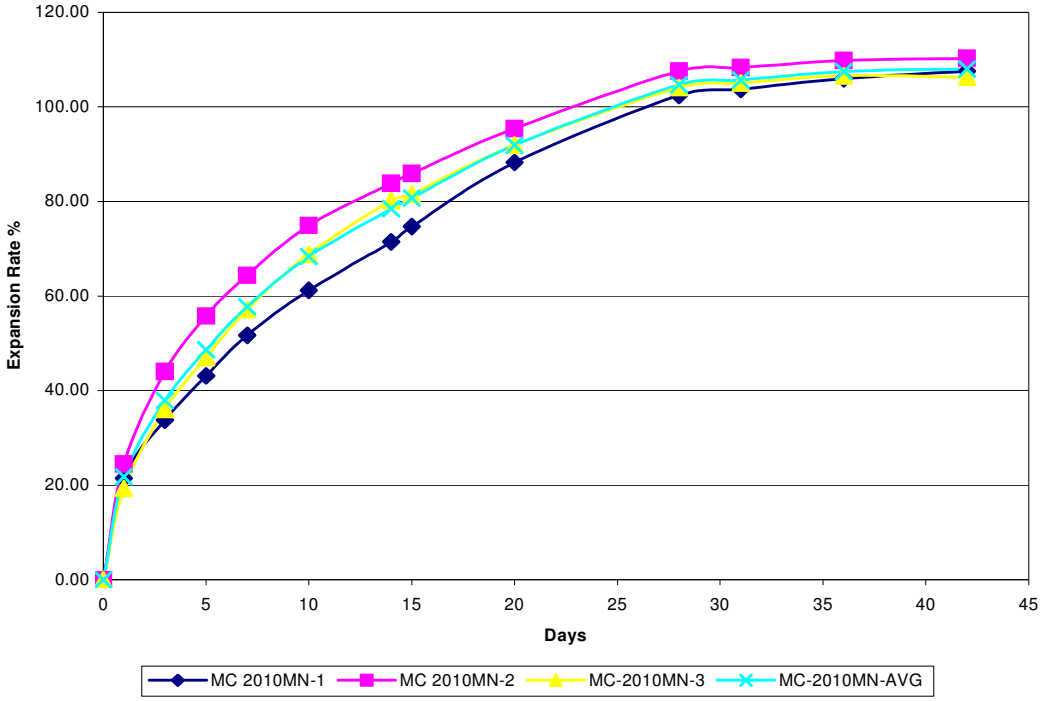

Figure 9.7 - Expansion rates of MC-2010MN samples in the third experiment.

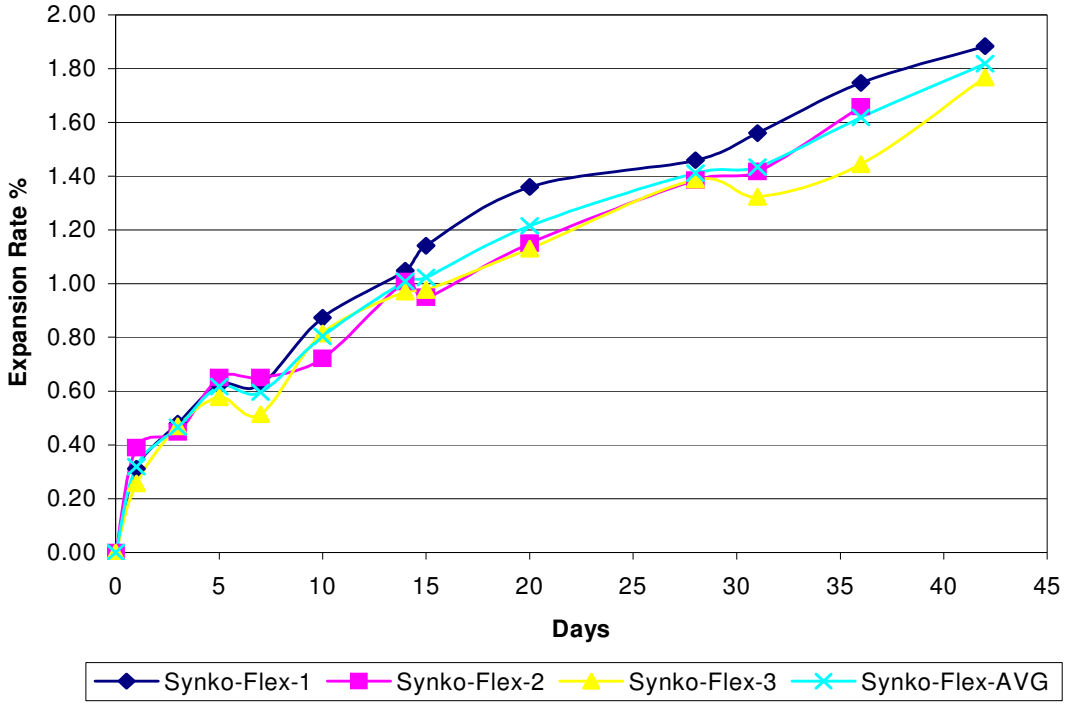

Figure 9.8 - Expansion rates of Synko-flex waterstop samples in the third experiment.

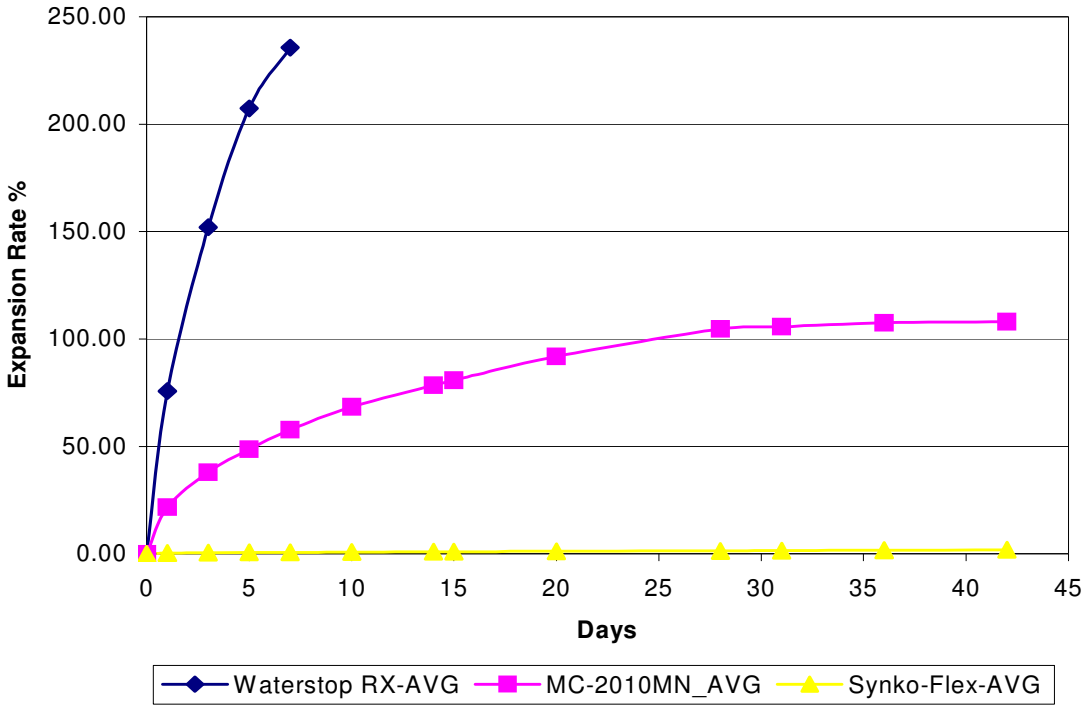

Figure 9.9 - Average expansion rates of the three waterstops tested in the third experiment.

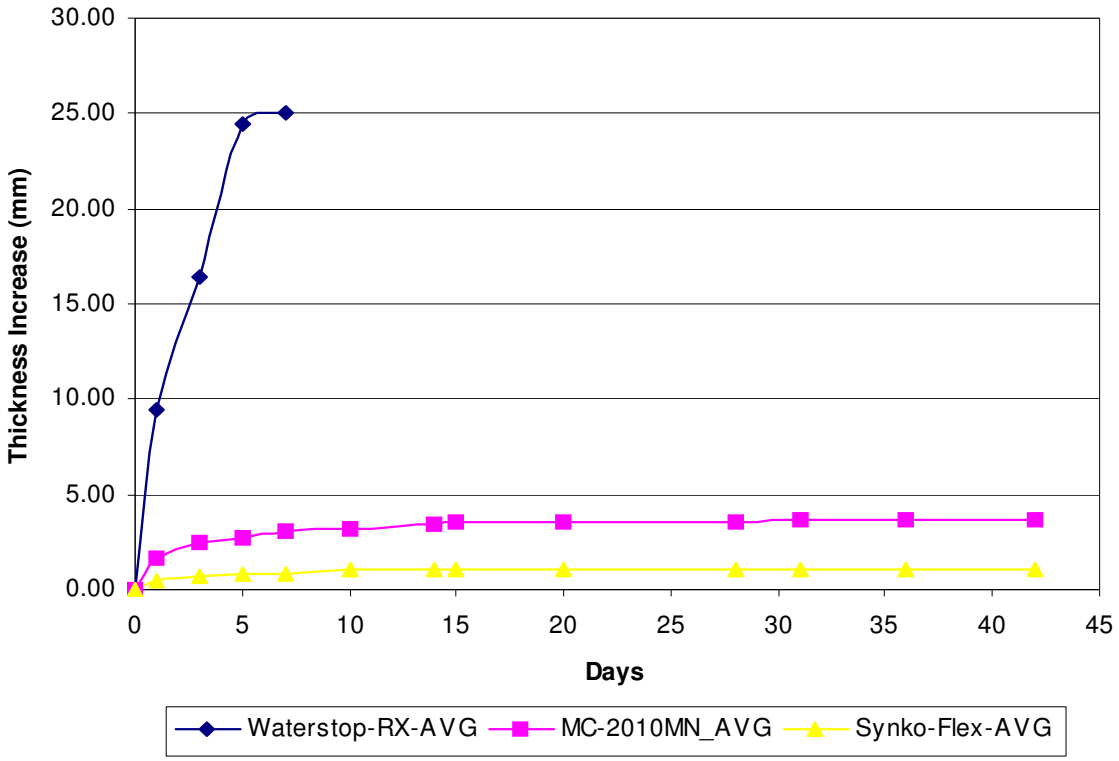

Figure 9.10 - Average thickness increases of waterstop samples in the third experiment.

CHAPTER 9: CONCLUSIONS AND RECOMMENDATIONS

9.1 CONCLUSIONS

The main objective of this study was to investigate alternatives for creating a watertight construction joint for inclusion in the specifications for the Hood Canal East Half Replacement Project. Determining the effectiveness of different products and construction methods at preventing water penetration will give WSDOT a starting point in building better more watertight joints for floating bridges.

The testing methods used in this study did not conform to a standard testing method due to the lack of such methods. The first experiment performed in this study worked correctly but the pressure applied by the system was too low to give any significant experimental results. Consequently, a second experimental procedure was used that applied a variable air pressure to the system. The system of the second experiment did increase the pressure applied to the specimens by over five times the pressure of experiment one but did not provide results for determining one products effectiveness over another at preventing water penetration.

The first two experiments were effective in showing that compaction is the deciding factor in water penetration through the construction joint. The greater the concrete compaction at the joint the less likely it will leak under pressure. Specimens in stages one and two were compacted to a higher level than stage three specimens through the use of a mechanical stinger. There was excellent compaction at the joint and no observed honeycombing in any of the specimens of the first two stages. Stage three specimens were compacted by stick strikes of the slump rod dropped into the freshly poured concrete. The compaction level of stage three specimens was much lower than

that of the first two stages. Honeycombing was observed in all specimens and was most severe near the joint. The honeycombing provided openings within the concrete to easily allow passage of water through the joint.

Product selection did not play an important role in preventing or decreasing water leakage through the joint. Poorly compacted specimens leaked immediately regardless of the applied product while all well-compacted specimens remained watertight. Honeycombing of the concrete near the joint signified poor compaction that has a high likelihood of leaking.

Products that should be most effective in helping to prevent water leakage through the joint are those that increase compaction at the joint. The mortar/slurry mixture applied to the first few inches of the joint helped improve compaction of the joint. The stage three specimen built using this construction method was one of only two specimens that did not leak before being placed within the testing setup. The removal of coarse aggregate from the first few inches of the second pour allowed the concrete to compact at a lower compaction effort than would be needed for a similar mix containing coarse aggregate. The mortar/slurry had the added benefit of helping to replace fines lost from segregation of the concrete when placed in a tall wall.

The third experiment was performed to determine the expansion rates of the three waterstops submerged in water. The Waterstop-RX 101TRH and MC-2010MN products saw significant expansion and thickness increases within the first two weeks of testing. The use of these two products in a joint exposed to significant moisture for an extended period of time could cause these products to lose their effectiveness as a water barrier. The Synko-flex waterstop retained its original shape and should not be damaged by

extended exposure to significant moisture. The Synko-flex product performed the best of the three waterstops tested in the third experiment but has not been proven to effectively reduce water penetration at the joint; more testing needs to be performed using a compaction level that demonstrates the Synko-Flex products ability to reduce water penetration more effectively than a similar jointed control specimen for a given air pressure.

9.2 GENERAL GUIDELINES FOR WATERTIGHT JOINT

The following general guidelines will help improve the resistance to water penetration for a concrete construction joint.

1. The top surface of the joint should be compacted to as high a compaction level as can be achieved in the field.
2. Repair any honeycombed concrete in the vicinity of the construction joint.
3. Use materials and construction methods to construct the joint that improve compaction at the joint such as the mortar/slurry mixture.
4. Products such as waterstops and surface coatings may help to decrease water penetration through the joint, but are far less important than good construction practices when building the joint.

9.3 RECOMMENDATIONS FOR FURTHER STUDY

Clearly, there is a need for further testing to determine the ability of individual products to prevent or reduce water penetration through a concrete construction joint.

The setup of the second experiment can be used to test these products. The products and testing methods used in this study along with additional products should be tested using the experimental setup of the second experiment with several small modifications.

The minimum compaction needed to prevent water leakage through the construction joint of the control specimen should be determined for the initial 16.48psi system pressure caused by the 4 foot water elevation. This minimum compaction should be used with all specimens to determine the air pressure necessary to cause leakage through the joint. Using this minimum compaction level will allow the most effective products for limiting water penetration to be determined.

Additional tests should be performed on admixtures that improve concrete compaction. The addition of these admixtures could limit water penetration through the joint by improving compaction at the joint without an increase in labor. The use of admixtures and other products that improve compaction should be studied further.

Testing should also be continued to determine the most effective surface preparation for limiting water penetration at the joint. The raking method, exposed aggregate surface and shear key should be further studied to determine the most effective method for preventing water penetration. Test results were inconclusive in determining the most effective surface preparation method for preventing water penetration; additional testing is necessary.

All testing completed in this study was performed under static loading. Pontoons in the field however are subjected to severe dynamic loading due to wind, wave and tidal fluctuations. These dynamic forces could cause significant movement of the construction joint that might lead to the formation of small cracks at the joint. Movement at the joint

could also cause damage to products applied to the joint. Testing should be performed to apply dynamic forces to concrete specimens to study joint movement and subsequent damage caused by this movement.

REFERENCES

Clear, C. A. (1985). "The Effects of Autogenous Healing Upon the Leakage of Water Through Cracks in Concrete." *Technical Report-Cement and Concrete Association*, 559(5).

Dusenberry, D. O., and DelloRusso, S. J. (1993). "Water Leakage Through Cracks in Reinforced Concrete." *Proc., International Conference on Hydropower*, 3(8), A. A. Balkema, Rotterdam, Netherlands, 2167-2176.

Henley, E. H., Wilson, D. L., and Kolle, G. A. (1997). " William A. Bugge Bridge Replacement Plan for the East-Half Floating Portion." *Report, Washington State Department of Transportation*.

Kishel, J. (1989). "Seepage and Contraction Joints in Concrete Canal Linings." *Journal of Irrigation and Drainage Engineering*, 115(3), 377-382.

Liou, D. D. (1996). "The Effects of Construction Joint in Mass Concrete." *Materials for the New Millenium. Proc. Fourth Materials Engineering Conference*, 1(11), ASCE, Washington DC, 193-202.

Lwin, M. M. (1993a). "The Lacey V. Murrow Floating Bridge, USA." *Structural Engineering International*, 145-148.

Lwin, M. M. (1993b). "Floating bridges-Solution to a difficult terrain." *Transporation Facilities through Difficult Terrain*, J. T. H. Wu and R. K. Barrett, eds., Balkema, Rotterdam, 581-591.

Lwin, M. M., Bruesch, A. W., and Evans, C. F. (1995). "High-Performance Concrete for a Floating Bridge." *Fourth International Bridge Engineering Conference*, National Academy Press, Washington DC, 155-162.

Lwin, M. M., Dusenberry, D. O. (1994). "Responding to a floating bridge failure." *Public Works*, 125(1), 39-43.

Lwin, M. M. and Gloyd, G. S. (1984) "Rebuilding the Hood Canal Floating Bridge." *Concrete International: Design and Construction*, 6(6), 30-35.

Nichols, C. C. (1964). "Construction and Performance of Hood Canal Floating Bridge." *Symposium on Concrete Construction in Aqueous Environment*, ACI SP-8, 97-106.

Rashed, A., Rogowsky, D. M., and Elwi, A. E. (2000). "Tests on Reinforced Partially Prestressed Concrete Tank Walls." *Journal of Structural Engineering*, 126(6), 675-683.

Tan, K., and Gjorv, O. E. (1996). "Performance of Concrete Under Different Curing Conditions." *Cement and Concrete Research*, 26(3), 355-361.

Tatro, S. B., and Waring, S. T. (1988). "Waterstop Technology-The Next Chapter." *Waterpower '87, Proc., International Conference on Hydropower,* 2, ASCE, New York, 1442-1451.

Wallis, S. (1992). "Putting Paid to Water Leakage Costs." *Tunnels and Tunnelling*, 24(1), 51-54.

Wiss, Janney, Elstner Associates, Inc. (1993). "Concrete for Lacey V. Murrow Bridge Pontoons." *Report, Washington State Department of Transportation*, ed., Robert LaFraugh.

WSDOT (2001). Standard Specifications for Road, Bridge and Municipal Construction 2002. Washington State Department of Transportation (WSDOT) Engineering Publications, Olympia, WA.

Young, D.A., Munson, B.A., and Okiishi, T.H. (1997). A Brief Introduction to Fluid Mechanics. John Wiley and Sons, Inc., New York, NY.

APPENDIX A

MEASURED MIX DATA

AND

STRAIN CALCULATIONS

Mix Design #1

LVM (Phase 1)

Mix # 1 - LVM Mix Design, Reference Mix w/c ratio= 0.3291

Concrete Constituent	mix proportions (per) 1 yd^3	**1.5 ft^3**	
Course Aggregate	1770 lb	**98.35**	lbs
Fine Aggregate	1295	**71.95**	lbs
Portland Cement Type II	624	**34.65**	lbs
Silica Fume (AASHTO M307)	50	**2.8**	lbs
Fly Ash (AASHTO M295)	100	**5.55**	lbs
Water (Total)	255	**14.15**	lbs
Water Reducer (ASTM C494)		**none**	
Superplasticizer (ASTM C494)	5.5floz/cwt	**70 mL**	

Slurry - Silica fume = **2.8 lbs**(all) **(1270.05grams)** Mix Water=total-slurry water
Water = **3.42lbs** **(1551.28grams)** = **10.73** **lbs**
HRWR = **6mL**

Concrete for Hood Canal Floating Bridge Replacement Project

Concrete Mix Design - **LVM Mix Design, Reference Mix**
Mix Design # - 1

Date Batched and Specimens Cast - November 14, 2002
Slump - 8.0"
Air Content - -
Batch Temperature - 66 F
Number of specimens cast (6x12 and 4x8) - 7 and 2 (#'s 1-9)

Date drilled and fitted with gage points - December 10, 2002

28-day Curing Date - December 12 (13), 2002

28-day Compressive Strength -

			Break notes
Cylinder f'c-1 =	8910psi	(252,170 lbs)	2 cones
Cylinder f'c-2 =	8650psi	(244,730 lbs)	Cone/Shear
Cylinder f'c-3 =	8570psi	(242,480 lbs)	Cone/Shear
Average =	8710psi		

Load to Apply for Creep Test - ASTM C 512
= 40% x f'c (28 day)
=.40 x 8710 psi = 3484 psi

Actual Applied Load = 30 tons = 24.4 % f'c (28 day) = 2122psi

Creep and Shrinkage Measurements

		Cylinder C-1 (mix #_____)			**Cylinder C-2 (mix #_____)**		
	Actual date	Creep Measurement			Creep Measurement		
Scheduled Time	and time	1	2	3	1	2	3
Before Loading	1/14 3:00pm	0.1649	0.1617	0.1592	0.1606	0.1561	0.1406
Immediately after Loading	1/14 3:53p	0.1615	0.1581	0.1554	0.1571	0.1529	0.137
15-20 minutes	1/14 4:20p	0.1614	0.1577	0.1551	0.156	0.1517	0.1362
1 hour	1/14 5:06p	0.1605	0.1569	0.1541	0.1553	0.1512	0.1364
2 hours: 45 minutes	1/14 6:45p	0.1603	0.1563	0.1541	0.1549	0.1503	0.1352
6 - 8 hours	1/14 9:56p	0.1602	0.1559	0.155	0.1541	0.1497	0.1354
2nd Day	1/15 1:50p	0.1597	0.1554	0.1548	0.1539	0.1494	0.1349
3rd Day	1/16 11:35a	0.1596	0.1549	0.1535	0.1533	0.1492	0.135
4th Day	1/17 1:40p	0.1589	0.1544	0.1535	0.153	0.1491	0.1348
6th Day	1/19 12:15p	0.1579	0.1541	0.153	0.1525	0.1486	0.1341
8th Day	1/21 1:35p	0.1573	0.1537	0.1526	0.1522	0.1485	0.1339
9th Day	1/22 1:52p	0.157	0.1535	0.1518	0.1519	0.1482	0.1337
14th Day	1/28 3:30p	0.1565	0.1532	0.1516	0.1516	0.1479	0.1335
21st Day	2/4 4:30p	0.156	0.1529	0.1513	0.1514	0.1474	0.1332
28th day	2/11 4:10p	0.1558	0.1527	0.1509	0.151	0.1469	0.1329
recovery	2/11 4:11p	0.159	0.1553	0.1538	0.1538	0.1495	0.1346

Creep and Shrinkage Measurements (Continued)

		Cylinder S-1 (mix #_____)			**Cylinder S-2 (mix #_____)**		
	Actual date	Shrinkage Measurement			Shrinkage Measurement		
Scheduled Time	and time	1	2	3	1	2	3
Before Loading	1/14 3:00pm	0.1536		0.1305	0.1228	0.1575	0.1429
Immediately after Loading	1/14 3:53p	0.1536		0.1305	0.1225	0.1575	0.1427
15-20 minutes	1/14 4:20p	0.1535	Gage	0.1302	0.1225	0.1572	0.1427
1 hour	1/14 5:06p	0.1535		0.1292	0.1225	0.1573	0.1428
2 hours: 45 minutes	1/14 6:45p	0.1534		0.1301	0.1227	0.1572	0.1429
6 - 8 hours	1/14 9:56p	0.1534	Length	0.1304	0.1227	0.158	0.1426
2nd Day	1/15 1:50p	0.1534		0.1297	0.1226	0.1579	0.1424
3rd Day	1/16 11:35a	0.1532		0.1306	0.1224	0.1577	0.1427
4th Day	1/17 1:40p	0.1534	Not	0.1304	0.1224	0.158	0.1422
6th Day	1/19 12:15p	0.1533		0.1302	0.1224	0.158	0.1422
8th Day	1/21 1:35p	0.1532		0.1301	0.1223	0.1575	0.1418
9th Day	1/22 1:52p	0.153	Good	0.1303	0.122	0.1574	0.1416
14th Day	1/28 3:30p	0.1529		0.1299	0.1218	0.1573	0.1415
21st Day	2/4 4:30p	0.1528		0.1294	0.1218	0.1571	0.1415
28th day	2/11 4:10p	0.1528		0.1293	0.1218	0.1571	0.1415
recovery	2/11 4:11p	0.1528		0.1293	0.1218	0.1571	0.1415

Mix Design #1 - LVM Mix Design

Creep Measurements

gage zero (10") = 0.1600

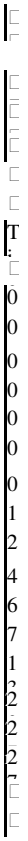

Shrinkage Measurements

gage zero (10") = 0.1600

(Creep)

		Cylinder #6 Cylinder plane #				average total strain	average total strain	Average total Strain - 2 Cylinders
1		2		3		(in)	(in/in)	(in)
0.1606	10.0006	0.1561	9.9961	0.1406	9.9806			
0.0000	0.00000	0.0000	0.00000	0.0000	0.00000	0.0000	0.00000	0.0000
0.0035	0.00035	0.0032	0.00032	0.0036	0.00036	0.0034	0.00034	0.0035
0.0046	0.00046	0.0044	0.00044	0.0044	0.00044	0.0045	0.00045	0.0042
0.0053	0.00053	0.0049	0.00049	0.0042	0.00042	0.0048	0.00048	0.0048
0.0057	0.00057	0.0058	0.00058	0.0054	0.00054	0.0056	0.00056	0.0053
0.0065	0.00065	0.0064	0.00064	0.0052	0.00052	0.0060	0.00060	0.0055
0.0067	0.00067	0.0067	0.00067	0.0057	0.00057	0.0064	0.00064	0.0058
0.0073	0.00073	0.0069	0.00069	0.0056	0.00056	0.0066	0.00066	0.0063
0.0076	0.00076	0.0070	0.00070	0.0058	0.00058	0.0068	0.00068	0.0066
0.0081	0.00081	0.0075	0.00075	0.0065	0.00065	0.0074	0.00074	0.0072
0.0084	0.00084	0.0076	0.00076	0.0067	0.00067	0.0076	0.00076	0.0075
0.0087	0.00087	0.0079	0.00079	0.0069	0.00069	0.0078	0.00078	0.0078
0.0090	0.00090	0.0082	0.00082	0.0071	0.00071	0.0081	0.00081	0.0081
0.0092	0.00092	0.0087	0.00087	0.0074	0.00074	0.0084	0.00084	0.0085
0.0096	0.00096	0.0092	0.00092	0.0077	0.00077	0.0088	0.00088	0.0088
0.0068	0.00068	0.0066	0.00066	0.0060	0.00060	0.0065	0.00065	0.0062

(Shrinkage)

		Cylinder #7 Cylinder plane				average shrinkage strain	average shrinkage strain (in/in)	Average Shrinkage Strain - 2 Cylinders (in)
1		2		3				
0.1228	9.9628	0.1575	9.9975	0.1429	9.9829			
0.0000	0.00000	0.0000	0.00000	0.0000	0.00000	0.0000	0.00000	0.0000
0.0003	0.00003	0.0000	0.00000	0.0002	0.00002	0.0002	0.00002	0.0001
0.0003	0.00003	0.0003	0.00003	0.0002	0.00002	0.0003	0.00003	0.0002
0.0003	0.00003	0.0002	0.00002	0.0001	0.00001	0.0002	0.00002	0.0004
0.0001	0.00001	0.0003	0.00003	0.0000	0.00000	0.0001	0.00001	0.0002
0.0001	0.00001	-0.0005	-0.00005	0.0003	0.00003	0.0000	0.00000	0.0001
0.0002	0.00002	-0.0004	-0.00004	0.0005	0.00005	0.0001	0.00001	0.0003
0.0004	0.00004	-0.0002	-0.00002	0.0002	0.00002	0.0001	0.00001	0.0001
0.0004	0.00004	-0.0005	-0.00005	0.0007	0.00007	0.0002	0.00002	0.0002
0.0004	0.00004	-0.0005	-0.00005	0.0007	0.00007	0.0002	0.00002	0.0003
0.0005	0.00005	0.0000	0.00000	0.0011	0.00011	0.0005	0.00005	0.0005
0.0008	0.00008	0.0001	0.00001	0.0013	0.00013	0.0007	0.00007	0.0006
0.0010	0.00010	0.0002	0.00002	0.0014	0.00014	0.0009	0.00009	0.0008
0.0010	0.00010	0.0004	0.00004	0.0014	0.00014	0.0009	0.00009	0.0009
0.0010	0.00010	0.0004	0.00004	0.0014	0.00014	0.0009	0.00009	0.0010
0.0010	0.00010	0.0004	0.00004	0.0014	0.00014	0.0009	0.00009	0.0010

Time,m	Time, day	**Average total Strain - 2** Cylinders **(in/in)**	(microstrain) (x 10^6)
0	0	**0**	0
53	0.0	**0.000351768**	351.8
80	0.1	**0.000416799**	416.8
126	0.1	**0.000478453**	478.5
225	0.2	**0.000533494**	533.5
416	0.3	**0.000546821**	546.8
1335	0.9	**0.0005835**	583.5
2670	1.9	**0.000626831**	626.8
4115	2.9	**0.00065683**	656.8
6910	4.8	**0.000715181**	715.2
9790	6.8	**0.000748516**	748.5
11247	7.8	**0.000783522**	783.5
18720	13.0	**0.000813525**	813.5
28800	20.0	**0.000848533**	848.5
38880	27.0	**0.000881878**	881.9
38881	27.0	**0.000618505**	618.5

Shrinkage Measurements

Time,m	Time, day	**Average Shrinkage Strain - 2 Cylinders (in/in)**	(microstrain) (x 10^6)	Creep= Total minus Shrinkage (in)	Creep= **Total minus Shrinkage (in/in)**	(microstrain) (x 10^6)
0	0	**0**	0	0.0000	**0.000000**	0
53	0.0	**8.33951E-06**	8.3	0.0034	**0.000343**	343.4
80	0.1	**2.33408E-05**	23.3	0.0039	**0.000393**	393.5
126	0.1	**4.50056E-05**	45.0	0.0043	**0.000433**	433.4
225	0.2	**2.16669E-05**	21.7	0.0051	**0.000512**	511.8
416	0.3	**5.83745E-06**	5.8	0.0054	**0.000541**	541.0
1335	0.9	**3.00125E-05**	30.0	0.0055	**0.000553**	553.5
2670	1.9	**1.41663E-05**	14.2	0.0061	**0.000613**	612.7
4115	2.9	**1.75168E-05**	17.5	0.0064	**0.000639**	639.3
6910	4.8	**2.5016E-05**	25.0	0.0069	**0.000690**	690.2
9790	6.8	**4.66977E-05**	46.7	0.0070	**0.000702**	701.8
11247	7.8	**5.67017E-05**	56.7	0.0073	**0.000727**	726.8
18720	13.0	**7.58716E-05**	75.9	0.0074	**0.000738**	737.7
28800	20.0	**9.4206E-05**	94.2	0.0075	**0.000754**	754.3
38880	27.0	**9.67062E-05**	96.7	0.0079	**0.000785**	785.2
38881	27.0	**9.67062E-05**	96.7	0.0052	**0.000522**	521.8

Mix #1
LVM Mix Design, Reference Mix (Phase 1)

Applied Creep Load = 2120psi

Time (min)	Total (in/in)	Creep (in/in)	Shrinkage (in/in)	Specific Creep plus Initial (microstrain/psi)	Specific Creep (microstrain/psi)	Specific Total (microstrain/psi)
0	0	0	0	0		0
53	.352E-3	.343E-3	.834E-5	0.162	0	0.166
80	.417E-3	.393E-3	.233E-4	0.186	0.024	0.197
126	.478E-3	.433E-3	.450E-4	0.204	0.042	0.226
225	.533E-3	.512E-3	.217E-4	0.241	0.079	0.252
416	.547E-3	.541E-3	.584E-5	0.255	0.093	0.258
1335	.584E-3	.553E-3	.300E-4	0.261	0.099	0.275
2670	.627E-3	.613E-3	.142E-4	0.289	0.127	0.296
4115	.657E-3	.639E-3	.175E-4	0.302	0.140	0.310
6910	.715E-3	.690E-3	.250E-4	0.326	0.164	0.337
9790	.749E-3	.702E-3	.467E-4	0.331	0.169	0.353
11247	.784E-3	.727E-3	.567E-4	0.343	0.181	0.370
18720	.814E-3	.738E-3	.759E-4	0.348	0.186	0.384
28800	.849E-3	.754E-3	.942E-4	0.356	0.194	0.400
38881	.619E-3	.522E-3	.967E-4	0.246		0.292

Mix Design #2

WJE, Inc Report Recommendation

Mix # 2 - 1st Alteration - WJE, Inc. Report Recommendation w/c ratio= 0.3287

Concrete Constituent	mix proportions (per) 1 yd^3	**1.5 ft^3**	
Course Aggregate	1770 lb	**98.35**	lbs
Fine Aggregate	1295	**71.95**	lbs
Portland Cement Type II	540	**30**	lbs
Silica Fume (AASHTO M307)	35	**1.95**	lbs
Fly Ash (AASHTO M295)	200	**11.1**	lbs
Water	255	**14.15**	lbs
Water Reducer (ASTM C494)		**none**	
Superplasticizer (ASTM C494)	4.3floz/cwt	**55 mL**	

Slurry - Silica fume=**1.95lbs**(all) **(884.5grams)** Mix Water=total-slurry water
Water=**2.38lbs** **(1079.5grams)** = **11.77 lbs**
HRWR=**6mL**

Concrete for Hood Canal Floating Bridge Replacement Project

Concrete Mix Design - **WJE, Inc Report Recommendation**
Mix Design **# 2**

Date Batched and Specimens Cast - November 14, 2002
Slump - 7.5 "
Air Content - -
Batch Temperature - 66 F
Number of specimens cast (6x12 and 4x8) - 7 and 2 (#'s 10 - 18)

Date drilled and fitted with gage points - December 10, 2002

28-day Curing Date - December 12 (13), 2002

28-day Compressive Strength -

		Break notes
Cylinder f'c-1 =	8140psi	(230360 lbs) 2 cones
Cylinder f'c-2 =	8200psi	(232130 lbs) 2 cones
Cylinder f'c-3 =	8150psi	(230790 lbs) 2 cones
Average =	8163.3psi	

Load to Apply for Creep Test - ASTM C 512
= 40% x f'c (28 day)
=.40 x 8163.3 psi = 3265.3 psi

Actual Applied Load = 28.1 tons psi = 24.4% f'c (28 day) = 1988 psi

Creep and Shrinkage Measurements

		#13			#14		
		Cylinder C-1 (mix #_____)			**Cylinder C-2 (mix #_____)**		
	Actual date	Creep Measurement			Creep Measurement		
Scheduled Time	and time	1	2	3	1	2	3
Before Loading	1/14 4:35pm	0.1545	0.1561	0.1599	0.163	0.157	0.154
Immediately after Loading	1/14 5:00p	0.1514	0.1544	0.1564	0.1611	0.1543	0.1519
15-20 minutes	1/14 5:20p	0.1477	0.1532	0.1565	0.1595	0.1544	0.1495
1 hour	1/14 6:07p	0.1474	0.152	0.1539	0.1593	0.1542	0.1485
2 hours: 45 minutes	1/14 7:59p	0.1478	0.1525	0.1542	0.16	0.155	0.149
6 - 8 hours	1/14 11:00p	0.1479	0.1525	0.1531	0.1593	0.155	0.149
2nd Day	1/15 1:53p	0.1466	0.1515	0.1528	0.1588	0.1551	0.1479
3rd Day	1/16 11:45a	0.147	0.1515	0.1525	0.1587	0.1548	0.1478
4th Day	1/17 1:51p	0.1466	0.1515	0.1523	0.1585	0.1547	0.1474
6th Day	1/19 12:30p	0.1459	0.1511	0.1519	0.1581	0.1541	0.1471
8th Day	1/21 1:40p	0.1456	0.1506	0.1516	0.1576	0.154	0.1468
9th Day	1/22 5:00p	0.1452	0.1502	0.1514	0.1572	0.1538	0.1464
14th Day	1/28 3:40p	0.1445	0.1499	0.1507	0.1566	0.1533	0.1456
21st Day	2/4 4:40p	0.1443	0.1496	0.1503	0.1563	0.1531	0.1454
28th day	2/11 4:15p	0.1441	0.1493	0.15	0.1561	0.153	0.1451
recovery	2/11 4:16p	0.1475	0.1522	0.1535	0.1595	0.1558	0.1491

Creep and Shrinkage Measurements (Continued)

		Cylinder S-1 (mix #_____)			**Cylinder S-2 (mix #_____)**		
Scheduled Time	Actual date and time	Shrinkage Measurement			Shrinkage Measurement		
		1	2	3	1	2	3
Before Loading	1/14 4:35pm	0.1506		0.1415	0.1421	0.1615	0.154
Immediately after Loading	1/14 5:00p	0.15		0.1415	0.142	0.1615	0.1542
15-20 minutes	1/14 5:20p	0.1491	Gage	0.1413	0.1421	0.1605	0.154
1 hour	1/14 6:07p	0.148		0.1397	0.1398	0.1595	0.1529
2 hours: 45 minutes	1/14 7:59p	0.149		0.1403	0.1402	0.1596	0.1524
6 - 8 hours	1/14 11:00p	0.1486	Length	0.1403	0.1396	0.1597	0.1524
2nd Day	1/15 1:53p	0.1481		0.1398	0.1396	0.1595	0.1522
3rd Day	1/16 11:45a	0.148		0.1397	0.1395	0.1594	0.1521
4th Day	1/17 1:51p	0.1481	Not	0.1396	0.14	0.1594	0.1522
6th Day	1/19 12:30p	0.1478		0.1394	0.1385	0.1593	0.1518
8th Day	1/21 1:40p	0.1476		0.1393	0.1395	0.1592	0.1517
9th Day	1/22 5:00p	0.1474	Good	0.1391	0.1394	0.1591	0.1517
14th Day	1/28 3:40p	0.148		0.1392	0.1393	0.1591	0.1516
21st Day	2/4 4:40p	0.1476		0.139	0.139	0.1588	0.1515
28th day	2/11 4:15p	0.1474		0.1388	0.1389	0.1587	0.1515
recovery	2/11 4:16p	0.1474		0.1388	0.1389	0.1587	0.1515

Mix # 2 - WJE, Inc Report Recommendation

Creep Measurements

gage zero (10") = 0.1600

				Cylinder # 13 Cylinder plane			average total	total strain
				T				
				0				
				0				
				0				
				0				
				0				
				0				
				0				
				1				
				2				
				4				
				6				
				7				
				1				
				2				
				2				
				2				
				7				

Shrinkage Measurements

gage zero (10") = 0.1600

				Cylinder #15 Cylinder plane			average shrinkage	average shrinkage strain
				T				
				0				
25	0.0	0.0006	0.0001	Gage	0.0000	0.0000	0.0003	0.000030
				0				
				0				
199	0.1	0.0016	0.0002	Length	0.0012	0.0001	0.0014	0.000140
				0				
				0				
2585	1.8	0.0026	0.0003	Not	0.0018	0.0002	0.0022	0.000220
				2				
				4				
9780	6.8	0.0030	0.0003	Good	0.0022	0.0002	0.0026	0.000260
				7				
				1				
				2				
				2				
				2				
				2				

(Creep)

Cylinder # 14								
Cylinder plane						average	average total strain	Average total
1		2		3		total strain	(in/in)	Strain - 2 Cylinders
0.163	10.0030	0.157	9.9970	0.154	9.9940			
0.0000	0.0000	0.0000	0.0000	0.0000	0.0000	0.0000	0.00000	0.0000
0.0019	0.0002	0.0027	0.0003	0.0021	0.0002	0.0022	0.00022	0.0025
0.0035	0.0003	0.0026	0.0003	0.0045	0.0005	0.0035	0.00035	0.0040
0.0037	0.0004	0.0028	0.0003	0.0055	0.0006	0.0040	0.00040	0.0049
0.0030	0.0003	0.0020	0.0002	0.0050	0.0005	0.0033	0.00033	0.0043
0.0037	0.0004	0.0020	0.0002	0.0050	0.0005	0.0036	0.00036	0.0046
0.0042	0.0004	0.0019	0.0002	0.0061	0.0006	0.0041	0.00041	0.0053
0.0043	0.0004	0.0022	0.0002	0.0062	0.0006	0.0042	0.00042	0.0054
0.0045	0.0004	0.0023	0.0002	0.0066	0.0007	0.0045	0.00045	0.0056
0.0049	0.0005	0.0029	0.0003	0.0069	0.0007	0.0049	0.00049	0.0060
0.0054	0.0005	0.0030	0.0003	0.0072	0.0007	0.0052	0.00052	0.0064
0.0058	0.0006	0.0032	0.0003	0.0076	0.0008	0.0055	0.00055	0.0067
0.0064	0.0006	0.0037	0.0004	0.0084	0.0008	0.0062	0.00062	0.0073
0.0067	0.0007	0.0039	0.0004	0.0086	0.0009	0.0064	0.00064	0.0076
0.0069	0.0007	0.0040	0.0004	0.0089	0.0009	0.0066	0.00066	0.0078
0.0035	0.0003	0.0012	0.0001	0.0049	0.0005	0.0032	0.00032	0.0045

(Shrinkage)

Cylinder #16								
Cylinder plane						average	average shrinkage strain	Average Shrinkage
1		2		3		shrinkage strain	(in/in)	Strain - 2 Cylinders
0.1421	9.9821	0.1615	10.0015	0.154	9.9940			
0.0000	0.0000	0.0000	0.0000	0.0000	0.0000	0.0000	0.00000	0.0000
0.0001	0.0000	0.0000	0.0000	-0.0002	0.0000	0.0000	0.00000	0.0001
0.0000	0.0000	0.0010	0.0001	0.0000	0.0000	0.0003	0.00003	0.0006
0.0023	0.0002	0.0020	0.0002	0.0011	0.0001	0.0018	0.00018	0.0020
0.0019	0.0002	0.0019	0.0002	0.0016	0.0002	0.0018	0.00018	0.0016
0.0025	0.0003	0.0018	0.0002	0.0016	0.0002	0.0020	0.00020	0.0018
0.0025	0.0003	0.0020	0.0002	0.0018	0.0002	0.0021	0.00021	0.0021
0.0026	0.0003	0.0021	0.0002	0.0019	0.0002	0.0022	0.00022	0.0022
0.0021	0.0002	0.0021	0.0002	0.0018	0.0002	0.0020	0.00020	0.0021
0.0036	0.0004	0.0022	0.0002	0.0022	0.0002	0.0027	0.00027	0.0026
0.0026	0.0003	0.0023	0.0002	0.0023	0.0002	0.0024	0.00024	0.0025
0.0027	0.0003	0.0024	0.0002	0.0023	0.0002	0.0025	0.00025	0.0026
0.0028	0.0003	0.0024	0.0002	0.0024	0.0002	0.0025	0.00025	0.0025
0.0031	0.0003	0.0027	0.0003	0.0025	0.0003	0.0028	0.00028	0.0028
0.0032	0.0003	0.0028	0.0003	0.0025	0.0003	0.0028	0.00028	0.0029
0.0032	0.0003	0.0028	0.0003	0.0025	0.0003	0.0028	0.00028	0.0029

Time,m	Time, day	**Average total Strain - 2 Cylinders (in/in)**	(x 10^6)
0	0	**0**	0
25	0.0	**0.000250065**	250.0651
40	0.0	**0.000395122**	395.1223
87	0.1	**0.00048681**	486.81
199	0.1	**0.000433464**	433.4642
380	0.3	**0.000461793**	461.7933
1273	0.9	**0.000530153**	530.1531
2585	1.8	**0.000536818**	536.8181
4151	2.9	**0.000558492**	558.492
6890	4.8	**0.000605172**	605.1718
9780	6.8	**0.000638512**	638.5122
11420	7.9	**0.000671855**	671.8548
18720	13.0	**0.000731871**	731.8708
28800	20.0	**0.000758543**	758.5428
38880	27.0	**0.000781882**	781.8825
38881	27.0	**0.000448461**	448.4615

Time,m	Time, day	**Average Shrinkage Strain - 2 Cylinders (in/in)**	(x 10^6)	Creep= Total minus Shrinkage	**Creep= Total minus Shrinkage (in/in)**	(x 10^6)
0	0	**0**	0	0.0000	**0**	0
25	0.0	**1.33484E-05**	13.34843	0.0024	**0.0002367**	236.7167
40	0.0	**5.92087E-05**	59.20872	0.0034	**0.0003359**	335.9136
87	0.1	**0.000200219**	200.2193	0.0029	**0.0002866**	286.5907
199	0.1	**0.000160161**	160.1613	0.0027	**0.0002733**	273.3029
380	0.3	**0.000178522**	178.5222	0.0028	**0.0002833**	283.2711
1273	0.9	**0.000210225**	210.2253	0.0032	**0.0003199**	319.9278
2585	1.8	**0.000220236**	220.236	0.0032	**0.0003166**	316.5821
4151	2.9	**0.000210222**	210.2224	0.0035	**0.0003483**	348.2697
6890	4.8	**0.000256121**	256.1206	0.0035	**0.0003491**	349.0512
9780	6.8	**0.000250267**	250.2675	0.0039	**0.0003882**	388.2447
11420	7.9	**0.000263618**	263.6175	0.0041	**0.0004082**	408.2373
18720	13.0	**0.000249436**	249.4361	0.0048	**0.0004824**	482.4347
28800	20.0	**0.000276131**	276.1307	0.0048	**0.0004824**	482.4122
38880	27.0	**0.000289481**	289.4807	0.0049	**0.0004924**	492.4018
38881	27.0	**0.000289481**	289.4807	0.0016	**0.000159**	158.9808

Mix #2
WJE, Inc Report Recommendation

Applied Creep Load = 1990psi

Time (min)	Total (in/in)	Creep (in/in)	Shrinkage (in/in)	Specific Creep plus Initial (microstrain/psi)	Specific Creep (microstrain/psi)	Specific Total (microstrain/psi)
0	0	0	0	0		0
25	.250E-3	.237E-3	.133E-4	0.119	0	0.126
40	.395E-3	.336E-3	.592E-4	0.169	0.050	0.199
87	.487E-3	.287E-3	.200E-3	0.144	0.025	0.245
199	.433E-3	.273E-3	.160E-3	0.137	0.018	0.218
380	.462E-3	.283E-3	.179E-3	0.142	0.023	0.232
1273	.530E-3	.320E-3	.210E-3	0.161	0.042	0.266
2585	.537E-3	.317E-3	.220E-3	0.159	0.040	0.270
4151	.558E-3	.348E-3	.210E-3	0.175	0.056	0.281
6890	.605E-3	.349E-3	.256E-3	0.175	0.056	0.304
9780	.639E-3	.388E-3	.250E-3	0.195	0.076	0.321
11420	.672E-3	.408E-3	.264E-3	0.205	0.086	0.338
18720	.732E-3	.482E-3	.249E-3	0.242	0.123	0.368
28800	.759E-3	.482E-3	.276E-3	0.242	0.123	0.381
38881	.448E-3	.159E-3	.289E-3	0.080		0.225

Mix Design #3

Metakaolin 5% OPC Replacement

Mix # 3 - 2nd Alteration - Metakaolin - 5% OPC Replacement* w/c ratio= 0.3287

Concrete Constituent	mix proportions (per) 1 yd^3	**1.5 ft^3**		
Course Aggregate	1770 lb	**98.35**	lbs	
Fine Aggregate	1295	**71.95**	lbs	
Portland Cement Type II	636.3	**35.35**	lbs	
Silica Fume (AASHTO M307)	none	**none**		
Fly Ash (AASHTO M295)	100	**5.55**	lbs-------->	**2517.4g**
Metakaolin (High Reactive)	38.75	**2.15**	lbs-------->	**975.2g**
Water	255	**14.15**	lbs	
Water Reducer (ASTM C494)		**none**		
Superplasticizer (ASTM C494)	5.5floz/cwt	**70 mL**		

* Based on 775 pounds of total cementitious materials

Concrete for Hood Canal Floating Bridge Replacement Project

Concrete Mix Design - **Metakaolin - 5% OPC Replacement**
Mix Design **# 3**

Date Batched and Specimens Cast - November 14, 2002
Slump - 9 "
Air Content - -
Batch Temperature - 66 F
Number of specimens cast (6x12 and 4x8) - 7 and 2 (#'s 19 - 27)

Date drilled and fitted with gage points - December 10, 2002

28-day Curing Date - December 12 (13), 2002

28-day Compressive Strength -

			Break notes
Cylinder f'c-1 =	8820psi	(249700 lbs)	2 cones
Cylinder f'c-2 =	8780psi	(248370 lbs)	Shear Plane
Cylinder f'c-3 =	8720psi	(246800 lbs)	2 cones
Average =	8773.3psi		

Load to Apply for Creep Test - ASTM C 512
= 40% x f'c (28 day)
=.40 x 8773.3 psi = 3509.3 psi

Actual Applied Load = 30.3 tons = 24.4% f'c (28 day) = 2140.7 psi

Creep and Shrinkage Measurements

		#23			#24		
		Cylinder C-1 (mix #_____)			**Cylinder C-2 (mix #_____)**		
	Actual date	Creep Measurement			Creep Measurement		
Scheduled Time	and time	1	2	3	1	2	3
Before Loading	1/14 5:37pm	0.1578	0.1501	0.1307	0.17	0.1635	0.1923
Immediately after Loading	1/14 6:01p	0.1551	0.1473	0.1279	0.1666	0.1603	0.1898
15-20 minutes	1/14 6:18p	0.155	0.147	0.1275	0.166	0.1599	0.1891
1 hour	1/14 7:00p	0.155	0.1467	0.1274	0.1657	0.1594	0.1876
2 hours: 45 minutes	1/14 8:45p	0.1555	0.1465	0.1279	0.1658	0.1594	0.1879
6 - 8 hours	1/14 12:01am	0.1559	0.1469	0.1279	0.1658	0.1594	0.1877
2nd Day	1/15 2:04p	0.1548	0.146	0.1264	0.1645	0.159	0.1868
3rd Day	1/16 11:51a	0.1543	0.1459	0.1255	0.1646	0.1582	0.1866
4th Day	1/17 1:55p	0.1539	0.145	0.1256	0.1643	0.1582	0.1865
6th Day	1/19 12:35p	0.1535	0.1443	0.1253	0.1638	0.1578	0.1861
8th Day	1/21 1:50p	0.1533	0.1435	0.1249	0.1634	0.1576	0.1855
9th Day	1/22 5:05p	0.1526	0.1433	0.1245	0.1632	0.157	0.1852
14th Day	1/28 4:00p	0.152	0.1428	0.1237	0.163	0.1566	0.1845
21st Day	2/4 4:45p	0.1512	0.1424	0.1234	0.1625	0.1564	0.1842
28th day	2/11 4:00p	0.1505	0.1422	0.1232	0.1623	0.1562	0.184
recovery	2/11 4:01p	0.1534	0.1456	0.1268	0.1649	0.1586	0.1879

		#22			#25		
		Cylinder S-1 (mix #_____)			**Cylinder S-2 (mix #_____)**		
Scheduled Time	Actual date and time	Shrinkage Measurement			Shrinkage Measurement		
		1	2	3	1	2	3
Before Loading	1/14 5:37pm	0.1655	0.0705	0.164	0.159	0.0641	0.12
Immediately after Loading	1/14 6:01p	0.1653	0.0704	0.1638	0.1593	0.064	0.12
15-20 minutes	1/14 6:18p	0.165	0.07	0.1636	0.1585	0.0653	0.119
1 hour	1/14 7:00p	0.1654	0.0708	0.164	0.1581	0.0649	0.1191
2 hours: 45 minutes	1/14 8:45p	0.1651	0.0705	0.1641	0.1591	0.0636	0.12
6 - 8 hours	1/14 12:01am	0.165	0.0706	0.164	0.1586	0.063	0.12
2nd Day	1/15 2:04p	0.1649	0.07	0.1636	0.1581	0.0628	0.12
3rd Day	1/16 11:51a	0.1646	0.07	0.164	0.158	0.063	0.1195
4th Day	1/17 1:55p	0.165	0.0701	0.1641	0.1576	0.0628	0.1195
6th Day	1/19 12:35p	0.1646	0.07	0.1636	0.1574	0.0628	0.1195
8th Day	1/21 1:50p	0.1645	0.0695	0.1633	0.1568	0.0625	0.1193
9th Day	1/22 5:05p	0.1645	0.0693	0.1632	0.1568	0.0625	0.1193
14th Day	1/28 4:00p	0.1646	0.0695	0.1636	0.157	0.0625	0.1194
21st Day	2/4 4:45p	0.1644	0.0693	0.1634	0.1569	0.0625	0.119
28th day	2/11 4:00p	0.1643	0.0693	0.1631	0.1568	0.0625	0.119
recovery	2/11 4:01p	0.1643	0.0693	0.1631	0.1568	0.0625	0.119

Mix # 3 - Metakaolin - 5% OPC Replacement

Creep Measurements

gage zero (10") = 0.1600

Cylinder # 23		average	total
Cylinder plane		total	strain
T			
0			
0			
0			
0			
0			
0			
0			
0			
1			
2			
4			
6			
8			
1			
2			
2			
2			

Shrinkage Measurements

gage zero (10") = 0.1600

Cylinder # 22		average	average
Cylinder plane		shrinkage	shrinkage
T			
0			
0			
0			
0			
0			
0			
0			
0			
1			
2			
4			
6			
8			
1			
2			
2			
2			

(creep)

Cylinder # 24 Cylinder plane								
1		2		3		average total strain	average total strain (in/in)	Average total Strain - 2 Cylinders
0.17	10.0100	0.1635	10.0035	0.1923	10.0323			
0.0000	0.00000	0.0000	0.00000	0.0000	0.00000	0.0000	0.00000	0.0000
0.0034	0.00034	0.0032	0.00032	0.0025	0.00025	0.0030	0.00030	0.0029
0.0040	0.00040	0.0036	0.00036	0.0032	0.00032	0.0036	0.00036	0.0033
0.0043	0.00043	0.0041	0.00041	0.0047	0.00047	0.0044	0.00044	0.0038
0.0042	0.00042	0.0041	0.00041	0.0044	0.00044	0.0042	0.00042	0.0036
0.0042	0.00042	0.0041	0.00041	0.0046	0.00046	0.0043	0.00043	0.0035
0.0055	0.00055	0.0045	0.00045	0.0055	0.00055	0.0052	0.00052	0.0045
0.0054	0.00054	0.0053	0.00053	0.0057	0.00057	0.0055	0.00055	0.0049
0.0057	0.00057	0.0053	0.00053	0.0058	0.00058	0.0056	0.00056	0.0052
0.0062	0.00062	0.0057	0.00057	0.0062	0.00062	0.0060	0.00060	0.0056
0.0066	0.00066	0.0059	0.00059	0.0068	0.00068	0.0064	0.00064	0.0060
0.0068	0.00068	0.0065	0.00065	0.0071	0.00071	0.0068	0.00068	0.0064
0.0070	0.00070	0.0069	0.00069	0.0078	0.00078	0.0072	0.00072	0.0070
0.0075	0.00075	0.0071	0.00071	0.0081	0.00081	0.0076	0.00076	0.0074
0.0077	0.00077	0.0073	0.00073	0.0083	0.00083	0.0078	0.00078	0.0077
0.0051	0.00051	0.0049	0.00049	0.0044	0.00044	0.0048	0.00048	0.0045

(shrinkage)

Cylinder # 25 Cylinder plane								
1		2		3		average shrinkage strain	average shrinkage strain (in/in)	Average Shrinkage Strain - 2 Cylinders (in)
0.159	9.9990	0.0641	9.9041	0.12	9.9600			
0.0000	0.00000	0.0000	0.00000	0.0000	0.00000	0.0000	0.00000	0.0000
-0.0003	-0.00003	0.0001	0.00001	0.0000	0.00000	-0.0001	-0.00001	0.0001
0.0005	0.00005	-0.0012	-0.00012	0.0010	0.00010	0.0001	0.00001	0.0003
0.0009	0.00009	-0.0008	-0.00008	0.0009	0.00009	0.0003	0.00003	0.0001
-0.0001	-0.00001	0.0005	0.00005	0.0000	0.00000	0.0001	0.00001	0.0001
0.0004	0.00004	0.0011	0.00011	0.0000	0.00000	0.0005	0.00005	0.0003
0.0009	0.00009	0.0013	0.00013	0.0000	0.00000	0.0007	0.00007	0.0006
0.0010	0.00010	0.0011	0.00011	0.0005	0.00005	0.0009	0.00009	0.0007
0.0014	0.00014	0.0013	0.00013	0.0005	0.00005	0.0011	0.00011	0.0007
0.0016	0.00016	0.0013	0.00013	0.0005	0.00005	0.0011	0.00011	0.0009
0.0022	0.00022	0.0016	0.00016	0.0007	0.00007	0.0015	0.00015	0.0012
0.0022	0.00022	0.0016	0.00016	0.0007	0.00007	0.0015	0.00015	0.0013
0.0020	0.00020	0.0016	0.00016	0.0006	0.00006	0.0014	0.00014	0.0011
0.0021	0.00021	0.0016	0.00016	0.0010	0.00010	0.0016	0.00016	0.0013
0.0022	0.00022	0.0016	0.00016	0.0010	0.00010	0.0016	0.00016	0.0014
0.0022	0.00022	0.0016	0.00016	0.0010	0.00010	0.0016	0.00016	0.0014

Time,m	Time, day	**Average total Strain - 2 Cylinders (in/in)**	(x 10^6)
0	0	**0**	0
24	0.0	**0.000289984**	289.9839
41	0.0	**0.000331626**	331.6256
83	0.1	**0.000376547**	376.547
188	0.1	**0.000356542**	356.5418
384	0.3	**0.000346523**	346.5229
1227	0.9	**0.00044821**	448.2097
2534	1.8	**0.000488244**	488.2435
4090	2.8	**0.000514911**	514.9113
6898	4.8	**0.000559907**	559.9069
9853	6.8	**0.000603234**	603.2337
11488	8.0	**0.000643236**	643.2363
18720	13.0	**0.000696576**	696.576
28800	20.0	**0.000738241**	738.2413
38880	27.0	**0.000766575**	766.5751
38881	27.0	**0.000453265**	453.2652

Time,m	Time, day	**Average Shrinkage Strain - 2 Cylinders (in/in)**	(x 10^6)	Creep= Total minus Shrinkage (in)	**Creep= Total minus Shrinkage (in/in)**	(x 10^6)
0	0	**0**	0	0.0000	**0.000000**	0
24	0.0	**5.01659E-06**	5.016592	0.0029	**0.000285**	284.9673
41	0.0	**2.8308E-05**	28.30803	0.0030	**0.000303**	303.3175
83	0.1	**1.32701E-05**	13.27013	0.0036	**0.000363**	363.2769
188	0.1	**1.1662E-05**	11.66199	0.0035	**0.000345**	344.8798
384	0.3	**3.16538E-05**	31.65377	0.0032	**0.000315**	314.8692
1227	0.9	**6.16742E-05**	61.67415	0.0039	**0.000387**	386.5356
2534	1.8	**6.66283E-05**	66.62833	0.0042	**0.000422**	421.6152
4090	2.8	**6.66125E-05**	66.61249	0.0045	**0.000448**	448.2988
6898	4.8	**8.66368E-05**	86.63677	0.0047	**0.000473**	473.2701
9853	6.8	**0.000119971**	119.9709	0.0048	**0.000483**	483.2628
11488	8.0	**0.000124979**	124.9791	0.0052	**0.000518**	518.2571
18720	13.0	**0.000108298**	108.2979	0.0059	**0.000588**	588.2781
28800	20.0	**0.000126622**	126.622	0.0061	**0.000612**	611.6194
38880	27.0	**0.000134969**	134.9687	0.0063	**0.000632**	631.6064
38881	27.0	**0.000134969**	134.9687	0.0032	**0.000318**	318.2965

Mix #3
Metakaolin - 5% OPC Replacement

Applied Creep Load = 2140psi

Time (min)	Total (in/in)	Creep (in/in)	Shrinkage (in/in)	Specific Creep plus Initial (microstrain/psi)	Specific Creep (microstrain/psi)	Specific Total (microstrain/psi)
0	0	0	0	0		0
24	.290E-3	.285E-3	.502E-5	0.133	0	0.136
41	.332E-3	.303E-3	.283E-4	0.142	0.009	0.155
83	.377E-3	.363E-3	.133E-4	0.170	0.037	0.176
188	.357E-3	.345E-3	.117E-4	0.161	0.028	0.167
384	.347E-3	.315E-3	.317E-4	0.147	0.014	0.162
1227	.448E-3	.387E-3	.617E-4	0.181	0.047	0.209
2534	.488E-3	.422E-3	.666E-4	0.197	0.064	0.228
4090	.515E-3	.448E-3	.666E-4	0.209	0.076	0.241
6898	.560E-3	.473E-3	.866E-4	0.221	0.088	0.262
9853	.603E-3	.483E-3	.120E-3	0.226	0.093	0.282
11488	.643E-3	.518E-3	.125E-3	0.242	0.109	0.301
18720	.697E-3	.588E-3	.108E-3	0.275	0.142	0.326
28800	.738E-3	.612E-3	.127E-3	0.286	0.153	0.345
38881	.453E-3	.318E-3	.135E-3	0.149		0.212

Mix Design #4

Metakaolin 10 % OPC Replacement

Mix # 4 - 3rd Alteration - Metakaolin - 10% OPC Replacement* w/c ratio= 0.3338

Concrete Constituent	mix proportions (per) 1 yd^3	**1.5 ft^3**		
Course Aggregate	1770 lb	**98.35**	lbs	
Fine Aggregate	1295	**71.95**	lbs	
Portland Cement Type II	597.5	**33.2**	lbs	
Silica Fume (AASHTO M307)	none	**none**		
Fly Ash (AASHTO M295)	100	**5.55**	lbs-------->	**2517.4g**
Metakaolin (High Reactive)	77.5	**4.3**	lbs-------->	**1950.4g**
Water	255	**14.37**	lbs	
Water Reducer (ASTM C494)		**none**		
Superplasticizer (ASTM C494)	7.0floz/cwt	**90 mL**		

* Based on 775 pounds of total cementitious materials

Concrete for Hood Canal Floating Bridge Replacement Project

Concrete Mix Design - **Metakaolin - 10% OPC Replacement**

Mix Design # - 4

Date Batched and Specimens Cast - December 14, 2002

Slump - 8.5"

Air Content - -

Batch Temperature - 62 F

Number of specimens cast (6x12 and 4x8) - 7 and 2 (#'s 28-36)

Date drilled and fitted with gage points -

28-day Curing Date - January 11, 2003

28-day Compressive Strength -

			Break notes
Cylinder f'c-1 =	9340psi	(264,240 lbs)	Shear Plane
Cylinder f'c-2 =	9080psi	(256,990 lbs)	Two cones
Cylinder f'c-3 =	9200psi	(260,400 lbs)	Two cones
Average =	9206.7psi		

Load to Apply for Creep Test - ASTM C 512

= 40% x f'c (28 day)

=.40 x 9207 psi = 3683 psi

Actual Applied Load = 33 tons = 25.4 % f'c (28 day) = 2334.3 psi

Creep and Shrinkage Measurements

		31			32		
		Cylinder C-1 (mix #__4__)			**Cylinder C-2 (mix #__4__)**		
	Actual date	Creep Measurement			Creep Measurement		
Scheduled Time	and time	1	2	3	1	2	3
Before Loading	2/18 2:20pm	0.1448	0.1567	0.1544	0.1369	0.1502	0.0959
Immediately after Loading	2/18 2:25pm	0.1414	0.153	0.1508	0.1336	0.1471	0.0928
15-20 minutes	2/18 2:40pm	0.1412	0.1532	0.1502	0.133	0.1469	0.0924
1 hour	2/18 3:25pm	0.141	0.1528	0.1501	0.1328	0.1468	0.0922
2 hours: 45 minutes	2/18 5:30pm	0.1411	0.1527	0.1499	0.1324	0.1469	0.0919
6 - 8 hours	2/18 8:50pm	0.141	0.1525	0.1499	0.1323	0.1469	0.092
2nd Day	2/19 5:05p	0.1406	0.152	0.1497	0.1321	0.1463	0.0917
3rd Day	2/20 1:30a	0.1397	0.1514	0.1494	0.1316	0.1454	0.0911
4th Day	2/21 2:05p	0.1395	0.1512	0.1489	0.1314	0.145	0.0909
7th Day	2/24 12:55p	0.1389	0.15	0.148	0.1311	0.1433	0.0888
14th Day	3/3 2:15p	0.1374	0.1488	0.1465	0.1301	0.1425	0.0882
21st Day	3/10 2:25p	0.1366	0.1479	0.1457	0.1292	0.1417	0.0877
28th day	3/17 1:35p	0.1361	0.1481	0.1451	0.1287	0.141	0.087
58th day	5/14 6:00p	0.1338	0.1446	0.1427	0.1269	0.1373	0.0845
recovery	5/14 6:00p	0.1372	0.1487	0.1468	0.1293	0.1426	0.0883

Creep and Shrinkage Measurements (Continued)

		33			34		
		Cylinder S-1 (mix #__4__)			**Cylinder S-2 (mix #__4__)**		
	Actual date	Shrinkage Measurement			Shrinkage Measurement		
Scheduled Time	and time	1	2	3	1	2	3
Before Loading	2/18 2:20pm	0.089	0.1593	0.1517	0.175	0.1552	0.1548
Immediately after Loading	2/18 2:25pm	0.089	0.1592	0.1516	0.1749	0.1551	0.1547
15-20 minutes	2/18 2:40pm	0.0889	0.1592	0.1515	0.1748	0.155	0.1546
1 hour	2/18 3:25pm	0.0888	0.1591	0.1514	0.1747	0.1549	0.1545
2 hours: 45 minutes	2/18 5:30pm	0.0888	0.1591	0.1514	0.1747	0.1549	0.1544
6 - 8 hours	2/18 8:50pm	0.0888	0.159	0.1514	0.1747	0.1549	0.1544
2nd Day	2/19 5:05p	0.0888	0.1589	0.1514	0.1746	0.1549	0.1543
3rd Day	2/20 1:30a	0.0887	0.1588	0.1513	0.1745	0.1548	0.1543
4th Day	2/21 2:05p	0.0887	0.1588	0.1513	0.1745	0.1548	0.1543
7th Day	2/24 12:55p	0.0887	0.1587	0.1513	0.1744	0.1547	0.1543
14th Day	3/3 2:15p	0.0885	0.1584	0.1509	0.1741	0.1545	0.154
21st Day	3/10 2:25p	0.0882	0.1583	0.1507	0.1737	0.1543	0.1538
28th day	3/17 1:35p	0.0881	0.158	0.1505	0.1735	0.1541	0.1535
58th day	5/14 6:00p	0.0865	0.1567	0.1488	0.1721	0.1527	0.152
recovery	5/14 6:00p	0.0865	0.1567	0.1488	0.1721	0.1527	0.152

Mix # 4 - Metakaolin -10% OPC Replacement

Creep Measurements

gage zero (10") = 0.1600

Cylinder plane #	strain	strain
T		
0		
0		
0		
0		
0		
0		
1		
2		
3		
5		
1		
2		
2		
2		
3		
5		
5		
6		

Shrinkage Measurements

gage zero (10") = 0.1600

Cylinder #33		average	average
Cylinder plane		shrinkage	shrinkage
T			
0			
0			
0			
0			
0			
0			
1			
2			
3			
5			
1			
2			
2			
2			
3			
5			
6			

(creep)

Cylinder #32 Cylinder plane # 1		2		3		average total strain (in)	average total strain (in/in)	Average total Strain - 2 Cylinders (in)
0.1369	9.9769	0.1502	9.9902	0.0959	9.9359			
0.0000	0.00000	0.0000	0.00000	0.0000	0.00000	0.0000	0.00000	0.0000
0.0033	0.00033	0.0031	0.00031	0.0031	0.00031	0.0032	0.00032	0.0034
0.0039	0.00039	0.0033	0.00033	0.0035	0.00035	0.0036	0.00036	0.0037
0.0041	0.00041	0.0034	0.00034	0.0037	0.00037	0.0037	0.00037	0.0039
0.0045	0.00045	0.0033	0.00033	0.0040	0.00040	0.0039	0.00039	0.0040
0.0046	0.00046	0.0033	0.00033	0.0039	0.00039	0.0039	0.00039	0.0041
0.0048	0.00048	0.0039	0.00039	0.0042	0.00042	0.0043	0.00043	0.0044
0.0053	0.00053	0.0048	0.00048	0.0048	0.00048	0.0050	0.00050	0.0051
0.0055	0.00055	0.0052	0.00052	0.0050	0.00050	0.0052	0.00053	0.0053
0.0058	0.00058	0.0069	0.00069	0.0071	0.00071	0.0066	0.00066	0.0065
0.0068	0.00068	0.0077	0.00077	0.0077	0.00077	0.0074	0.00074	0.0076
0.0077	0.00077	0.0085	0.00085	0.0082	0.00083	0.0081	0.00082	0.0084
0.0082	0.00082	0.0092	0.00092	0.0089	0.00090	0.0088	0.00088	0.0088
0.0100	0.00100	0.0129	0.00129	0.0114	0.00115	0.0114	0.00115	0.0115
0.0076	0.00076	0.0076	0.00076	0.0076	0.00076	0.0076	0.00076	0.0077

(shrinkage)

Cylinder #34 Cylinder plane 1		2		3		average shrinkage strain	average shrinkage strain (in/in)	Average Shrinkage Strain - 2 Cylinders (in)
0.175	10.0150	0.1552	9.9952	0.1548	9.9948			
0.0000	0.00000	0.0000	0.00000	0.0000	0.00000	0.0000	0.00000	0.0000
0.0001	0.00001	0.0001	0.00001	0.0001	0.00001	0.0001	0.00001	0.0001
0.0002	0.00002	0.0002	0.00002	0.0002	0.00002	0.0002	0.00002	0.0002
0.0003	0.00003	0.0003	0.00003	0.0003	0.00003	0.0003	0.00003	0.0003
0.0003	0.00003	0.0003	0.00003	0.0004	0.00004	0.0003	0.00003	0.0003
0.0003	0.00003	0.0003	0.00003	0.0004	0.00004	0.0003	0.00003	0.0003
0.0004	0.00004	0.0003	0.00003	0.0005	0.00005	0.0004	0.00004	0.0003
0.0005	0.00005	0.0004	0.00004	0.0005	0.00005	0.0005	0.00005	0.0004
0.0005	0.00005	0.0004	0.00004	0.0005	0.00005	0.0005	0.00005	0.0004
0.0006	0.00006	0.0005	0.00005	0.0005	0.00005	0.0005	0.00005	0.0005
0.0009	0.00009	0.0007	0.00007	0.0008	0.00008	0.0008	0.00008	0.0008
0.0013	0.00013	0.0009	0.00009	0.0010	0.00010	0.0011	0.00011	0.0010
0.0015	0.00015	0.0011	0.00011	0.0013	0.00013	0.0013	0.00013	0.0012
0.0029	0.00029	0.0025	0.00025	0.0028	0.00028	0.0027	0.00027	0.0027

0.0029	0.00029	0.0025	0.00025	0.0028	0.00028	0.0027	0.00027	0.0027

Time,m	Time, day	**Average total Strain - 2 Cylinders (in/in)**	(x 10^-6)
0	0	**0**	0
5	0.0	**0.000337**	337.3183
20	0.0	**0.000367**	367.3973
65	0.0	**0.000387**	387.4363
190	0.1	**0.000401**	400.8156
390	0.3	**0.000406**	405.8123
1605	1.1	**0.000443**	442.5436
2830	2.0	**0.000506**	506.0044
4305	3.0	**0.000534**	534.3843
8555	5.9	**0.000648**	648.013
18715	13.0	**0.000758**	758.1879
28805	20.0	**0.000837**	836.6555
38835	27.0	**0.000883**	883.4454
83520	58.0	**0.001154**	1153.944
83521	58.0	**0.000768**	768.2092

Time,m	Time, day	**Average Shrinkage Strain - 2 Cylinders (in/in)**	(x 10^-6)	Creep= Total minus Shrinkage (in)	**Creep= Total minus Shrinkage (in/in)**	(x 10^-6)
0	0	**0**	0	0.0000	**0.000000**	0
5	0.0	**8.33E-06**	8.334006	0.0033	**0.000329**	328.9842
20	0.0	**1.67E-05**	16.67981	0.0035	**0.000351**	350.7175
65	0.0	**2.67E-05**	26.6924	0.0036	**0.000361**	360.7439
190	0.1	**2.84E-05**	28.35994	0.0037	**0.000372**	372.4557
390	0.3	**3E-05**	30.02672	0.0038	**0.000376**	375.7856
1605	1.1	**3.5E-05**	35.02521	0.0041	**0.000408**	407.5184
2830	2.0	**4.34E-05**	43.37026	0.0046	**0.000463**	462.6341
4305	3.0	**4.34E-05**	43.37026	0.0049	**0.000491**	491.014
8555	5.9	**4.84E-05**	48.36869	0.0060	**0.000600**	599.6443
18715	13.0	**7.67E-05**	76.72846	0.0068	**0.000681**	681.4594
28805	20.0	**0.0001**	100.0938	0.0074	**0.000737**	736.5617
38835	27.0	**0.000122**	121.7747	0.0076	**0.000762**	761.6707
83520	58.0	**0.00027**	270.313	0.0088	**0.000884**	883.6311

83521	58.0	**0.00027**	270.313		0.0050	**0.000498**	497.8962

Mix #4

Metakaolin - 10% OPC Replacement

Applied Creep Load = 2340psi

Time (min)	Total (in/in)	Creep (in/in)	Shrinkage (in/in)	Specific Creep plus Initial (microstrain/psi)	Specific Creep (microstrain/psi)	Specific Total (microstrain/psi)
0	0	0	0	0		0
5	.337E-3	.329E-3	.833E-5	0.141	0	0.144
20	.367E-3	.351E-3	.167E-4	0.150	0.009	0.157
65	.387E-3	.361E-3	.267E-4	0.154	0.014	0.166
190	.401E-3	.372E-3	.284E-4	0.159	0.019	0.171
390	.406E-3	.376E-3	.300E-4	0.161	0.020	0.173
1605	.443E-3	.408E-3	.350E-4	0.174	0.034	0.189
2830	.506E-3	.463E-3	.434E-4	0.198	0.057	0.216
4305	.534E-3	.491E-3	.434E-4	0.210	0.069	0.228
8555	.648E-3	.600E-3	.484E-4	0.256	0.116	0.277
18715	.758E-3	.681E-3	.767E-4	0.291	0.151	0.324
28805	.837E-3	.737E-3	.100E-3	0.315	0.174	0.358
83520	.115E-2	.884E-3	.270E-3	0.378	0.237	0.493
83521	.768E-3	.498E-3	.270E-3	0.213		0.328

Mix Design #5

LVM (Phase 2)

Mix # 5 - LVM Mix Design #2 w/c ratio= 0.3342

Concrete Constituent	mix proportions (per) 1 yd^3	**1.5 ft^3**	
Course Aggregate	1770 lb	**98.35**	lbs
Fine Aggregate	1295	**71.95**	lbs
Portland Cement Type II	624	**34.65**	lbs
Silica Fume (AASHTO M307)	50	**2.8**	lbs
Fly Ash (AASHTO M295)	100	**5.55**	lbs
Water	258.66	**14.37**	lbs
Water Reducer (ASTM C494)		**none**	
Superplasticizer (ASTM C494)	5.3floz/cwt	**65 mL**	

slurry - Silica fume=**2.8 lbs**(all) **(1270.05grams)** Mix Water=total-slurry water
Water=**3.42lbs** **(1551.28grams)** = **10.73 lbs**
HRWR=**6mL**

Concrete for Hood Canal Floating Bridge Replacement Project

Concrete Mix Design - **LVM Mix Design (2nd), Reference Mix**

Mix Design # - 5

Date Batched and Specimens Cast - December 14, 2002

Slump - 8.5"

Air Content - -

Batch Temperature - 62 F

Number of specimens cast (6x12 and 4x8) - 7 and 2 (#'s 37-45)

Date drilled and fitted with gage points -

28-day Curing Date - January 11, 2003

28-day Compressive Strength -

		Break notes
Cylinder f'c-1 =	8870psi	(251,000 lbs) 2 cones
Cylinder f'c-2 =	8820psi	(249,550 lbs) Cone/Shear
Cylinder f'c-3 =	8910psi	(252,040 lbs) Cone/Shear
Average =	8866.7psi	

Load to Apply for Creep Test - ASTM C 512

= 40% x f'c (28 day)

=.40 x 8867 psi = 3547 psi

Actual Applied Load = 30.6 tons = 24.4 % f'c (28 day) = 2163.6 psi

Creep and Shrinkage Measurements

		40			41		
		Cylinder C-1 (mix #__5__)			**Cylinder C-2 (mix #__5__)**		
	Actual date	Creep Measurement			Creep Measurement		
Scheduled Time	and time	1	2	3	1	2	3
Before Loading	2/18 2:30pm	0.154	0.1566	0.1519	0.1538	0.1548	0.1571
Immediately after Loading	2/18 2:35pm	0.1506	0.153	0.149	0.1509	0.1509	0.153
15-20 minutes	2/18 2:58pm	0.1502	0.1527	0.1478	0.1505	0.1508	0.1532
1 hour	2/18 3:35pm	0.15	0.1526	0.1477	0.1504	0.1507	0.1527
2 hours: 45 minutes	2/18 5:35pm	0.1499	0.1524	0.1476	0.1501	0.1505	0.1525
6 - 8 hours	2/18 8:55pm	0.1499	0.1522	0.1474	0.1498	0.1504	0.1523
2nd Day	2/19 5:10p	0.1496	0.1519	0.1474	0.1496	0.15	0.1521
3rd Day	2/20 1:40a	0.149	0.1516	0.1469	0.1489	0.1493	0.1515
4th Day	2/21 2:07p	0.149	0.1514	0.1469	0.1487	0.1493	0.1512
7th Day	2/24 1:00p	0.1483	0.1505	0.1461	0.1481	0.1484	0.1502
14th Day	3/3 2:25p	0.1474	0.1497	0.1452	0.1472	0.1476	0.1491
21st Day	3/10 2:30p	0.1466	0.1488	0.1445	0.1463	0.147	0.1483
28th day	3/17 1:40p	0.1463	0.1484	0.1439	0.146	0.1462	0.148
58th day	5/14 6:00p	0.1446	0.1462	0.1422	0.1445	0.1442	0.1461
recovery	5/14 6:00p	0.1483	0.1501	0.146	0.1482	0.1488	0.1507

Creep and Shrinkage Measurements (Continued)

		42			43		
		Cylinder S-1 (mix #__5__)			**Cylinder S-2 (mix #__5__)**		
	Actual date	Shrinkage Measurement			Shrinkage Measurement		
Scheduled Time	and time	1	2	3	1	2	3
Before Loading	2/18 2:30pm	0.1422	0.1585	0.1421	0.1529	0.1605	0.1536
Immediately after Loading	2/18 2:35pm	0.1421	0.1585	0.1421	0.1529	0.1605	0.1536
15-20 minutes	2/18 2:58pm	0.1421	0.1583	0.142	0.1528	0.1604	0.1535
1 hour	2/18 3:35pm	0.142	0.1582	0.1419	0.1527	0.1603	0.1535
2 hours: 45 minutes	2/18 5:35pm	0.1421	0.1581	0.1419	0.1527	0.1603	0.1535
6 - 8 hours	2/18 8:55pm	0.1421	0.1581	0.1419	0.1526	0.1602	0.1535
2nd Day	2/19 5:10p	0.1421	0.1581	0.1418	0.1525	0.1602	0.1534
3rd Day	2/20 1:40a	0.1421	0.1581	0.1418	0.1525	0.1602	0.1533
4th Day	2/21 2:07p	0.142	0.1581	0.1417	0.1524	0.1601	0.1533
7th Day	2/24 1:00p	0.1419	0.1581	0.1417	0.1524	0.1601	0.1533
14th Day	3/3 2:25p	0.1419	0.1579	0.1414	0.1522	0.16	0.1532
21st Day	3/10 2:30p	0.1417	0.1579	0.1413	0.1522	0.1598	0.1531
28th day	3/17 1:40p	0.1416	0.1576	0.1412	0.152	0.1594	0.153
58th day	5/14 6:00p	0.1411	0.1564	0.1401	0.1503	0.1585	0.1517
recovery	5/14 6:00p	0.1411	0.1564	0.1401	0.1503	0.1585	0.1517

Mix # 5 -2nd LVM Mix Design

gage zero (10") = 0.1600

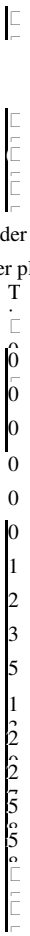

Cylinder #40	total	total
Cylinder plane #	strain	strain
T		
0		
0		
0		
0		
0		
0		
1		
2		
3		
5		
1		
2		
2		
2		
3		
5		
5		
8		

Shrinkage Measurements

gage zero (10") = 0.1600

Cylinder #42	average	average shrinkage
Cylinder plane	shrinkage	strain
T		
0		
0		
0		
0		
0		
0		
1		
2		
3		
5		
1		
2		
2		
2		
3		
5		
5		
8		

(creep)

Cylinder #41 Cylinder plane # 1		2		3		average total strain (in)	average total strain (in/in)	Average total Strain - 2 Cylinders (in)
0.1538	9.9938	0.1548	9.9948	0.1571	9.9971			
0.0000	0.00000	0.0000	0.00000	0.0000	0.00000	0.0000	0.00000	0.0000
0.0029	0.00029	0.0039	0.00039	0.0041	0.00041	0.0036	0.00036	0.0035
0.0033	0.00033	0.0040	0.00040	0.0039	0.00039	0.0037	0.00037	0.0038
0.0034	0.00034	0.0041	0.00041	0.0044	0.00044	0.0040	0.00040	0.0040
0.0037	0.00037	0.0043	0.00043	0.0046	0.00046	0.0042	0.00042	0.0042
0.0040	0.00040	0.0044	0.00044	0.0048	0.00048	0.0044	0.00044	0.0044
0.0042	0.00042	0.0048	0.00048	0.0050	0.00050	0.0047	0.00047	0.0046
0.0049	0.00049	0.0055	0.00055	0.0056	0.00056	0.0053	0.00053	0.0052
0.0051	0.00051	0.0055	0.00055	0.0059	0.00059	0.0055	0.00055	0.0053
0.0057	0.00057	0.0064	0.00064	0.0069	0.00069	0.0063	0.00063	0.0061
0.0066	0.00066	0.0072	0.00072	0.0080	0.00080	0.0073	0.00073	0.0070
0.0075	0.00075	0.0078	0.00078	0.0088	0.00088	0.0080	0.00080	0.0078
0.0078	0.00078	0.0086	0.00086	0.0091	0.00091	0.0085	0.00085	0.0082
0.0093	0.00093	0.0106	0.00106	0.0110	0.00110	0.0103	0.00103	0.0101
0.0056	0.00056	0.0060	0.00060	0.0064	0.00064	0.0060	0.00060	0.0060

(shrinkage)

Cylinder #43 Cylinder plane 1		2		3		average shrinkage strain	average shrinkage strain (in/in)	Average Shrinkage Strain - 2 Cylinders (in)
0.1529	9.9929	0.1605	10.0005	0.1536	9.9936			
0.0000	0.00000	0.0000	0.00000	0.0000	0.00000	0.0000	0.00000	0.0000
0.0000	0.00000	0.0000	0.00000	0.0000	0.00000	0.0000	0.00000	0.0000
0.0001	0.00001	0.0001	0.00001	0.0001	0.00001	0.0001	0.00001	0.0001
0.0002	0.00002	0.0002	0.00002	0.0001	0.00001	0.0002	0.00002	0.0002
0.0002	0.00002	0.0002	0.00002	0.0001	0.00001	0.0002	0.00002	0.0002
0.0003	0.00003	0.0003	0.00003	0.0001	0.00001	0.0002	0.00002	0.0002
0.0004	0.00004	0.0003	0.00003	0.0002	0.00002	0.0003	0.00003	0.0003
0.0004	0.00004	0.0003	0.00003	0.0003	0.00003	0.0003	0.00003	0.0003
0.0005	0.00005	0.0004	0.00004	0.0003	0.00003	0.0004	0.00004	0.0004
0.0005	0.00005	0.0004	0.00004	0.0003	0.00003	0.0004	0.00004	0.0004
0.0007	0.00007	0.0005	0.00005	0.0004	0.00004	0.0005	0.00005	0.0005
0.0007	0.00007	0.0007	0.00007	0.0005	0.00005	0.0006	0.00006	0.0006
0.0009	0.00009	0.0011	0.00011	0.0006	0.00006	0.0009	0.00009	0.0008
0.0026	0.00026	0.0020	0.00020	0.0019	0.00019	0.0022	0.00022	0.0020
0.0026	0.00026	0.0020	0.00020	0.0019	0.00019	0.0022	0.00022	0.0020

Time,m	Time, day	**Average total Strain - 2 Cylinders (in/in)**	(microstrain) (x 10^6)
0	0	**0**	0
5	0.0	**0.000347**	346.84
28	0.0	**0.000384**	383.54
65	0.0	**0.000402**	401.88
185	0.1	**0.000420**	420.22
385	0.3	**0.000437**	436.90
1600	1.1	**0.000460**	460.24
2830	2.0	**0.000517**	516.94
4297	3.0	**0.000529**	528.61
8550	5.9	**0.000610**	610.32
18710	13.0	**0.000700**	700.37
28800	20.0	**0.000779**	778.74
38830	27.0	**0.000824**	823.76
83520	58.0	**0.001007**	1007.19
83521	58.0	**0.000602**	601.98

Time,m	Time, day	**Average Shrinkage Strain - 2 Cylinders (in/in)**	(microstrain) (x 10^6)	Creep= Total minus Shrinkage (in)	**Creep= Total minus Shrinkage (in/in)**	(microstrain) (x 10^6)
0	0	**0**	0	0.0000	**0.000000**	0
5	0.0	**1.668E-06**	1.668	0.0034	**0.000345**	345.18
28	0.0	**1.167E-05**	11.673	0.0037	**0.000372**	371.86
65	0.0	**2.001E-05**	20.011	0.0038	**0.000382**	381.87
185	0.1	**2.001E-05**	20.010	0.0040	**0.000400**	400.21
385	0.3	**2.335E-05**	23.345	0.0041	**0.000414**	413.55
1600	1.1	**2.835E-05**	28.348	0.0043	**0.000432**	431.89
2830	2.0	**3.002E-05**	30.016	0.0049	**0.000487**	486.92
4297	3.0	**3.669E-05**	36.686	0.0049	**0.000492**	491.92
8550	5.9	**3.835E-05**	38.354	0.0057	**0.000572**	571.96
18710	13.0	**5.336E-05**	53.363	0.0065	**0.000647**	647.00
28800	20.0	**6.337E-05**	63.368	0.0072	**0.000715**	715.37
38830	27.0	**8.338E-05**	83.378	0.0074	**0.000740**	740.39
83520	58.0	**1.951E-04**	195.103	0.0081	**0.000812**	812.09
83521	58.0	**1.951E-04**	195.103	0.0041	**0.000407**	406.88

Mix #5
LVM Mix Design, Reference Mix (Phase 2)

Applied Creep Load = 2160psi

Time (min)	Total (in/in)	Creep (in/in)	Shrinkage (in/in)	Specific Creep plus Initial (microstrain/psi)	Specific Creep (microstrain/psi)	Specific Total (microstrain/psi)
0	0	0	0	0		0
5	.347E-3	.345E-3	.167E-5	0.160	0	0.161
28	.384E-3	.372E-3	.117E-4	0.172	0.012	0.178
65	.402E-3	.382E-3	.200E-4	0.177	0.017	0.186
185	.420E-3	.400E-3	.200E-4	0.185	0.025	0.195
385	.437E-3	.414E-3	.233E-4	0.191	0.032	0.202
1600	.460E-3	.432E-3	.283E-4	0.200	0.040	0.213
2830	.517E-3	.487E-3	.300E-4	0.225	0.066	0.239
4297	.529E-3	.492E-3	.367E-4	0.228	0.068	0.245
8550	.610E-3	.572E-3	.384E-4	0.265	0.105	0.283
18710	.700E-3	.647E-3	.534E-4	0.300	0.140	0.324
28800	.779E-3	.715E-3	.634E-4	0.331	0.171	0.361
.						
83520	.101E-2	.812E-3	.195E-3	0.376	0.216	0.466
83521	.602E-3	.407E-3	.195E-3	0.188		0.279

Mix Design #6

LVM Mix with Caltite Waterproofing Admixture

Mix # 6 - 4th Alteration - LVM Mix with Caltite Admixture w/c ratio= 0.3514

Concrete Constituent	mix proportions (per) 1 yd^3	**1.5 ft^3**	
Course Aggregate	1770 lb	**98.35**	lbs
Fine Aggregate	1295	**71.95**	lbs
Portland Cement Type II	624	**34.65**	lbs
Silica Fume (AASHTO M307)	50	**2.8**	lbs
Fly Ash (AASHTO M295)	100	**5.55**	lbs
Water	222.12	**12.34**	lbs
Water Reducer (ASTM C494)		**none**	
Superplasticizer (ASTM C494)	5.5floz/cwt	**70 mL**	
Caltite	6 gallons	**2.77 lbs**	

Slurry - Silica fume=**2.8 lbs**(all) **(1270.05grams)** Mix Water=total-slurry water
Water=**3.42lbs** **(1551.28grams)** = **8.92 lbs**
HRWR=**6mL**

Concrete for Hood Canal Floating Bridge Replacement Project

Concrete Mix Design - **LVM Mix with Caltite Waterproofing Admixture**

Mix Design # - 6

Date Batched and Specimens Cast - December 14, 2002

Slump - 8.5"

Air Content - -

Batch Temperature - 62 F

Number of specimens cast (6x12 and 4x8) - 7 and 2 (#'s 46-54)

Date drilled and fitted with gage points -

28-day Curing Date - January 11, 2003

28-day Compressive Strength -

		Break notes	
Cylinder f'c-1 =	7010psi	(198,330 lbs)	Cone/Shear
Cylinder f'c-2 =	6800psi	(192,420 lbs)	Shear Plane
Cylinder f'c-3 =	6860psi	(194,190 lbs)	Cone/Shear
Average =	6890psi		

Load to Apply for Creep Test - ASTM C 512

= 40% x f'c (28 day)

=.40 x 6890 psi = 2756 psi

Actual Applied Load = 23.8 tons = 24.4 % f'c (28 day) = 1681.2 psi

Creep and Shrinkage Measurements

		49			50		
		Cylinder C-1 (mix #__6__)			**Cylinder C-2 (mix #__6__)**		
	Actual date	Creep Measurement			Creep Measurement		
Scheduled Time	and time	1	2	3	1	2	3
Before Loading	2/18 2:45pm	0.1114	0.1594	0.1509	0.1614	0.1592	0.1771
Immediately after Loading	2/18 2:55pm	0.1084	0.1568	0.1475	0.1588	0.1572	0.173
15-20 minutes	2/18 3:10pm	0.1083	0.1568	0.1473	0.1586	0.1574	0.1728
1 hour	2/18 3:55pm	0.1081	0.1564	0.147	0.1585	0.157	0.1725
2 hours: 45 minutes	2/18 5:40pm	0.1078	0.1562	0.1466	0.1581	0.1569	0.1722
6 - 8 hours	2/18 9:00pm	0.1077	0.1558	0.1465	0.158	0.1568	0.172
2nd Day	2/19 5:15p	0.1075	0.1558	0.146	0.1577	0.1565	0.1718
3rd Day	2/20 1:45a	0.107	0.1554	0.1454	0.1572	0.1562	0.1712
4th Day	2/21 2:10p	0.107	0.1554	0.145	0.1574	0.1563	0.1708
7th Day	2/24 1:05p	0.1064	0.1547	0.1444	0.1569	0.1558	0.1702
14th Day	3/3 2:30p	0.1054	0.1542	0.1434	0.1561	0.1548	0.169
21st Day	3/10 2:35p	0.1048	0.1533	0.1424	0.1553	0.1542	0.1682
28th day	3/17 1:45p	0.1044	0.1529	0.1421	0.1549	0.1538	0.1678
58th day	5/14 6:00p	0.1026	0.1513	0.1402	0.1531	0.1523	0.1659
recovery	5/14 6:00p	0.1057	0.1541	0.144	0.1564	0.1548	0.1703

Creep and Shrinkage Measurements (Continued)

		51			52		
		Cylinder S-1 (mix #__6__)			**Cylinder S-2 (mix #__6__)**		
	Actual date	Shrinkage Measurement			Shrinkage Measurement		
Scheduled Time	and time	1	2	3	1	2	3
Before Loading	2/18 2:45pm	0.154	0.1551	0.152	0.162	0.1631	0.156
Immediately after Loading	2/18 2:55pm	0.154	0.1551	0.152	0.162	0.1631	0.156
15-20 minutes	2/18 3:10pm	0.1539	0.155	0.1518	0.1619	0.1629	0.1559
1 hour	2/18 3:55pm	0.1538	0.155	0.1517	0.1618	0.1628	0.1558
2 hours: 45 minutes	2/18 5:40pm	0.1538	0.155	0.1517	0.1618	0.1627	0.1558
6 - 8 hours	2/18 9:00pm	0.1538	0.1549	0.1516	0.1618	0.1627	0.1557
2nd Day	2/19 5:15p	0.1537	0.1548	0.1513	0.1617	0.1626	0.1556
3rd Day	2/20 1:45a	0.1536	0.1547	0.1511	0.1616	0.1625	0.1554
4th Day	2/21 2:10p	0.1536	0.1547	0.1511	0.1616	0.1625	0.1554
7th Day	2/24 1:05p	0.1536	0.1547	0.151	0.1616	0.1625	0.1553
14th Day	3/3 2:30p	0.1533	0.1545	0.1507	0.1615	0.1623	0.1551
21st Day	3/10 2:35p	0.1531	0.1542	0.1506	0.1613	0.1622	0.1548
28th day	3/17 1:45p	0.1528	0.1541	0.1504	0.1613	0.1621	0.1545
58th day	5/14 6:00p	0.1519	0.153	0.1492	0.1601	0.1614	0.1531
recovery	5/14 6:00p	0.1519	0.153	0.1492	0.1601	0.1614	0.1531

Mix #6 - LVM Mix w/ Caltite

gage zero (10") = 0.1600

Cylinder #49	total	total
Cylinder plane #	strain	strain
T		
0		
0		
0		
0		
0		
0		
1		
2		
3		
5		
1		
2		
2		
3		
5		
5		
6		

Shrinkage Measurements

gage zero (10") = 0.1600

Cylinder #51	average	average shrinkage
Cylinder plane	shrinkage	strain
T		
0		
0		
0		
0		
0		
0		
1		
2		
3		
5		
1		
2		
2		
3		
5		
5		
6		

(creep)

Cylinder #50 Cylinder plane # 1		2		3		average total strain (in)	average total strain (in/in)	Average total Strain - 2 Cylinders (in)
0.1614	10.0014	0.1592	9.9992	0.1771	10.0171			
0.0000	0.00000	0.0000	0.00000	0.0000	0.00000	0.0000	0.00000	0.0000
0.0026	0.00026	0.0020	0.00020	0.0041	0.00041	0.0029	0.00029	0.0030
0.0028	0.00028	0.0018	0.00018	0.0043	0.00043	0.0030	0.00030	0.0030
0.0029	0.00029	0.0022	0.00022	0.0046	0.00046	0.0032	0.00032	0.0033
0.0033	0.00033	0.0023	0.00023	0.0049	0.00049	0.0035	0.00035	0.0036
0.0034	0.00034	0.0024	0.00024	0.0051	0.00051	0.0036	0.00036	0.0038
0.0037	0.00037	0.0027	0.00027	0.0053	0.00053	0.0039	0.00039	0.0040
0.0042	0.00042	0.0030	0.00030	0.0059	0.00059	0.0044	0.00044	0.0045
0.0040	0.00040	0.0029	0.00029	0.0063	0.00063	0.0044	0.00044	0.0046
0.0045	0.00045	0.0034	0.00034	0.0069	0.00069	0.0049	0.00049	0.0052
0.0053	0.00053	0.0044	0.00044	0.0081	0.00081	0.0059	0.00059	0.0061
0.0061	0.00061	0.0050	0.00050	0.0089	0.00089	0.0067	0.00067	0.0069
0.0065	0.00065	0.0054	0.00054	0.0093	0.00093	0.0071	0.00071	0.0072
0.0083	0.00083	0.0069	0.00069	0.0112	0.00112	0.0088	0.00088	0.0090
0.0050	0.00050	0.0044	0.00044	0.0068	0.00068	0.0054	0.00054	0.0057

(shrinkage)

Cylinder #52 Cylinder plane 1		2		3		average shrinkage strain	average shrinkage strain (in/in)	Average Shrinkage Strain - 2 Cylinders (in)
0.162	10.0020	0.1631	10.0031	0.156	9.9960			
0.0000	0.00000	0.0000	0.00000	0.0000	0.00000	0.0000	0.00000	0.0000
0.0000	0.00000	0.0000	0.00000	0.0000	0.00000	0.0000	0.00000	0.0000
0.0001	0.00001	0.0002	0.00002	0.0001	0.00001	0.0001	0.00001	0.0001
0.0002	0.00002	0.0003	0.00003	0.0002	0.00002	0.0002	0.00002	0.0002
0.0002	0.00002	0.0004	0.00004	0.0002	0.00002	0.0003	0.00003	0.0002
0.0002	0.00002	0.0004	0.00004	0.0003	0.00003	0.0003	0.00003	0.0003
0.0003	0.00003	0.0005	0.00005	0.0004	0.00004	0.0004	0.00004	0.0004
0.0004	0.00004	0.0006	0.00006	0.0006	0.00006	0.0005	0.00005	0.0005
0.0004	0.00004	0.0006	0.00006	0.0006	0.00006	0.0005	0.00005	0.0005
0.0004	0.00004	0.0006	0.00006	0.0007	0.00007	0.0006	0.00006	0.0006
0.0005	0.00005	0.0008	0.00008	0.0009	0.00009	0.0007	0.00007	0.0008
0.0007	0.00007	0.0009	0.00009	0.0012	0.00012	0.0009	0.00009	0.0010
0.0007	0.00007	0.0010	0.00010	0.0015	0.00015	0.0011	0.00011	0.0012
0.0019	0.00019	0.0017	0.00017	0.0029	0.00029	0.0022	0.00022	0.0023
0.0019	0.00019	0.0017	0.00017	0.0029	0.00029	0.0022	0.00022	0.0023

Time,m	Time, day	**Average total Strain - 2 Cylinders (in/in)**	(x 10^-6)
0	0	**0**	0
5	0.0	**0.000295**	295.1784
20	0.0	**0.000304**	303.5164
65	0.0	**0.000332**	331.8628
170	0.1	**0.000360**	360.2175
370	0.3	**0.000377**	376.8884
1585	1.1	**0.000402**	401.9063
2815	2.0	**0.000450**	450.272
4280	3.0	**0.000459**	458.6003
8535	5.9	**0.000517**	516.9747
18700	13.0	**0.000609**	608.7038
28785	20.0	**0.000687**	687.0782
38815	27.0	**0.000725**	725.4373
83520	58.0	**0.000901**	900.558
83521	58.0	**0.000569**	568.7081

Time,m	Time, day	**Average Shrinkage Strain - 2 Cylinders (in/in)**	(x 10^-6)	Creep= Total minus Shrinkage (in)	**Creep= Total minus Shrinkage (in/in)**	(x 10^-6)
0	0	**0**	0	0.0000	**0.000000**	0
5	0.0	**0**	0	0.0030	**0.000295**	295.1784
20	0.0	**1.3E-05**	13.3418	0.0029	**0.000290**	290.1746
65	0.0	**2.2E-05**	21.68184	0.0031	**0.000310**	310.1809
170	0.1	**2.3E-05**	23.34864	0.0034	**0.000337**	336.8688
370	0.3	**2.8E-05**	28.34742	0.0035	**0.000349**	348.541
1585	1.1	**4.2E-05**	41.6906	0.0036	**0.000360**	360.2157
2815	2.0	**5.5E-05**	55.02942	0.0040	**0.000395**	395.2426
4280	3.0	**5.5E-05**	55.02942	0.0040	**0.000404**	403.5709
8535	5.9	**5.8E-05**	58.36142	0.0046	**0.000459**	458.6133
18700	13.0	**8.0E-05**	80.05161	0.0053	**0.000529**	528.6522
28785	20.0	**1.0E-04**	100.0608	0.0059	**0.000587**	587.0174
38815	27.0	**1.2E-04**	116.7467	0.0061	**0.000609**	608.6906
83520	58.0	**2.3E-04**	225.1309	0.0068	**0.000675**	675.4271
83521	58.0	**2.3E-04**	225.1309	0.0034	**0.000344**	343.5772

Mix #6
LVM Mix with Caltite Waterproofing Admixture

Applied Creep Load = 1680 psi

Time (min)	Total (in/in)	Creep (in/in)	Shrinkage (in/in)	Specific Creep plus Initial (microstrain/psi)	Specific Creep (microstrain/psi)	Specific Total (microstrain/psi)
0	0	0	0	0		0
5	.295E-3	.295E-3	.000E+0	0.176	0	0.176
20	.304E-3	.290E-3	.133E-4	0.173	-0.003	0.181
65	.332E-3	.310E-3	.217E-4	0.185	0.009	0.198
170	.360E-3	.337E-3	.233E-4	0.201	0.025	0.214
370	.377E-3	.349E-3	.283E-4	0.207	0.032	0.224
1585	.402E-3	.360E-3	.417E-4	0.214	0.039	0.239
2815	.450E-3	.395E-3	.550E-4	0.235	0.060	0.268
4280	.459E-3	.404E-3	.550E-4	0.240	0.065	0.273
8535	.517E-3	.459E-3	.584E-4	0.273	0.097	0.308
18700	.609E-3	.529E-3	.801E-4	0.315	0.139	0.362
28785	.687E-3	.587E-3	.100E-3	0.349	0.174	0.409
83520	.901E-3	.675E-3	.225E-3	0.402	0.226	0.536
83521	.569E-3	.344E-3	.225E-3	0.205		0.339

Mix Design #7

Caltite Mix Design

Mix # 7 - 5th Alteration - Mix w/Caltite w/o Silica Fume w/c ratio= 0.2826

Concrete Constituent	mix proportions (per) 1 yd^3	**1.5 ft^3**	
Course Aggregate	1770 lb	**98.35**	lbs
Fine Aggregate	1295	**71.95**	lbs
Portland Cement Type II	624	**34.65**	lbs
Silica Fume (AASHTO M307)	none	**none**	lbs
Fly Ash (AASHTO M295)	100	**5.55**	lbs
Water	154.64	**8.59**	lbs
Water Reducer (ASTM C494)		**none**	
Superplasticizer (ASTM C494)	6.3floz/cwt	**75 mL**	
Caltite	6 gallons	**2.77 lbs**	

Concrete for Hood Canal Floating Bridge Replacement Project

Concrete Mix Design - **Caltite Mix Design**

Mix Design # - 7

Date Batched and Specimens Cast - December 14, 2002

Slump - 9.0"

Air Content - -

Batch Temperature - 62 F

Number of specimens cast (6x12 and 4x8) - 7 and 2 (#'s 55-63)

Date drilled and fitted with gage points -

28-day Curing Date - January 11, 2003

28-day Compressive Strength -

			Break notes
Cylinder f'c-1 =	6100psi	(172,550 lbs)	Vertical Planes
Cylinder f'c-2 =	6350psi	(179,770 lbs)	Crushing
Cylinder f'c-3 =	6250psi	(176,790 lbs)	Crushing
Average =	6233.3psi		

Load to Apply for Creep Test - ASTM C 512

= 40% x f'c (28 day)

=.40 x 6233.3 psi = 2493 psi

Actual Applied Load = 21.5 tons = 24.4 % f'c (28 day) = 1520.9 psi

Creep and Shrinkage Measurements

		58			59		
		Cylinder C-1 (mix #__7__)			**Cylinder C-2 (mix #__7__)**		
	Actual date	Creep Measurement			Creep Measurement		
Scheduled Time	and time	1	2	3	1	2	3
Before Loading	2/18 3:05pm	0.152	0.1585	0.1505	0.1354	0.1419	0.1165
Immediately after Loading	2/18 3:10pm	0.1507	0.1562	0.1484	0.134	0.1379	0.1143
15-20 minutes	2/18 3:25pm	0.1505	0.1561	0.148	0.134	0.1377	0.1141
1 hour	2/18 4:25pm	0.1504	0.1558	0.148	0.1338	0.1377	0.1141
2 hours: 45 minutes	2/18 5:45pm	0.1502	0.1554	0.1478	0.1332	0.1372	0.1139
6 - 8 hours	2/18 9:05pm	0.1499	0.1553	0.1476	0.1328	0.137	0.1138
2nd Day	2/19 5:20p	0.1497	0.155	0.1475	0.1326	0.1368	0.1137
3rd Day	2/20 1:50a	0.1494	0.1545	0.1472	0.1323	0.1366	0.1132
4th Day	2/21 2:15p	0.1496	0.1543	0.1475	0.1324	0.1363	0.1133
7th Day	2/24 1:10p	0.1489	0.1535	0.1472	0.1314	0.1355	0.1127
14th Day	3/3 2:35p	0.1486	0.1527	0.1467	0.1308	0.1346	0.1122
21st Day	3/10 2:40p	0.1481	0.1521	0.1461	0.1302	0.1336	0.1116
28th day	3/17 1:50p	0.1478	0.1517	0.1457	0.13	0.1327	0.1109
58th day	5/14 6:00p	0.1462	0.149	0.1435	0.1284	0.1303	0.1092
recovery	5/14 6:00p	0.1483	0.1521	0.1458	0.1298	0.1344	0.1115

Creep and Shrinkage Measurements (Continued)

		60			61		
		Cylinder S-1 (mix #__7__)			**Cylinder S-2 (mix #__7__)**		
	Actual date	Shrinkage Measurement			Shrinkage Measurement		
Scheduled Time	and time	1	2	3	1	2	3
Before Loading	2/18 2:45pm	0.1557	0.1582	0.1575	0.1581	0.1558	0.1532
Immediately after Loading	2/18 2:55pm	0.1557	0.1582	0.1575	0.1581	0.1558	0.1532
15-20 minutes	2/18 3:10pm	0.1556	0.1582	0.1574	0.1579	0.1557	0.1531
1 hour	2/18 3:55pm	0.1555	0.1581	0.1573	0.1578	0.1556	0.153
2 hours: 45 minutes	2/18 5:40pm	0.1555	0.1581	0.1573	0.1577	0.1556	0.153
6 - 8 hours	2/18 9:00pm	0.1554	0.1581	0.1573	0.1576	0.1556	0.153
2nd Day	2/19 5:15p	0.1553	0.158	0.1572	0.1575	0.1555	0.1528
3rd Day	2/20 1:45a	0.1552	0.1579	0.1571	0.1575	0.1555	0.1527
4th Day	2/21 2:10p	0.1552	0.1578	0.157	0.1575	0.1556	0.1527
7th Day	2/24 1:05p	0.1551	0.1577	0.1569	0.1575	0.1556	0.1527
14th Day	3/3 2:30p	0.155	0.1575	0.1567	0.1573	0.1554	0.1526
21st Day	3/10 2:35p	0.1548	0.1572	0.1565	0.1569	0.1552	0.1522
28th day	3/17 1:45p	0.1546	0.1569	0.1563	0.1564	0.1547	0.1519
58th day	5/14 6:00p	0.1533	0.1556	0.1553	0.1554	0.1537	0.1512
recovery	5/14 6:00p	0.1533	0.1556	0.1553	0.1554	0.1537	0.1512

Mix #7 - Caltite Mix Design

gage zero (10") = 0.1600

Cylinder #	58	total strain	total strain
Cylinder plane #			
T			
0			
0			
0			
0			
0			
0			
1			
1			
3			
5			
1			
2			
2			
5			
5			

Shrinkage Measurements

gage zero (10") = 0.1600

Cylinder #	60	average shrinkage	average shrinkage
Cylinder plane			
T			
0			
0			
0			
0			
0			
0			
1			
1			
3			
5			
1			
2			
2			
5			
5			

(creep)

Cylinder #59 Cylinder plane #						average total strain	average total strain	Average total Strain - 2 Cylinders
1		2		3		(in)	(in/in)	(in)
0.1354	9.9754	0.1419	9.9819	0.1165	9.9565			
0.0000	0.00000	0.0000	0.00000	0.0000	0.00000	0.0000	0.00000	0.0000
0.0014	0.00014	0.0040	0.00040	0.0022	0.00022	0.0025	0.00025	0.0022
0.0014	0.00014	0.0042	0.00042	0.0024	0.00024	0.0027	0.00027	0.0024
0.0016	0.00016	0.0042	0.00042	0.0024	0.00024	0.0027	0.00027	0.0025
0.0022	0.00022	0.0047	0.00047	0.0026	0.00026	0.0032	0.00032	0.0029
0.0026	0.00026	0.0049	0.00049	0.0027	0.00027	0.0034	0.00034	0.0031
0.0028	0.00028	0.0051	0.00051	0.0028	0.00028	0.0036	0.00036	0.0033
0.0031	0.00031	0.0053	0.00053	0.0033	0.00033	0.0039	0.00039	0.0036
0.0030	0.00030	0.0056	0.00056	0.0032	0.00032	0.0039	0.00039	0.0036
0.0040	0.00040	0.0064	0.00064	0.0038	0.00038	0.0047	0.00047	0.0043
0.0046	0.00046	0.0073	0.00073	0.0043	0.00043	0.0054	0.00054	0.0049
0.0052	0.00052	0.0083	0.00083	0.0049	0.00049	0.0061	0.00061	0.0055
0.0054	0.00054	0.0092	0.00092	0.0056	0.00056	0.0067	0.00068	0.0060
0.0070	0.00070	0.0116	0.00116	0.0073	0.00073	0.0086	0.00087	0.0080
0.0056	0.00056	0.0075	0.00075	0.0050	0.00050	0.0060	0.00060	0.0055

(shrinkage)

Cylinder #61 Cylinder plane						average shrinkage strain	average shrinkage strain (in/in)	Average Shrinkage Strain - 2 Cylinders (in)
1		2		3				
0.1581	9.9981	0.1558	9.9958	0.1532	9.9932			
0.0000	0.00000	0.0000	0.00000	0.0000	0.00000	0.0000	0.00000	0.0000
0.0000	0.00000	0.0000	0.00000	0.0000	0.00000	0.0000	0.00000	0.0000
0.0002	0.00002	0.0001	0.00001	0.0001	0.00001	0.0001	0.00001	0.0001
0.0003	0.00003	0.0002	0.00002	0.0002	0.00002	0.0002	0.00002	0.0002
0.0004	0.00004	0.0002	0.00002	0.0002	0.00002	0.0003	0.00003	0.0002
0.0005	0.00005	0.0002	0.00002	0.0002	0.00002	0.0003	0.00003	0.0003
0.0006	0.00006	0.0003	0.00003	0.0004	0.00004	0.0004	0.00004	0.0004
0.0006	0.00006	0.0003	0.00003	0.0005	0.00005	0.0005	0.00005	0.0004
0.0006	0.00006	0.0002	0.00002	0.0005	0.00005	0.0004	0.00004	0.0005
0.0006	0.00006	0.0002	0.00002	0.0005	0.00005	0.0004	0.00004	0.0005
0.0008	0.00008	0.0004	0.00004	0.0006	0.00006	0.0006	0.00006	0.0007
0.0012	0.00012	0.0006	0.00006	0.0010	0.00010	0.0009	0.00009	0.0009
0.0017	0.00017	0.0011	0.00011	0.0013	0.00013	0.0014	0.00014	0.0013
0.0027	0.00027	0.0021	0.00021	0.0020	0.00020	0.0023	0.00023	0.0023
0.0027	0.00027	0.0021	0.00021	0.0020	0.00020	0.0023	0.00023	0.0023

Time,m	Time, day	**Average total Strain - 2 Cylinders (in/in)**	(microstrain) (x 10^-6)
0	0	**0**	0
5	0.0	**0.000222**	222.1
20	0.0	**0.000240**	240.4
80	0.1	**0.000250**	250.4
160	0.1	**0.000285**	285.5
360	0.3	**0.000307**	307.2
1571	1.1	**0.000326**	325.6
2805	1.9	**0.000361**	360.6
4267	3.0	**0.000357**	357.3
8525	5.9	**0.000427**	427.4
18690	13.0	**0.000488**	487.5
28775	20.0	**0.000553**	552.6
38805	26.9	**0.000601**	601.1
83520	58.0	**0.000805**	804.7
83521	58.0	**0.000549**	549.3

Time,m	Time, day	**Average Shrinkage Strain - 2 Cylinders (in/in)**	(microstrain) (x 10^-6)	Creep= Total minus Shrinkage (in)	**Creep= Total minus Shrinkage (in/in)**	(microstrain) (x 10^-6)
0	0	**0**	0	0.0000	**0.000000**	0
5	0.0	**0**	0	0.0022	**0.000222**	222.1
20	0.0	**1.00E-05**	10.0	0.0023	**0.000230**	230.4
80	0.1	**2.00E-05**	20.0	0.0023	**0.000230**	230.4
160	0.1	**2.17E-05**	21.7	0.0026	**0.000264**	263.8
360	0.3	**2.50E-05**	25.0	0.0028	**0.000282**	282.2
1571	1.1	**3.67E-05**	36.7	0.0029	**0.000289**	288.8
2805	1.9	**4.34E-05**	43.4	0.0032	**0.000317**	317.2
4267	3.0	**4.51E-05**	45.1	0.0031	**0.000312**	312.2
8525	5.9	**5.01E-05**	50.1	0.0038	**0.000377**	377.3
18690	13.0	**6.68E-05**	66.8	0.0042	**0.000421**	420.7
28775	20.0	**9.52E-05**	95.2	0.0046	**0.000457**	457.5
38805	26.9	**1.29E-04**	128.6	0.0047	**0.000472**	472.5
83520	58.0	**2.34E-04**	233.7	0.0057	**0.000571**	571.0
83521	58.0	**2.34E-04**	233.7	0.0032	**0.000316**	315.6

Mix #7
Caltite Mix Design

Applied Creep Load = 1520psi

Time (min)	Total (in/in)	Creep (in/in)	Shrinkage (in/in)	Specific Creep plus Initial (microstrain/psi)	Specific Creep (microstrain/psi)	Specific Total (microstrain/psi)
0	0	0	0	0		0
5	.222E-3	.222E-3	.000E+0	0.146	0	0.146
20	.240E-3	.230E-3	.100E-4	0.152	0.005	0.158
80	.250E-3	.230E-3	.200E-4	0.152	0.005	0.165
160	.285E-3	.264E-3	.217E-4	0.174	0.027	0.188
360	.307E-3	.282E-3	.250E-4	0.186	0.040	0.202
1571	.326E-3	.289E-3	.367E-4	0.190	0.044	0.214
2805	.361E-3	.317E-3	.434E-4	0.209	0.063	0.237
4267	.357E-3	.312E-3	.451E-4	0.205	0.059	0.235
8525	.427E-3	.377E-3	.501E-4	0.248	0.102	0.281
18690	.488E-3	.421E-3	.668E-4	0.277	0.131	0.321
28775	.553E-3	.457E-3	.952E-4	0.301	0.155	0.364
83520	.805E-3	.571E-3	.234E-3	0.376	0.230	0.529
83521	.549E-3	.316E-3	.234E-3	0.208		0.361

APPENDIX B

EXPERIMENT 2

B1. - Water level changes – second experiment – stage one.

		Water Column Height			
		Specimen			
Time	Air Pressure Gauge Reading (psi)	A1	B1	C1	D1
		Control, No Joint	Control, Joint	MC-2010MN	Synko-flex
10:00	0	20.3	19	17.2	17.5
10:35	5	24.5	23.5	22.1	48.5 *
11:05	10	27.4	26.7	25	N.A.
11:35	15	29.4	28.9	27.2	N.A.
12:00	20	31.8	31.8	29.5	N.A.
12:30	25	33.8	37.3	31.2	N.A.
1:00	30	36	52 *	33.2	N.A.
1:30	35	38	54	35	N.A.
2:00	40	40.3	56.3	37	N.A.
2:30	50	44.2	N.A.	39.8	N.A.
3:00	60	47.8	N.A.	43.2	N.A.
3:30	70	51	67.4	46.4	N.A.
4:30	80	55.8	73.4	48.6	N.A.
5:00	90	N.A.	82.3	52.5	N.A.
5:30	100	77	87.5	55.6	N.A.

*** Pressure system leak observed.**

B2. - Water volume changes – second experiment – stage one.

Time	Air Pressure Gauge Reading (psi)	Volume Changes (cm^3)			
		Specimen			
		A1	B1	C1	D1
		Control, No Joint	Control, Joint	MC-2010MN	Synko-flex
10:00	0	0	0	0	0
10:35	5	532.0	570.0	620.7	3927.0
11:05	10	899.4	975.4	988.1	
11:35	15	1152.8	1254.1	1266.8	
12:00	20	1456.8	1621.5	1558.1	
12:30	25	1710.1	2318.2	1773.5	
1:00	30	1988.8	4180.3	2026.8	
1:30	35	2242.2	4433.7	2254.8	
2:00	40	2533.5	4725.0	2508.2	
2:30	50	3027.6		2862.9	
3:00	60	3483.6		3293.6	
3:30	70	3889.0		3699.0	
4:30	80	4497.0		3977.7	
5:00	90			4471.7	
5:30	100			4864.4	

B3. - Water level changes – second experiment – stage two.

	Water Column Height (cm)
	5 3 . 2 2 1 N . A . N . A . N . A

*** Pressure system leak observed.**

B4. - Water volume changes – second experiment - stage two.

	Volume Decrease (cm^3)
A	
	2 4 8 2 3

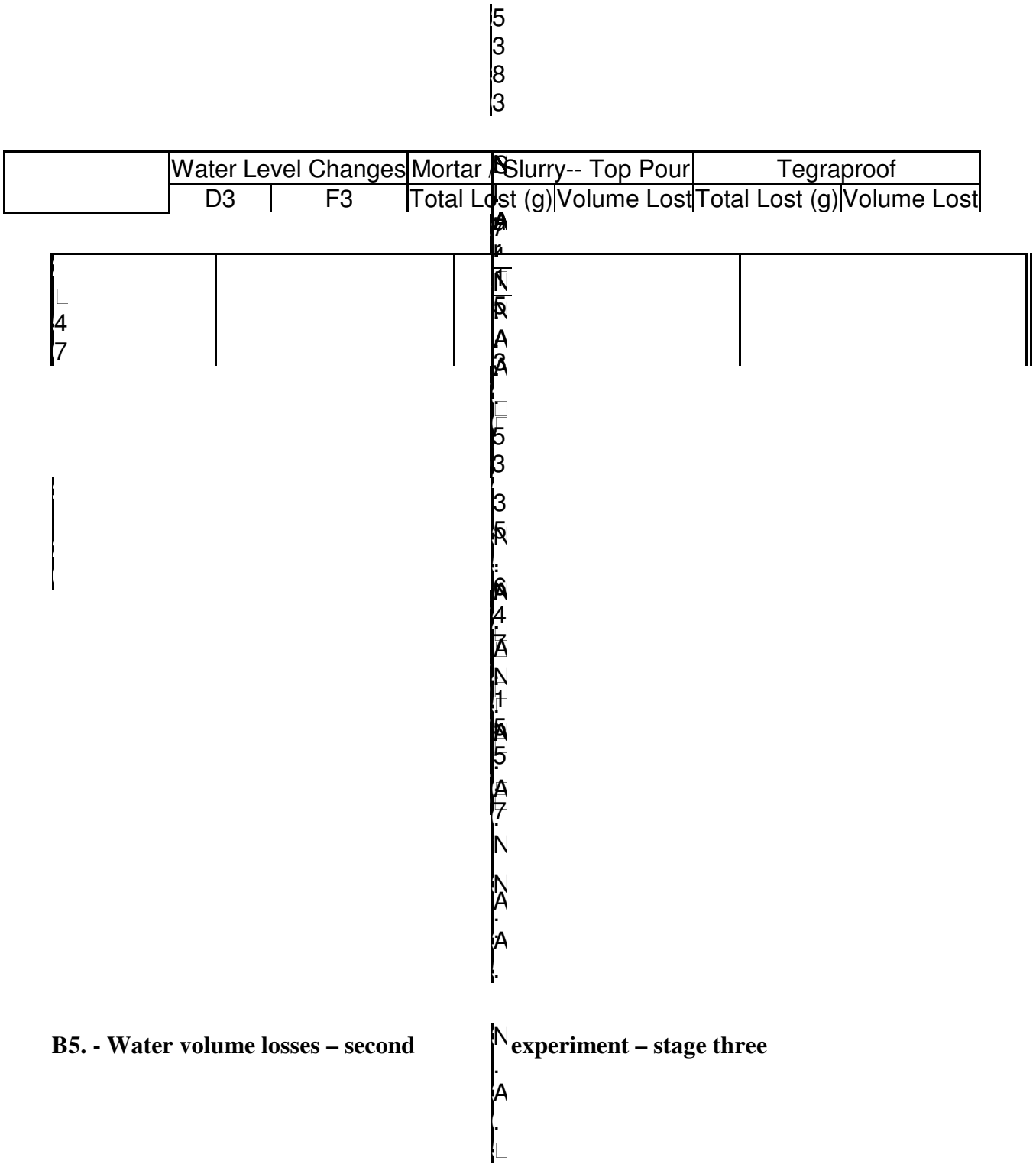

	Water Level Changes		Mortar	Slurry-- Top Pour		Tegraproof	
	D3	F3	Total Lost (g)	Volume Lost		Total Lost (g)	Volume Lost

B5. - Water volume losses – second experiment – stage three

APPENDIX C

EXPERIMENT 3

Waterstop RX-1						
Time	Weight	Length	Thickness (mm)	Width (mm)	Expansion Rate	Thickness Increase

C1. - Waterstop-RX 101TRH - specimen one.

C2. - Waterstop-RX 101TRH - specimen two.

Waterstop RX-2						
Time	Weight	Length	Thickness (mm)	Width (mm)	Expansion Rate	Thickness Increase

C3. - Waterstop-RX 101TRH - specimen three.

Waterstop RX-3						
Time	Weight	Length	Thickness (mm)	Width (mm)	Expansion Rate	Thickness Increase

C4. - Waterstop-RX 101TRH - averages.

Waterstop RX-AVG						
Time	Weight	Length	Thickness	Width	Expansion Rate	Thickness Increase
(Day)	(g)	(mm)	(mm)	(mm)	(%)	(mm)
0	156.5	198.7	17.7	25.9	0.0	0.0
1	275.0	229.5	27.2	39.3	75.7	9.5
3	394.4	186.3	34.0	48.4	151.9	16.4
5	481.2	220.0	42.0	55.8	207.4	24.4
7	525.3	116.3	42.3	59.3	235.6	25.0

C5. - MC-2010MN – specimen one.

MC 2010-MN-1						
Time	Weight	Length	Thickness (mm)	Width (mm)	Expansion Rate	Thickness Increase

C6. - MC-2010MN – specimen two.

MC 2010-MN-2						
Time	Weight	Length	Thickness (mm)	Width (mm)	Expansion Rate	Thickness Increase

2

2

2

C7. - MC-2010MN – specimen three.

MC 2010-MN-3						
Time	Weight	Length	Thickness (mm)	Width (mm)	Expansion Rate	Thickness Increase

2

2

2
0

2

2

2
1

C8. - MC-2010MN – averages.

MC-2010MN-AVG						
Time	Weight	Length	Thickness	Width	Expansion Rate	Thickness Increase
(Day)	(g)	(mm)	(mm)	(mm)	(%)	(mm)
0	23.4	200.0	9.0	15.0	0.0	0.0
1	28.5	202.3	10.7	16.8	21.7	1.7
3	32.3	204.5	11.5	17.3	37.9	2.5
5	34.8	205.7	11.7	17.7	48.6	2.7
7	37.0	206.3	12.1	17.9	57.8	3.1
10	39.5	208.0	12.2	18.0	68.3	3.2
14	41.8	208.3	12.4	18.0	78.5	3.4
15	42.4	208.3	12.6	18.0	80.7	3.6
20	45.0	208.7	12.6	18.0	91.9	3.6
28	48.0	208.7	12.6	18.0	104.7	3.6
31	48.2	208.7	12.6	18.0	105.7	3.6
36	48.6	208.7	12.7	18.0	107.5	3.7
42	48.7	208.7	12.7	18.0	108.0	3.7

C9. - Synko-Flex – specimen one.

Synko-Flex-1						
Time	Weight	Length	Thickness (mm)	Width (mm)	Expansion Rate	Thickness Increase
				(		
				2		
				0		
				2		
				1		
				2		
				1		
				2		
				.		
				2		
				1		
				2		
				1		
				2		
				1		

C10. - Synko-Flex – specimen two.

Synko-Flex-2						
Time	Weight	Length	Thickness (mm)	Width (mm)	Expansion Rate	Thickness Increase
				2 2 0 2 2 0 2 2 0 2 2 0		

C11. - Sykno-Flex – specimen three.

Synko-Flex-3						
Time	Weight	Length	Thickness (mm)	Width (mm)	Expansion Rate	Thickness Increase
				1 9 2 2 0 2 0		

2
0

2
2
2
2

C12. - Synko-Flex – averages.

Synko-Flex-AVG						
Time	Weight	Length	Thickness	Width	Expansion Rate	Thickness Increase
(Day)	(g)	(mm)	(mm)	(mm)	(%)	(mm)
0	156.6	200.0	16.9	33.7	0.0	0.0

1	157.1	204.3	17.4	34.1	0.3	0.5
3	157.3	206.0	17.7	33.6	0.5	0.7
5	157.6	206.0	17.7	33.7	0.6	0.8
7	157.5	206.0	17.7	33.9	0.6	0.8
10	157.9	206.3	18.0	33.9	0.8	1.1
14	158.2	207.0	18.1	33.9	1.0	1.1
15	158.2	207.0	18.1	33.9	1.0	1.1
20	158.5	207.3	18.1	33.9	1.2	1.1
28	158.8	207.7	18.1	33.9	1.4	1.1
31	158.8	208.0	18.1	33.9	1.4	1.1
36	159.1	208.7	18.1	33.9	1.6	1.1
42	159.4	208.7	18.1	33.9	1.8	1.1